SUSTAINABLE PRODUCTION OF AROMATIC AMINO ACIDS BY ENGINEERED CYANOBACTERIA

by

Arnav Deshpande

A Dissertation

Submitted to the Faculty of Purdue University

In Partial Fulfillment of the Requirements for the degree of

Doctor of Philosophy

Davidson School of Chemical Engineering

West Lafayette, Indiana

May 2022

THE PURDUE UNIVERSITY GRADUATE SCHOOL

STATEMENT OF COMMITTEE APPROVAL

Dr. John A. Morgan, Chair

Davidson School of Chemical Engineering

Dr. Natalia Dudareva

Department of Biochemistry

Dr. Doraiswami Ramkrishna

Davidson School of Chemical Engineering

Dr. Julie Liu

Davidson School of Chemical Engineering

Approved by:

Dr. John A. Morgan

This dissertation is dedicated to my beloved parents,

my world.

ACKNOWLEDGMENTS

I would like to express my gratitude to my advisor and mentor, Dr. John A. Morgan for his guidance and support throughout my time at Purdue. It is because of him that I chose to work in the field of metabolic engineering after taking his class at the start of my graduate school. His guidance, patience, curiosity, and support have given me the right tools to succeed as a researcher. I would also like to express my gratitude to Dr. Natalia Dudareva, who is not only part of my committee but also was one of my favorite instructors who motivated and inspired me with her endless passion for science. I also feel privileged to have Dr. Doraiswami Ramkrishna as a part of my committee, whose excellence and expertise are exemplary. I would also like to thank Dr. Xiaoping Bao for being part of my preliminary exam committee and Dr. Julie Liu for serving as my committee member.

I want to thank Dr. Shaunak (Rick) Ray for his mentorship, support, and friendship during my time at Purdue. His guidance, technical expertise, patience, and curiosity helped me transition into the field of metabolic engineering and helped me succeed. Rick showed me what it is to be a great mentor enriching my mentoring experience with the undergraduate researchers in our lab who I have had the privilege to work with throughout my time at Purdue. I would also like to thank Dr. Iskander M. Ibrahim and Dr. Sujith Puthiyaveetil for their excellent collaboration and for teaching me so much in a few short months. I would like to also thank all my group members, Meng-Ling, Joel, Melissa, and Jeremiah for their support, input, and contribution in creating a wonderful work environment. I would also like to show my appreciation to Dr. Gabriela Nagy, head of the safety committee who contributed to developing my leadership skills and helped develop a safe working environment.

Lastly, I would like to thank my friends. Charlie and Blake were instrumental in making me feel at home after first coming to the United States. Murali, Sukirt, and Charlie were always there for me. I also want to thank my family. My parents Unmesh and Jayanti have shown me unconditional love, and support and have been the best parents I could have wished for. My brother Advik is my support and although we have been thousands of miles apart, I have thoroughly enjoyed his companionship playing WarThunder and watching Liverpool play every weekend. Finally, I would like to express my love and appreciation for my partner Carsyn, who has helped me experience joy in the small things, and for her endless support.

TABLE OF CONTENTS

LIST OF TABLES

LIST OF FIGURES

NOMENCLATURE

List of notations

Φ_{PSII}: Effective quantum yield of photosystem II

$\Phi_{PSIImax}$: Maximum quantum yield of photosystem II

q_P: Photochemical quenching

q_L: Estimate of fraction of open PSII centres

F_m: Maximum fluorescence for dark adapted state

F_s: Steady fluorescence signal

F_m': Maximum fluorescence under actinic light

F_m^{DCMU}: Maximum fluorescence under actinic light with the addition of DCMU

F_0: Basal fluorescence for dark adapted state

F_0': Basal Fluorescence under dark after actinic light treatment

P_m: Maximum Absorbance change with saturating pulse post Far Red light treatment

P: Steady State Absorbance change under actinic light

P_m': Maximum absorbance change with saturating pulse under actinic light

P_0: Steady absorbance change after P700 re-reduction

Y(I): Quantum yield of photosystem I

Y(ND): Non-photochemical quenching due to donor side limitation

Y(NA): Non-photochemical quenching due to acceptor side limitation

List of frequently used abbreviations

2-PE: 2-Phenylethanol

3,2-TA: 3-(2-thienyl)-DL-alanine

5-FT: 5-fluoro-DL-tryptophan

A: Adenine

ADH: Alcohol dehydrogenase

AEF: Alternate electron flow

AGN: Arogenate

ALE: Adaptive laboratory evolution

ANT: Anthranilate

APRT: Anthranilate phosphoribosyltransferase

AS: Anthranilate Synthase

ATP: Adenosine triphosphate

BCA: Bicinchoninic acid

BSA: Bovine Serum Albumin

C: Cytosine

CBB: Calvin Benson Bassham

CE: Collision energy

CEF: Cyclic electron flow

CHA: Chorismate

CM: Chorismate mutase

CS: Chorismate Synthase

CRP: 1-(2-carboxyphenylamino)-1-deoxy-D-ribulose 5-phosphate

CXP: Cell exit potential

Cyt *b6f*: Cytochrome *b6f*

DAHP: 3-deoxy-D-arabinoheptulosonate 7-phosphate

DAHPS: 3-deoxy-D-arabinoheptulosonate 7-phosphate synthase

DBMIB: Dibromothymoquinone

DCMU: 3-(3,4-dichlorophenyl)-1,1-dimethylurea

DCW: Dry cell weight

DNA: Deoxyribonucleic acid

DHQ: 3-dehydroquinate

DHQD: 3-dehydroquinate dehydrogenase

DHQS: 3-dehydroquinate synthase

DHS: 3-dehydroshikimate

DP: Declustering potential

E4P: Erythrose-4-phosphate

EDTA: Ethylenediamine tetraacetic acid

EP: Entrance potential

EPSP: 5-enolpyruvylshikimate 3-phosphate

EPSPS: 5-enolpyruvylshikimate 3-phosphate synthase

E. coli: *Escherichia coli*

ESI: Electrospray ionization

Fd: Ferridoxin

FMS: Fluorescence monitoring system

FNR: Ferridoxin $NADP^+$ oxidoreductase

FR: Far red

G: Guanine

HA: Hydroxylamine

IGP: Indole glycerol phosphate

IPTG: Isopropyl-β-D-thiogalactopyranoside

KDC: 2-keto acid decarboxylase

Km: Kanamycin

LC-MS: Liquid chromatography mass spectrometry

LEF: Linear electron flow

MMS: Methyl methanesulfonate

NADPH: nicotinamide adenine dinucleotide phosphate

NGS: Next generation sequencing

NPQ: Non-photochemical quenching

NS: Neutral site

OD: Optical density

PAAS: Phenylacetaldehyde synthase

PAM: Pulse amplitude modulated fluorometry

PAT: Prephenate aminotransferase

PC: Plastocyanin

PCR: Polymerase chain reaction

PEA: Phenylethylamine

PEP: Phosphoenolpyruvate

PD: Prephenate dehydratase

Phe: L-phenylalanine

PPA: Prephenate

PPY: Phenylpyruvate

PQ: Plastoquinone

PRA: Phosphoribosylanthranilate

PRAI: Phosphoribosylanthranilate isomerase

PSI: Photosystem I

PSII: Photosystem II

rETR: Relative electron transport rate

RT: Retention time

RuBisCO: Ribulose-1,5-bisphosphate carboxylase/oxygenase

S3P: Shikimate-3-phosphate

SDH: Shikimate dehydrogenase

SDS: Sodium dodecyl sulfate

SHK: Shikimate

SK: Shikimate Kinase

SNP: Single nucleotide polymorphism

T: Thymine

Trp: L-tryptophan

TRPS: Tryptophan synthase

Tyr: L-tyrosine

WT: Wild type

ABSTRACT

With the increasing concern of climate change, engineering strategies to capture and fix carbon dioxide to produce valuable chemicals is a promising proposition. Metabolic engineering efforts have recently been focused on using cyanobacteria as hosts for the production biochemicals due to their ability to utilize carbon dioxide and sunlight as the sole carbon and energy sources, respectively. Unlike fermentation which uses plant derived sugars, cyanobacterial biochemical production does not compete for arable land that can be utilized for food production. Aromatic amino acids such as L-phenylalanine (Phe) and L-tryptophan (Trp) are essential amino acids since they cannot be synthesized by animals and thus are needed as supplements. They are valuable as animal feed supplements in the agricultural industry and find wide applications in the food, cosmetic and pharmaceutical industries as precursors. However, investigation of cyanobacteria for production of aromatic amino acids such as Phe and Trp is limited. This dissertation studies (*i*) combining random mutagenesis and metabolic engineering techniques for Trp and Phe production in *Synechocystis* sp. PCC 6803, (*ii*) development of a fast-growing cyanobacteria strain *Synechococcus elongatus* PCC 11801 for Phe production and (*iii*) investigating the effect of creation of Phe sink on photosynthetic efficiency under different light intensities.

Aromatic amino acid biosynthesis is tightly regulated by feedback inhibition in cyanobacteria. To enable overproduction of Trp in *Synechocystis* sp PCC 6803, we utilized chemical mutagenesis coupled with analog selection followed by genome sequencing to identify single nucleotide polymorphisms (SNPs) responsible for the Trp overproduction phenotypes. Interestingly, overproducers had mutations in the competing Phe biosynthetic pathway gene chorismate mutase (CM) which resulted in a lower enzyme activity and redirection of flux to Trp. We subsequently overexpressed genes encoding feedback insensitive enzymes in our randomly engineered Trp overproducing strain. The best strain isolated was able to accumulate 212±23 mg/L Trp in 10 days under 3% (vol/vol) CO_2. We demonstrate that combining random mutagenesis and metabolic engineering is superior to either approach alone.

Initial efforts in engineering cyanobacteria have resulted in low titers and productivities due to slow growth. Recently a fast-growing cyanobacterial strain *Synechococcus elongatus* PCC 11801 was discovered with growth rates comparable to yeast. Due to the lack of well characterized synthetic biology tools available for metabolic engineering of this strain, we use two rounds of

ultraviolet (UV) mutagenesis and analog selection to develop Phe overproducing strains. The best strain obtained using this strategy can produce 1.2 ± 0.1 g/L of Phe in 3 days under 3% (vol/vol) CO_2. This is the highest titer and productivity for Phe production currently reported by cyanobacteria highlighting the promise of engineering fast-growing strains for biochemical production.

Interestingly, Phe overproduction does not compete with growth but happens by fixing carbon at a higher rate. It is thought that the introduction of this carbon and energy sink relieves "sink limitation" by improving light use. However, neither the molecular mechanism nor the effect of light on enhancement in carbon fixation by introduction of an additional sink are known. Therefore, we investigated the effect of light intensity on photosynthetic efficiency, linear and cyclic electron flow in the strain containing the Phe sink. Our results indicate that under excess light, introduction of the Phe sink improves carbon fixation by improving photosynthetic efficiency and substantially reducing the cyclic electron flow around photosystem I (PSI). Taken together, our results show the previously untapped potential of cyanobacteria to improve carbon fixation by the unintuitive strategy of introducing a native carbon product sink and highlight the importance of the light environment on its performance.

Although further improvements in titer, productivity, and scale up will be necessary for cyanobacteria to compete economically at the industrial scale, this dissertation adds to the scientific knowledge and techniques for further metabolic engineering efforts.

1. INTRODUCTION

1.1 Cyanobacteria as hosts for the sustainable production of biochemicals

There is an urgent need to devise sustainable solutions to move away from fossil fuels to produce chemicals while still improving on the standard of living of the society. The severity of human induced climate change due to the magnitude of increase in carbon dioxide emission is irreversible for one thousand years after emissions stop (Susan et al., 2009). Thus, it is crucial to investigate novel solutions that could utilize one carbon substrates responsible for climate change for the conversion to valuable products.

Cyanobacteria are photosynthetic prokaryotes capable of oxygenic photosynthesis. Due to faster growth, ease of genetic manipulation, and stress tolerance compared to plants and green algae, they possess great potential as hosts for metabolic engineering for biochemical production (Jaiswal et al., 2022). Unlike, other conventional bio-based fermentation processes which utilize engineered heterotrophs such as *E. coli*, *C. glutamicum* and different yeasts, cyanobacteria do not require sugars for growth (Knoot et al., 2018). Traditional fermentation-based bio-chemical production is a two-step process. The first step involves production of sugars in plants such as corn and sugarcane and suffers and is land intensive and a direct competitor for arable land for food production. The second step is fermentation of sugars to biochemicals by industrial microbes which results in CO_2 emission (Bongaerts et al., 2001). Engineered cyanobacteria on the other hand, can convert this two-step process by directly utilizing CO_2 and sunlight from the atmosphere and converting it to biofuels or biochemicals as shown in figure 1.1 (Deshpande et al., 2020; Knoot et al., 2018; Oliver et al., 2013).

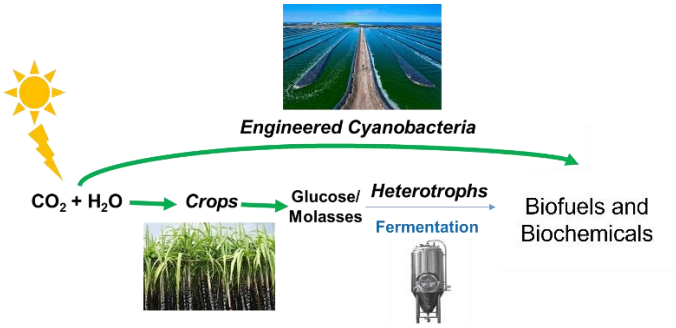

Figure 1.1 Cyanobacteria can convert a two-step sugar fermentation process into a single step by for the sustainable production of biochemicals.

Cyanobacteria can convert CO_2 to several relevant compounds such as alcohols, diols, terpenes, acids, and sugars (Pattharaprachayakul et al., 2020). However, several valuable products are either present in low amounts or are not synthesized by using the native genome set. Thus, metabolic engineering has been a valuable tool for introduction of genes for the production of value-added products as well as improving the production of native products (Knoot et al., 2018; Nielsen et al., 2016; Pattharaprachayakul et al., 2020). A summary of the metabolic engineering of biosynthetic pathways is shown in figure 1.2.

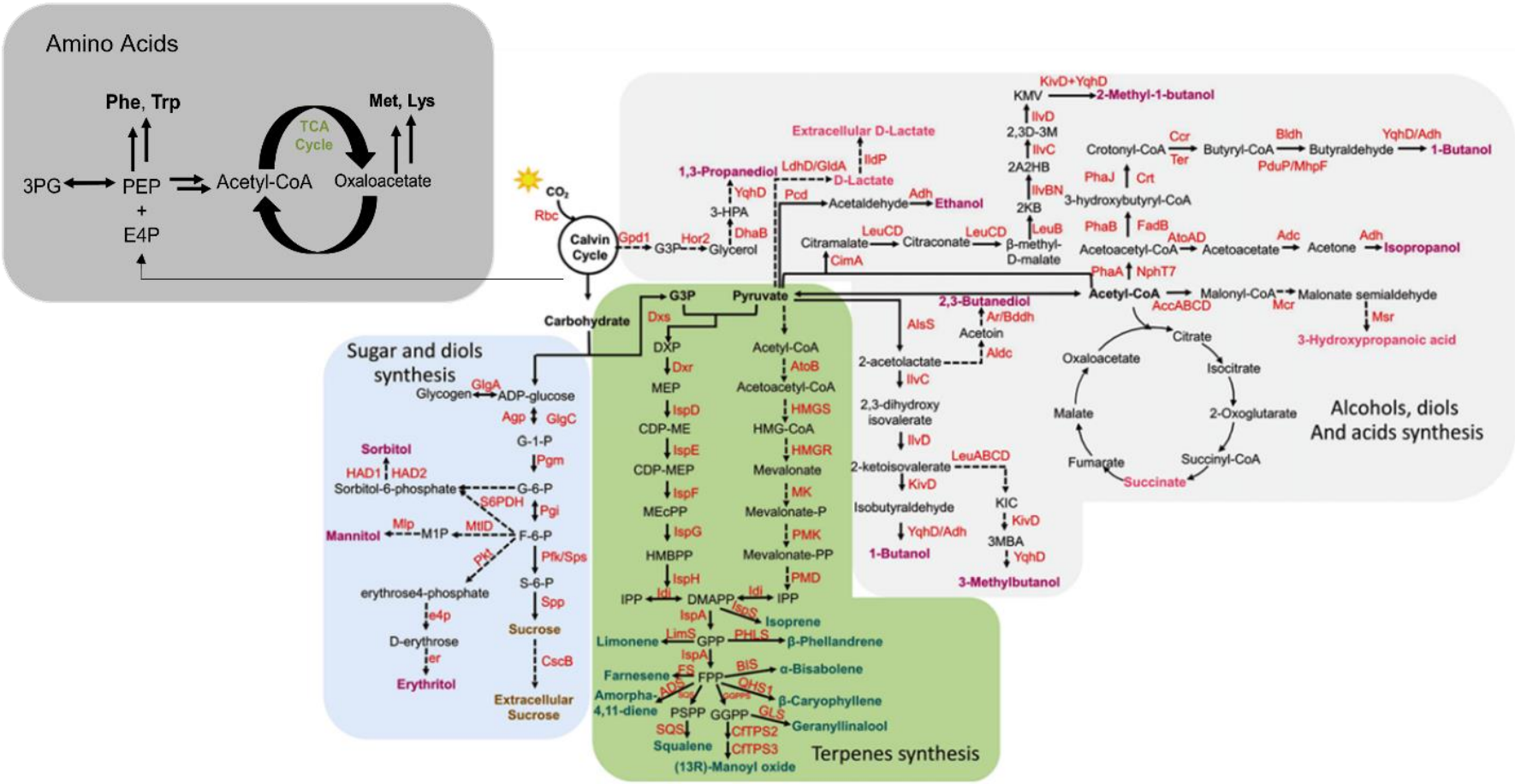

Figure 1.2 Summary of engineered pathways and products in cyanobacteria. Adapted and modified from (Nielsen et al., 2016; Pattharaprachayakul et al., 2020). Dotted lines indicate heterologous pathways, and the solid lines indicate homologous pathways. Abbreviations: Amino Acids; Met, Methionine; 3PG, 3-phosphoglycerate; E4P, erythrose-4-phosphate; PEP, phosphoenolpyruvate; Lys, Lysine; Phe, phenylalanine; Trp, tryptophan. Calvin cycle; Rbc, RuBisCo; Sugar and diols synthesis pathway; glgA, glycogen synthase; Agp, ADP-glucose pyrophosphorylase; Pgm, phosphoglucomutase; Pgi, glucose-6- phosphate isomerase; Sps, sucrose phosphate synthase; Spp, sucrose phosphate phosphatase; CscB, sucrose transporter; S6PDH, sorbitol6-phosphate dehydrogenase; HAD1 and 2, haloacid dehalogenase-like hydrolases 1 and 2; MtlD, mannitol-1-phosphate dehydrogenase; Mlp, mannitol-1-phosphatase; Pkt, phosphoketolase;

Figure 1.2 continued

E4p, erythrose-4-phosphatase; Er, erythrose reductase. G-1-P, glucose-1-phosphate; G-6-P, glucose-6-phosphate; F-6-P, fructose-6-phosphate; S-6-P, sucrose-6-phosphate; M1P, mannitol-1-phosphate. Terpenes synthesis pathway; Dxs, 1-deoxy-D-xylulose-5-phosphate synthase; Dxr, deoxyxylulose 5-phosphate reductoisomerase; IspD, diphosphocytidylyl methylerythritol synthase; IspE, diphosphocytidylyl methylerythritol kinase; IspF, methyl erythritol-2,4-cyclodiphosphate synthase; IspG, hydroxymethylbutenyl diphosphate synthase; IspH, hydroxymethylbutenyl diphosphate reductase; Idi, isopentenyl diphosphate isomerase; IspA, farnesyl diphosphate synthase; IspS, isoprene synthase; LimS, limonene synthase; PHLS, phellandrene synthase; FS, farnesene synthase; ADS, amorphadiene synthase; BIS, α-bisabolene synthase; QHS1, β-caryophyllene synthase; SQS, squalene synthase; GGPPS, geranylgeranyl diphosphate synthase; GLS, geranyllinalool synthase; CfTPS2 and 3, diterpene synthases; AtoB, acetyl-CoA acetyltransferase; HMGS, hydroxymethylglutaryl-CoA synthase; HMGR, 3-hydroxy-3-methylglutaryl-CoA reductase; MK, mevalonate kinase; PMD, phosphomevalonate decarboxylase; HMG-CoA, 3-hydroxy-3-methyl-glutaryl-coenzyme A. G3P, glyceraldehyde 3-phosphate; DXP, 1-deoxy-D-xylulose-5-phosphate; MEP, 2-C-methyl-D-erythritol-4-phosphate; CDP-ME, 4-diphosphocytidyl-2-Cmethyl-D-erythritol; CDP-MEP, 4-diphosphocytidyl-2C-methyl-D-erythritol-2-phosphate; MEcPP, 2C-methyl-D-erythritol-2,4- cyclodiphosphate; HMBPP, (E)-4-hydroxy-3-methylbut-2-enyl-diphosphate; IPP, isopentenyl diphosphate; DMAPP, dimethylallyl diphosphate; GPP, geranyl diphosphate; FPP, farnesyl diphosphate; GGPP, geranylgeranyl diphosphate; PSPP, presqualene diphosphate. Alcohols, diols and alcohols synthesis pathway; AlsS, acetolactate synthase; IlvC; acetohydroxy acid isomeroreductase; IlvD, dihydroxyacid dehydratase; LeuABCD, operon of leucine synthesis; alpha acetolactate decarboxylase; Ar, acetoin reductase; Bddh, 2,3-butanediol dehydrogenase; AccABCD, Acetyl-CoA carboxylase four subunits; Mcr, malonyl-CoA reductase; KivD, α-ketoisovalerate decarboxylase; PhaA, β-ketothiolase; PhaB, acetoacetyl-CoA reductase; PhaJ, enoyl-CoA hydratase; Ccr; cinnamoyl coenzyme A reductase; Bldh, CoA-acylating butyraldehyde dehydrogenase; NphT7, acetoacetyl-CoA synthase; FadB, Fatty acid oxidation complex subunit alpha; Crt, 3-hydroxybutyryl-CoA dehydratase; Ter, enoyl-CoA reductase; PduP/MhpF, propionaldehyde dehydrogenase; YqhD; NADPH-dependent aldehyde reductase/alcohol dehydrogenase; Adh, alcohol dehydrogenase; AtoAD, CoA-transferase operon A and D; Adc, acetoacetate decarboxylase; CimA, citramalate synthase; LeuCD, 3-isopropylamalate dehydratase; LeuB, citramalate synthase; IlvBN, acetohydroxy acid synthase; Pdc, pyruvate decarboxylase; LdhD, lactate dehydrogenase D; GldA; glycerol dehydrogenase; IldP, lactate exporter; Gdp1, Glyceraldehyde-3-phosphate dehydrogenase; Hor2, glycerol-1-phosphatase; DhaB, glycerol dehydratase; 3-HPA, 3-hydroxypropionaldehyde; KIC, 2-ketoisocaproate; 3MBA, 3-methylbutanal; 2KB, 2-ketobutyrate; 2A2HB, 2-aceto-2-hydroxybutyrate; 2,3D-3M, 2,3-dihydroxy-3methylvalerate; KMV, 2-keto-3-methylvalerate.

Although metabolic engineering has been used widely in cyanobacteria, random mutagenesis has been largely ignored after initial work in the early 1980's to identify regulation of the shikimate pathway in cyanobacteria. Random mutagenesis has been a highly successful strategy in industry, especially in the development of heterotrophic organisms for fermentation. This opens the opportunity to explore random mutagenesis as an engineering strategy, especially when combined with genome sequencing to decipher fundamental understanding of bottlenecks in the native pathway. Table 1.1 shows the studies on engineering production of endogenous products in cyanobacteria and highlights the need to further explore random mutagenesis as a strain development strategy.

Table 1.1 Engineering strategies for the production of endogenous products from CO_2 in cyanobacteria. * indicates combination of metabolic engineering and random mutagenesis techniques. Isoprene and Squalene are natively produced only in some cyanobacterial strains

Product	Mutagenesis	Metabolic Engineering	Max Titer/ Productivity
L-Lactate	-	(Angermayr et al., 2014)	836 mg/L, 60 mg/L/d
D-Lactate	-	(Selão et al., 2020)	1 g/L, 0.2 g/L/d
Succinate	-	(Sengupta et al., 2020)	0.93 g/L, 0.19 g/L/d
Sucrose	-	(Lin et al., 2020)	8 g/L, 1.9 g/L/d
Isoprene	-	(Gao et al., 2016)	1.26 g/L, 0.1 g/L/d
Squalene	-	(Choi et al., 2017)	12 mg/L/OD_{730}
Free Fatty Acids	-	(Kato et al., 2016)	0.64 g/L, 36 mg/L/d
Phenylalanine	This dissertation, (G. C. Hall et al., 1983; Hall & Jensen, 1980)	(Brey et al., 2020; Ni et al., 2018)	3 g/L, 0.4 g/L/d
Tyrosine	(G. C. Hall et al., 1983)	(Brey et al., 2020)	40 mg/L, 4 mg/L/d
Tryptophan	(G. Hall et al., 1980)	(Deshpande et al., 2020)	212 mg/L, 21 mg/L/d
Lysine	-	(Dookeran & Nielsen, 2021)	0.55 g/L, 0.11 g/L/d

1.2 Aromatic amino acid biosynthesis and engineering efforts

The shikimate pathway is used by microorganisms for the biosynthesis of the three aromatic amino acids namely L-Phenylalanine (Phe), L-Tryptophan (Trp), and L-Tyrosine (Tyr). The aromatic amino acids are essential components of the animal diet as they cannot be synthesized by animals and thus are valuable in the nutrition industry. The aromatic amino acid industry is growing with wide use in the food and feed, pharmaceutical, and nutraceutical industries (Bongaerts et al., 2001; Brey et al., 2020; Y. Liu et al., 2018).

Much of the engineering efforts have concentrated on model heterotrophs such as *E. coli*, *S. cerevisiae*, and *C. glutamicum* (Bongaerts et al., 2001; Ikeda, 2006; Rodriguez et al., 2014, 2015). The shikimate pathway starts with the precursors erythrose-4-phosphate and phosphoenolpyruvate followed by seven consecutive steps that lead to the formation of chorismate which is the common precursor for the biosynthesis for Phe, Tyr, and Trp. A representative pathway in cyanobacteria is shown in figure 2.1. Engineering the overproduction of aromatic amino acids has typically targeted genes that are subject to feedback inhibition by the end products on the enzymes such as 3-deoxy-D-*arabino*-heptulosonate-7-phosphate synthase (DAHPS), anthranilate synthase (AS), chorismate mutase/prephenate dehydratase (CM-PD) within the shikimate pathway (Denenut & Demain, 1981; Ikeda, 2006; Ikeda & Katsumata, 1999; Prasad et al., 1987). There have also been efforts on targeting transcriptional regulators of the shikimate pathway in *E. coli* (L. Liu et al., 2016; Song et al., 2005). Increasing the availability of precursors, overexpression of enzymes as well as preventing re-uptake of secreted amino acids are other techniques that has been widely employed (Draths et al., 1992; Rodriguez et al., 2014).

Although significant progress has been made in engineering model heterotrophs, only two studies in the last three years have reported successful overproduction of aromatic amino acids in cyanobacteria. This is mainly due to the lack of abundance of omics-scale datasets and extensive synthetic biology toolbox (Rodriguez et al., 2014), presence of multiple copies of the genome (Zerulla et al., 2016), as well as slower growth and larger development and testing times when compared to models such as *E. coli*. In cyanobacteria, Phe overproduction has been achieved in *Synechococcus elongatus* PCC 7942 and *Synechocystis* sp PCC 6803 by heterologous overexpression of feedback resistant forms of DAHP synthase and CM-PD from *E.coli* (Brey et al., 2020; Ni et al., 2018). However, there have not been any attempts to engineer tryptophan production or improve productivities which remain crucial for the success of cyanobacteria for aromatic amino acid production on a larger scale.

1.3 Objectives of dissertation

This dissertation seeks to utilize random mutagenesis and metabolic engineering techniques towards enabling sustainable and efficient production of aromatic amino acids and understanding its effect on carbon fixation by studying photosynthesis using bioanalytical techniques and

fluorescence/absorbance based photosynthetic measurements. The objectives can be summarized as follows:

I. Combine random mutagenesis and metabolic engineering strategies to develop *Synechocystis* sp PCC 6803 for the production of tryptophan
II. Engineer recently discovered fast growing cyanobacteria *Synechococcus elongatus* PCC 11801 for the production of phenylalanine
III. Evaluate the effect of Phe sink on the carbon fixation by studying electron flow through photosystem I and II

1.4 References

Angermayr, S. A., van der Woude, A. D., Correddu, D., Vreugdenhil, A., Verrone, V., & Hellingwerf, K. J. (2014). Exploring metabolic engineering design principles for the photosynthetic production of lactic acid by *Synechocystis* sp. PCC6803. *Biotechnology for Biofuels*, *7*(1), 99. https://doi.org/10.1186/1754-6834-7-99

Bongaerts, J., Krämer, M., Müller, U., Raeven, L., & Wubbolts, M. (2001). Metabolic engineering for microbial production of aromatic amino acids and derived compounds. *Metabolic Engineering* (Vol. 3, Issue 4, pp. 289–300). Academic Press Inc. https://doi.org/10.1006/mben.2001.0196

Brey, L. F., Włodarczyk, A. J., Bang Thøfner, J. F., Burow, M., Crocoll, C., Nielsen, I., Zygadlo Nielsen, A. J., & Jensen, P. E. (2020). Metabolic engineering of *Synechocystis* sp. PCC 6803 for the production of aromatic amino acids and derived phenylpropanoids. *Metabolic Engineering*, *57*, 129–139. https://doi.org/10.1016/j.ymben.2019.11.002

Choi, S. Y., Wang, J.-Y., Kwak, H. S., Lee, S.-M., Um, Y., Kim, Y., Sim, S. J., Choi, J., & Woo, H. M. (2017). Improvement of Squalene Production from CO_2 in Synechococcus elongatus PCC 7942 by Metabolic Engineering and Scalable Production in a Photobioreactor. *ACS Synthetic Biology*, *6*(7), 1289–1295. https://doi.org/10.1021/acssynbio.7b00083

Denenut, E. 0, & Demain, A. L. (1981). Enzymatic Basis for Overproduction of Tryptophan and Its Metabolites in Hansenula polymorpha Mutants. *Applied and Environmental Microbiology*. https://journals.asm.org/journal/aem

Deshpande, A., Vue, J., & Morgan, J. (2020). Combining Random Mutagenesis and Metabolic Engineering for Enhanced Tryptophan Production in *Synechocystis* sp. Strain PCC 6803. *Applied and Environmental Microbiology* https://doi.org/10.1128/AEM

Dookeran, Z. A., & Nielsen, D. R. (2021). Systematic Engineering of Synechococcus elongatus UTEX 2973 for Photosynthetic Production of l-Lysine, Cadaverine, and Glutarate. *ACS Synthetic Biology*, *10*(12), 3561–3575. https://doi.org/10.1021/acssynbio.1c00492

Draths, K. M., Pompliano, D. L., Conley, D. L., Frost, J. W., Berry, A., Disbrow, G. L., Staversky, R. J., & Lievense, J. C. (1992). Biocatalytic synthesis of aromatics from D-glucose: the role of transketolase. *Journal of the American Chemical Society*, *114*(10), 3956–3962. https://doi.org/10.1021/ja00036a050

Gao, X., Gao, F., Liu, D., Zhang, H., Nie, X., & Yang, C. (2016). Engineering the methylerythritol phosphate pathway in cyanobacteria for photosynthetic isoprene production from CO2. *Energy & Environmental Science*, *9*(4), 1400–1411. https://doi.org/10.1039/C5EE03102H

Hall, G., Flick, M., & Jensen, R. (1983). Regulation of the aromatic pathway in the cyanobacterium Synechococcus sp. strain Pcc6301 (Anacystis nidulans). *Journal Of Bacteriology*, *153*(1), 423-428. doi: 10.1128/jb.153.1.423-428.

Ikeda, M. (2006). Towards bacterial strains overproducing L-tryptophan and other aromatics by metabolic engineering. In *Applied Microbiology and Biotechnology* (Vol. 69, Issue 6, pp. 615–626). https://doi.org/10.1007/s00253-005-0252-y

Ikeda, M., & Katsumata, R. (1999). Hyperproduction of Tryptophan by Corynebacterium glutamicum with the Modified Pentose Phosphate Pathway. *Applied and Environmental Microbiology* (Vol. 65, Issue 6). https://journals.asm.org/journal/aem

Jaiswal, D., Sahasrabuddhe, D., & Wangikar, P. P. (2022). Cyanobacteria as cell factories: the roles of host and pathway engineering and translational research. *Current Opinion in Biotechnology* (Vol. 73, pp. 314–322). Elsevier Ltd. https://doi.org/10.1016/j.copbio.2021.09.010

Kato, A., Use, K., Takatani, N., Ikeda, K., Matsuura, M., Kojima, K., Aichi, M., Maeda, S., & Omata, T. (2016). Modulation of the balance of fatty acid production and secretion is crucial for enhancement of growth and productivity of the engineered mutant of the cyanobacterium *Synechococcus elongatus*. *Biotechnology for Biofuels*, *9*(1), 91. https://doi.org/10.1186/s13068-016-0506-1

Knoot, C. J., Ungerer, J., Wangikar, P. P., & Pakrasi, H. B. (2018). Cyanobacteria: Promising biocatalysts for sustainable chemical production. In *Journal of Biological Chemistry* (Vol. 293, Issue 14, pp. 5044–5052). American Society for Biochemistry and Molecular Biology Inc. https://doi.org/10.1074/jbc.R117.815886

Lin, P.-C., Zhang, F., & Pakrasi, H. B. (2020). Enhanced production of sucrose in the fast-growing cyanobacterium Synechococcus elongatus UTEX 2973. *Scientific Reports*, *10*(1), 390. https://doi.org/10.1038/s41598-019-57319-5

Liu, L., Duan, X., & Wu, J. (2016). Modulating the direction of carbon flow in Escherichia coli to improve L-tryptophan production by inactivating the global regulator FruR. *Journal of Biotechnology*, *231*, 141–148. https://doi.org/10.1016/j.jbiotec.2016.06.008

Liu, Y., Xu, Y., Ding, D., Wen, J., Zhu, B., & Zhang, D. (2018). Genetic engineering of Escherichia coli to improve L-phenylalanine production. *BMC Biotechnology*, *18*(1). https://doi.org/10.1186/s12896-018-0418-1

Ni, J., Liu, H. Y., Tao, F., Wu, Y. T., & Xu, P. (2018). Remodeling of the Photosynthetic Chain Promotes Direct CO_2 Conversion into Valuable Aromatic Compounds. *Angewandte Chemie - International Edition*, *57*(49), 15990–15994. https://doi.org/10.1002/anie.201808402

Nielsen, A. Z., Mellor, S. B., Vavitsas, K., Wlodarczyk, A. J., Gnanasekaran, T., Perestrello Ramos H de Jesus, M., King, B. C., Bakowski, K., & Jensen, P. E. (2016). Extending the biosynthetic repertoires of cyanobacteria and chloroplasts. In *Plant Journal* (Vol. 87, Issue 1, pp. 87–102). Blackwell Publishing Ltd. https://doi.org/10.1111/tpj.13173

Oliver, J. W. K., Machado, I. M. P., Yoneda, H., & Atsumi, S. (2013). Cyanobacterial conversion of carbon dioxide to 2,3-butanediol. *Proceedings of the National Academy of Sciences of the United States of America*, *110*(4), 1249–1254. https://doi.org/10.1073/pnas.1213024110

Pattharaprachayakul, N., Choi, J., Incharoensakdi, A., & Woo, H. M. (2020). Metabolic Engineering and Synthetic Biology of Cyanobacteria for Carbon Capture and Utilization. *Biotechnology and Bioprocess Engineering*, *25*(6), 829–847. https://doi.org/10.1007/s12257-019-0447-1

Prasad, R., Niederberger, P., & Hütter, R. (1987). Tryptophan accumulation in Saccharomyces cerevisiae under the influence of an artificial yeast TRP gene cluster. *Yeast*, *3*(2), 95–105. https://doi.org/https://doi.org/10.1002/yea.320030206

Rodriguez, A., Kildegaard, K. R., Li, M., Borodina, I., & Nielsen, J. (2015). Establishment of a yeast platform strain for production of p-coumaric acid through metabolic engineering of aromatic amino acid biosynthesis. *Metabolic Engineering*, *31*, 181-188. https://doi.org/10.1016/j.ymben.2015.08.003

Rodriguez, A., Martínez, J. A., Flores, N., Escalante, A., Gosset, G., & Bolivar, F. (2014). Engineering Escherichia coli to overproduce aromatic amino acids and derived compounds. *Microbial Cell Factories* (Vol. 13, Issue 1). BioMed Central Ltd. https://doi.org/10.1186/s12934-014-0126-z

Selão, T. T., Jebarani, J., Ismail, N. A., Norling, B., & Nixon, P. J. (2020). Enhanced Production of D-Lactate in Cyanobacteria by Re-Routing Photosynthetic Cyclic and Pseudo-Cyclic Electron Flow. *Frontiers in Plant Science*, *10*. https://www.frontiersin.org/article/10.3389/fpls.2019.01700

Sengupta, S., Jaiswal, D., Sengupta, A., Shah, S., Gadagkar, S., & Wangikar, P. P. (2020). Metabolic engineering of a fast-growing cyanobacterium Synechococcus elongatus PCC 11801 for photoautotrophic production of succinic acid. *Biotechnology for Biofuels*, *13*(1). https://doi.org/10.1186/s13068-020-01727-7

Song, J., Bonner, C. A., Wolinsky, M., & Jensen, R. A. (2005). The TyrA family of aromatic-pathway dehydrogenases in phylogenetic context. *BMC Biology*, *3*. https://doi.org/10.1186/1741-7007-3-13

Susan, S., Gian-Kasper, P., Reto, K., & Pierre, F. (2009). Irreversible climate change due to carbon dioxide emissions. *Proceedings of the National Academy of Sciences*, *106*(6), 1704–1709. https://doi.org/10.1073/pnas.0812721106

Zerulla, K., Ludt, K., & Soppa, J. (2016). The ploidy level of Synechocystis sp. PCC 6803 is highly variable and is influenced by growth phase and by chemical and physical external parameters. *Microbiology*, *162*(5), 730–739. https://doi.org/10.1099/mic.0.000264

2. COMBINING RANDOM MUTAGENESIS AND METABOLIC ENGINEERING FOR ENHANCED AROMATIC AMINO ACID PRODUCTION IN *SYNECHOCYSTIS* SP PCC 6803

2.1 Abstract

Tryptophan (Trp) is an essential aromatic amino acid that has value as an animal feed supplement, as the amount found in plant-based sources is insufficient. Phenylalanine and tyrosine are widely used in the food and pharmaceutical industries. An alternative to production by engineered microbial fermentation is to have tryptophan biosynthesized by a photosynthetic microorganism that could replace or supplement both the plant and industrially used microbes. We selected *Synechocystis* sp. strain PCC 6803, a model cyanobacterium, as the host and studied metabolic engineering and random mutagenesis approaches. Previous work on engineering heterotrophic microbes for improved Phe and Trp titers has targeted allosteric feedback regulation in enzymes 3-deoxy-D-arabinoheptulosonate 7-phosphate synthase (DAHPS), chorismate mutase (CM) and anthranilate synthase (AS) as major bottlenecks in the shikimate pathway. In this work, the genes encoding feedback-resistant enzymes from *Escherichia coli*, $aroG^{fbr}$ and $trpE^{fbr}$, were overexpressed in the host wild-type (WT) strain. Separately, the WT strain was subjected to random mutagenesis and selection using an amino acid analog to isolate phenylalanine and tryptophan-overproducing strains. The randomly mutagenized strains were sequenced in order to identify the mutations that resulted in the desirable phenotypes. Interestingly, the tryptophan overproducers had mutations in the gene encoding chorismate mutase (CM), which catalyzes the conversion of chorismate to prephenate. We hypothesized that mutant CM has a reduced activity that leads to redirection of flux to tryptophan. *In vitro* enzyme kinetics confirmed that the mutation in CM resulted not only in a 2.3-fold higher K_m, but also a lower maximum rate V_{max}. The best tryptophan overproducer from random mutagenesis was selected as a host for metabolic engineering where $aroG^{fbr}$ and $trpE^{fbr}$ were overexpressed. The best strain developed produced 212 ± 23 mg/liter of tryptophan after 10 days of photoautotrophic growth under 3% (vol/vol) CO_2. We demonstrated that a combination of random mutagenesis and metabolic engineering was superior to either individual approach.

Importance: Aromatic amino acids such as phenylalanine and tryptophan are primarily used as additives in the animal feed industry and are typically produced using genetically engineered

heterotrophic organisms such as *Escherichia coli*. This involves a two-step process, where the substrate such as molasses is first obtained from plants followed by fermentation by heterotrophic organisms. We have engineered photoautotrophic cyanobacterial strains by a combination of random mutagenesis and metabolic engineering. These strains grow on CO_2 as the sole carbon source and utilize light as the sole energy source to produce tryptophan, thus converting the two-step process into a single step. Our results show that combining random mutagenesis and metabolic engineering was superior to either approach alone. This study also builds a foundation for further engineering of cyanobacteria for industrial tryptophan production.

2.2 Introduction

Aromatic amino acids are high value biochemicals with industrial and agricultural applications (Ikeda, 2006; Leuchtenberger et al., 2005; Sprenger, 2007). Tryptophan is used in feed, food, and pharmaceutical industries and serves as the precursor for the synthesis of 5-hydroxytryptophan and for the treatment of pellagra, a disease caused by the deficiency of niacin (Bongaerts et al., 2001; Ikeda, 2006; Leuchtenberger et al., 2005). Phenylalanine is used as a feedstock to produce the artificial sweetener aspartame and has been used as an intermediate for pharmaceuticals such as HIV protease inhibitor, anti-inflammatory drugs, and catecholamines as well (Bongaerts et al., 2001). Tryptophan is produced in biotechnological processes using engineered heterotrophic microorganisms such as *Escherichia coli* and *Corynebacterium glutamicum* from carbon sources such as glucose (Ikeda, 2006; Ikeda & Katsumata, 1999). As an alternative, photoautotrophic cyanobacteria can fix carbon dioxide to produce aromatic amino acids via the shikimate pathway. This approach converts the two-step process of obtaining a carbon source such as molasses/glucose from plants and its subsequent conversion to aromatic amino acids into a single step.

Hall et al. (Hall et al., 1982) surveyed the regulation of the shikimate pathway in their study of 48 cyanobacterial strains and found they differ greatly from those of *E. coli* and *C. glutamicum*. They tested allosteric feedback inhibition of the first enzyme, 3-deoxy-Darabinoheptulosonate 7-phosphate synthase (DAHPS), across several species and showed that it is predominantly due to phenylalanine (Hall et al., 1982), whereas the three isoforms of DAHPS are each individually inhibited by phenylalanine, tyrosine, and tryptophan in *E. coli* (Sprenger, 2007). Further differences between *E. coli* and cyanobacteria include the regulation of the Phe/Tyr and Trp

branches. Chorismate mutase (CM) was only found to be feedback inhibited by Phe, Tyr, or Trp in a few cyanobacterial strains (Hall et al., 1982), whereas CM-prephenate dehydrogenase (PDH) is inhibited by tyrosine and the CM-prephenate dehydratase (PD) complex is inhibited by phenylalanine in *E. coli* (Ikeda, 2006). A summary of the observed regulation of the pathways of aromatic amino acid biosynthesis in cyanobacteria is provided in Fig. 2.1, but does not necessarily represent regulation in any single cyanobacteria strain.

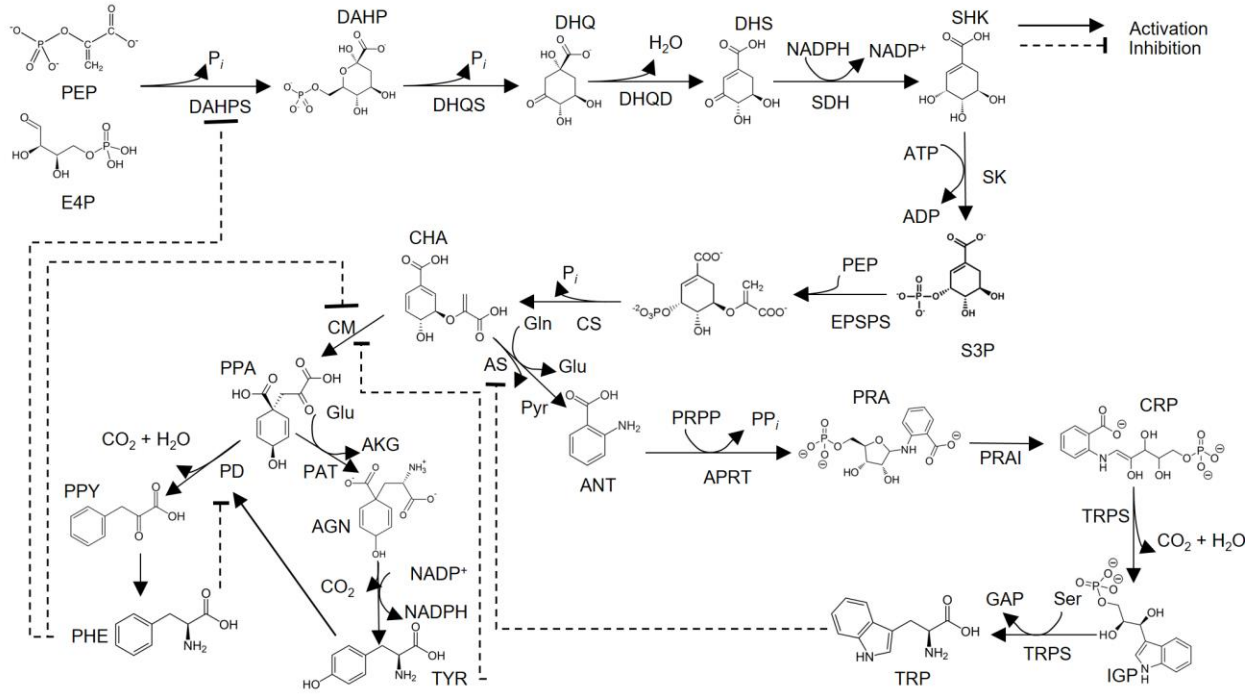

Figure 2.1 Observed enzyme regulation of the shikimate and aromatic amino acid pathways in cyanobacteria. Not all regulation necessarily exists in a single cyanobacterial species. Adapted and modified from (Riccardi et al., 1989; Song et al., 2005). E4P, erythrose-4-phosphate; PEP, phosphoenolpyruvate; DAHP, 3-deoxy-D-arabinoheptulosonate 7-phosphate; DHQ, 3-dehydroquinate; DHS, 3-dehydroshikimate; SHK, shikimate; S3P, shikimate-3-phosphate; EPSP, 5-enolpyruvylshikimate 3-phosphate; CHA, chorismate; ANT, anthranilate; PRA, phosphoribosylanthranilate; CRP, 1-(2-carboxyphenylamino)-1-deoxy-D-ribulose 5-phosphate; IGP, indole glycerol phosphate; TRP, tryptophan; PPA, prephenate; PPY, phenylpyruvate; AGN, arogenate; PHE, phenylalanine; TYR, tyrosine; DAHPS, 3-deoxy-D-arabinoheptulosonate 7-phosphate synthase; DHQS, 3-dehydroquinate synthase; DHQD, 3-dehydroquinate dehydrogenase; SDH, shikimate dehydrogenase; SK, shikimate kinase; EPSPS, 5-enolpyruvylshikimate 3-phosphate synthase; CS, chorismate synthase; AS, anthranilate synthase; APRT, anthranilate phosphoribosyltransferase; PRAI, phosphoribosylanthranilate isomerase; TRPS, tryptophan synthase; CM, chorismate mutase; PD, prephenate dehydratase; PAT, prephenate aminotransferase.

In general, the first step for microbial overproduction of phenylalanine or tryptophan is the removal of allosteric feedback inhibition of DAHPS to increase flux into the shikimate pathway (Ikeda, 2006). Further deregulation of enzymes downstream of DAHPS is also required to improve the productivity of the microbes. In *E. coli*, the branch point enzyme CM is deregulated to produce phenylalanine, and anthranilate synthase (AS) is deregulated to produce tryptophan (Rodriguez et al., 2015). The removal of feedback inhibition of DAHPS by phenylalanine alone in a mutant of *Synechocystis* sp. strain 29108 was sufficient to confer resistance to phenylalanine analogs and produce measurable amounts of extracellular Phe and Tyr compared to nondetectable amounts in the wild type (Hall & Jensen, 1980).

Random mutagenesis followed by selection on amino acid analogs is a common strain development technique for the production of valuable amino acids. With the reduced cost of whole-genome sequencing using next-generation sequencing (NGS), random mutagenesis has become a feasible option to discover favorable mutations and has been used in *Corynebacterium* for enhancing the production of lysine, methionine, and serine. Moreover, random mutagenesis, screening, and resequencing may identify gene regulation of key features of the shikimate pathway in less-characterized species. Previous work demonstrated that DAHPS and other shikimate pathway enzymes lost feedback inhibition in analog-resistant cyanobacterial mutants through enzyme assays (Hall & Jensen, 1980; Hall et al., 1983; Rao et al., 1995) but did not determine the biochemical nature, either of alterations in the gene coding region or amino acids in the sequence of the resistant enzyme. In contrast, specific amino acid substitutions are known to occur in feedback resistant DAHPS (Hu et al., 2003), CM-PD (Nelms et al., 1992), and AS in *E. coli*, allowing for direct expression of genes encoding these allosteric feedback-resistant enzymes.

In this study, we heterologously overexpressed $aroG^{L175D}$ (Hu et al., 2003) and $trpE^{S40F}$ (Ramos & Downs, 2003) from *E. coli*, which code for feedback-resistant DAHPS and AS, respectively, individually as well as in combination to study their effect on aromatic amino acid production. In parallel, methyl methanesulfonate (MMS), a potent DNA alkylating agent that induces base substitutions, was used for random mutagenesis, followed by selection on phenylalanine and tryptophan analog. Three overproducing mutants were sequenced using the Illumina MiSeq platform to identify novel mutations that could lead to overproduction of aromatic amino acids. The effect of a common mutation identified that enabled tryptophan production was tested by studying enzyme kinetics using *in vitro* assays of the purified wild type and mutant

enzymes. Finally, the randomly mutagenized strain with the highest tryptophan titer was selected to be further engineered by the individual and combined overexpression of feedback-resistant forms of DAHPS and AS to develop strains with higher tryptophan titers.

We show that the combination of metabolic engineering and random mutagenesis approaches was a strategy superior to either approach alone. This method could be used in the future to guide the development of cyanobacterial strains or other microbes for production of valuable chemicals on larger scales.

2.3 Materials and Methods

2.3.1 Bacterial strains, media and growth conditions

In this study, the cyanobacteria wild type strain is *Synechocystis* sp. PCC 6803 substrain GT-I. All the strains (Table 2.1) were grown in triplicate in 250 mL Erlenmeyer flasks at 30°C and 200 rpm under 240 μE (μmol photons/m^2/s) fluorescent light and atmospheric CO_2 conditions in 50 mL of BG-11 medium (Rippka et al., 1979) with a starting optical density (OD) of 0.05 or on BG-11 agar plates with 1.5% w/v DifcoBacto agar (Becton Dickinson) with 3 g/L sodium thiosulfate unless stated otherwise. Randomly mutagenized strains were regularly cultured with 0.3 mg/ml of analog 5-fluoro-DL-tryptophan or 3-(2-thienyl)-DL-alanine apart from when used in an experiment to maintain their observed phenotype whereas rationally engineered strains were grown with 50 μg/mL levels of kanamycin. Strains developed using both rational and random approaches were cultured with both kanamycin as well as the appropriate analog apart from when used in experiments. The growth of the cultures is determined by measuring the optical density (OD) at 730 nm using a Beckman DU Series 500 spectrophotometer. The relationship between the biomass and the OD_{730} was determined to be 0.286 g CDW/L/OD_{730}.

Table 2.1 List of cyanobacteria strains used and developed in this study

Strains		Characteristic	Source
SYNY3		*Synechocystis* sp. PCC 6803 substrain GT-I	ATCC
SYNY3-JV1, SYNY3-JV2, SYNY3-JV3		Tryptophan overproducer	This work
SYNY3-JV4, SYNY3-JV5, SYNY3-JV6		Phenylalanine overproducer	This work
Strain	Parent Strain	Integrative Plasmid	Source
SYNY3-AD1	SYNY3	pEERM1	This work
SYNY3-AD2	SYNY3	pEERM1a	This work
SYNY3-AD3	SYNY3	pEERM1b	This work
SYNY3-AD4	SYNY3	pEERM1c	This work
SYNY3-AD5	SYNY3-JV1	pEERM1	This work
SYNY3-AD6	SYNY3-JV1	pEERM1a	This work
SYNY3-AD7	SYNY3-JV1	pEERM1b	This work
SYNY3-AD8	SYNY3-JV1	pEERM1c	This work

2.3.2 Construction of plasmids for metabolic engineering

Plasmid pEERM1 was a gift from Dr. Pia Lindberg and acquired from Addgene (Addgene plasmid #64024 ; http://n2t.net/addgene:64024 ; RRID:Addgene_64024) (Englund et al., 2015). Genes coding feedback resistant DAHPS and AS were codon optimized for expression in cyanobacteria and synthesized by GenScript (GenScript, Piscataway, NJ). To develop plasmid pEERM1a and pEERM1b, $aroG^{L175D}$ and $trpE^{S40F}$ was inserted in the open reading frame between cloning sites XbaI and SpeI respectively in plasmid pEERM1. Plasmid pEERM1c contains both $aroG^{L175D}$ and $trpE^{S40F}$ and was constructed by insertion of gene $trpE^{S40F}$ between cloning sites SpeI and PstI in plasmid pEERM1a. Table 2.2 lists all the plasmids used in this study. Successful cloning was verified by gel electrophoresis.

Table 2.2 List of plasmids developed and used in this study

Plasmid	Integration Site	Promoter	Antibiotic Resistance	Genes Expressed (*E.coli*)	Source
pEERM1	*psbA2*	P*psbA2*	Km	-	Englund et al. (2015)
pEERM1a	*psbA2*	P*psbA2*	Km	$aroG^{L175D}$	This work
pEERM1b	*psbA2*	P*psbA2*	Km	$trpE^{S40F}$	This work
pEERM1c	*psbA2*	P*psbA2*	Km	$aroG^{L175D}$, $trpE^{S40F}$	This work

Figure 2.2 shows the vector diagram of the plasmid pEERM1 and the proposed strategy used in this develop feedback resistant gene expression vectors. Previously, pEERM1 was developed for use in *Synechocystis* sp. PCC 6803 for production for plant diterpenoid manoyl oxide (Englund et al., 2015).

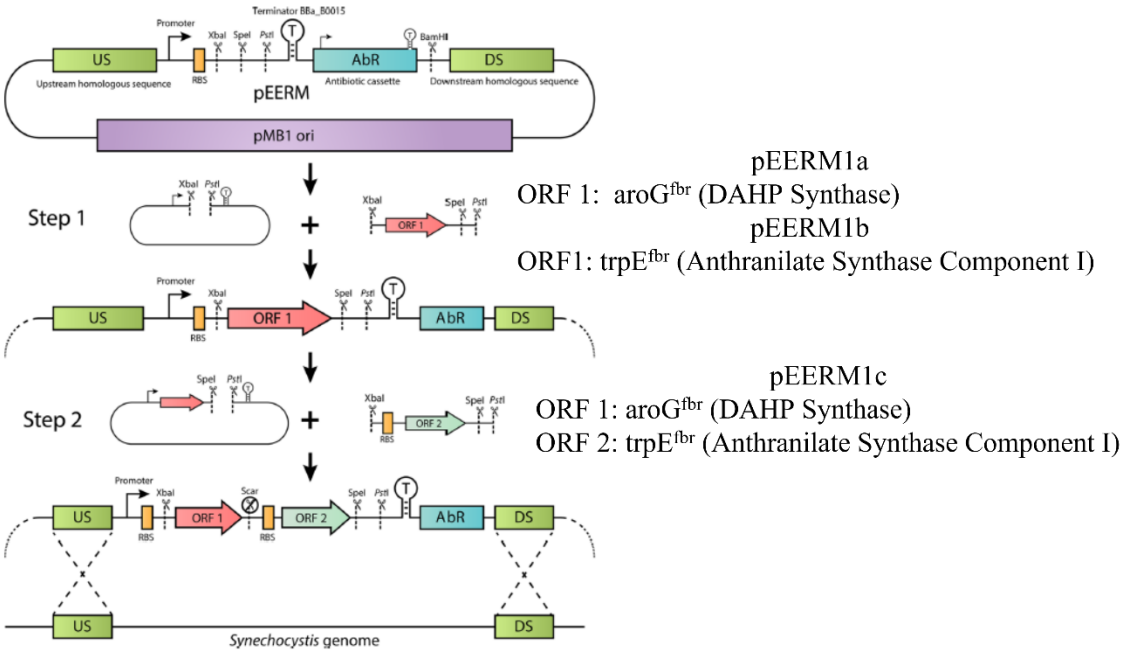

Figure 2.2 Plasmid development strategy for the overexpression of feedback resistant genes *aroG*^{fbr} and *trpE*^{fbr} separately and together

2.3.3 Construction of metabolically engineered strains

Transgenic SYNY3 strains were constructed by overexpression of feedback resistant DAHPS and AS from *E. coli*. Briefly, the integrative plasmid pEERM1 integrates into the *Synechocystis* genome at the *psbA2* site and expression of the cloned genes is driven by the strong light inducible promoter P*psbA2* (Englund et al., 2015). The plasmid has a kanamycin antibiotic

resistance cassette which was used for selecting transformed strains. The plasmids pEERM1a, pEERM1b and pEERM1c were transformed into the SYNY3 (wild type) or randomly mutagenized strain SYNY3-JV1 by a previously described protocol (Brey et al., 2020; Englund et al., 2015). The transformed cells were selected by re-streaking individual colonies on BG-11 plates containing 50 µg/mL kanamycin a minimum of three times. Individual colonies were then selected and grown in liquid media containing 50 µg/mL kanamycin and successful transformation was verified by PCR amplification followed by gel electrophoresis.

2.3.4 Verification of cloning and bacterial transformation

Plasmids in this study were separated on 1% agarose gels in 1X TAE buffer with 0.5 µg/L EtBr on a Bio-Rad Mini-Sub Cell GT gel electrophoresis system prior to UV light imaging using a transilluminator. A super coiled DNA ladder was used as a marker to verify that the inserts were as expected. Figure 2.3 shows the DNA bands obtained after the plasmids were run on the gel. The plasmid pEERM1 is 3728 bp whereas the genes *aroG*^{fbr} and *trpE*^{fbr} are1053 bp and 1563 bp long. Figure 2.3 thus confirms that the plasmids pEERM1a-c have the expected sizes (~4.7 kb, 5.3 kb and 6.3 kb respectively).

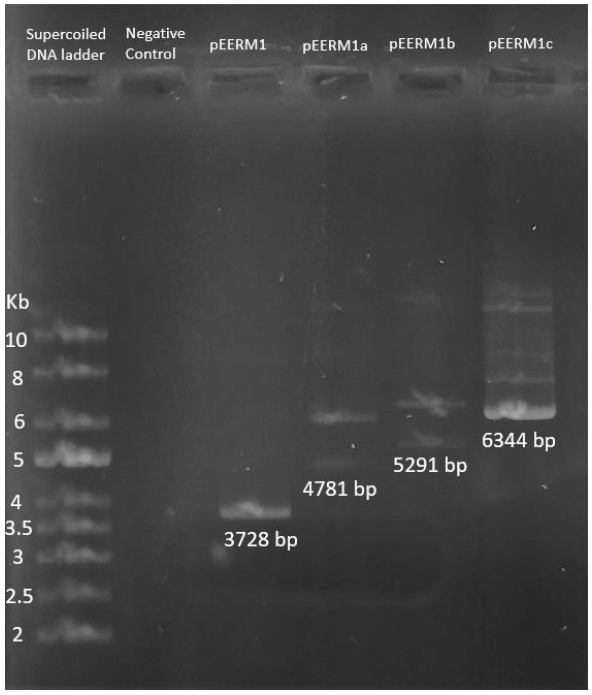

Figure 2.3 Gel electrophoresis image showing DNA bands of plasmids used in this study run on 1% agarose gel stained with ethidium bromide with a supercoiled DNA ladder

Successful transformation was checked using a combination of PCR and gel electrophoresis. Transformed strains listed in Table 2.1 were grown until they reached exponential growth phase when samples were taken. Genomic DNA was extracted using Applied Biosystems DNA All Reagents Kit to serve as template for PCR. Primers were designed to amplify the psbA2 integration region. The forward primer was 5'- CCAATCTGAACATCGACAAATACAT-3' while 5'-CCCATTGAAGGAGAGTGCAA-3' served as the reverse primer. ThermoScientific DreamTaq Green PCR Mastermix was used for the PCR reaction and the conditions were set as follows: Denaturation at 95°C for 5 mins on initial cycle followed by 30 cycles of 94° for 30s, 60°C for 30s and 68°C for 210s. This was followed by a final extension at 68°C for 5 mins before holding at 4°C. The amplified PCR products obtained were then run on 1% agarose gels as previously described with a 1 kB DNA ladder as a marker lane. Figure 2.3 shows the DNA bands obtained after the amplified PCR products. The size integration region amplified by the primers is roughly 1.2 kb. Figure 2.4 shows successful transformation and segregation for all our developed strains where incorporation of the EV corresponds to ~1.2 kb while $aroG^{fbr}$, $trpE^{fbr}$ and a combination of both the genes correspond to DNA bands of ~ 2.3 kb, 2.8 kb and 3.8 kb respectively.

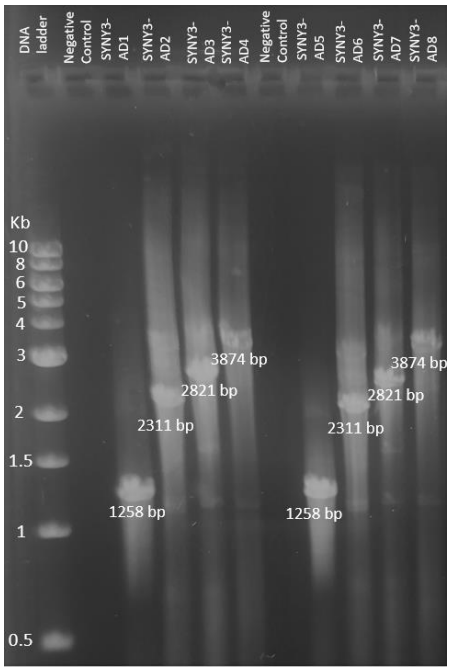

Figure 2.4 Gel electrophoresis image showing DNA bands obtained after running PCR amplified psbA2 integration regions of different strains developed in this study

2.3.5 Random mutagenesis and selection

Random mutagenesis was carried out using a modified procedure previously described using methyl methanesulfonate (MMS) as the chemical mutagen (Bose, 2016; Tillich et al., 2012). Briefly, 1% (v/v) MMS was added to cyanobacteria cultures in exponential growth phase for 60 seconds and quenched with sodium thiosulfate for reaction volumes greater than 1.5 mL. The cells were then pelleted by centrifugation at 2760 x *g* and washed a total of three times in fresh growth medium to remove the mutagen.

Cells were then incubated at room temperature in the dark for 24 hours before spreading on agar plates containing increasing concentrations of amino acid analog 5-fluoro-DL-tryptophan or 3-(2-thienyl)-DL-alanine (Sigma Aldrich, St. Louis, MO) ranging from 0.3 mg/ml to 0.9 mg/ml to select for tryptophan or phenylalanine overproducers respectively. Individual colonies resistant to the highest analog concentration were re-streaked on analog containing plates a minimum of three times before being shifted to liquid media to test for amino acid production.

2.3.6 Metabolite extraction

Synechocystis cells were pelleted by centrifugation at 2760 x *g*. The supernatant was collected and stored at -20°C until further analysis for extracellular metabolites. The cell pellet was extracted with 500 µL of methanol followed by incubation at -20°C for 30 minutes. Two more extractions using 50% methanol with *p*-fluoro-DL-phenylalanine as internal standard were performed and all the extracts were pooled. Both the supernatant and the extracts were dried to completeness using either a stream of pure N_2 or with a Labconco CentriVap Concentrator. The dried samples were reconstituted in 50% methanol before injection into the LC-MS/MS.

2.3.7 Quantification of aromatic amino acids production

Intracellular and extracellular aromatic amino acid concentrations were separately calculated using reverse-phase chromatography on a Shimadzu HPLC-20 AD system (Columbia, MD) and quantified by external standards using ABSciex 5500 triple quadrupole mass spectrometer (Redwood City, CA) in negative ion mode. The cell extracts were spiked with the internal standard *p*-fluoro-DL-phenylalanine to account for volume changes. Chromatographic separations were performed on a 150 mm x 4.6 mm Zorbax Eclipse C8 column, 5 µm, (Agilent

Technologies, Santa Clara, CA) at column temperature 30°C and a flow rate of 1 mL/min. The injection volume was set to 10 µL. A linear gradient of aqueous solvent A (2.5 mM ammonium acetate in ultrapure water, adjusted to pH 5.3 using glacial acetic acid) and organic solvent B (97.8% acetonitrile, 2% ultrapure water and 0.2% formic acid) was used as follows: 10% B (*v/v*) for 1 min, 10-20% B over 3 min, 20-70% B over 3 min, hold at 70% B for 3 min, return to 10% B in 1 min followed by equilibrating at 10% B for 3 min resulting in 14 min runtime for each sample.

For metabolite profiling, the mass spectrometer is equipped with an electrospray ionization (ESI) and all the analysis was performed using the Analyst 1.5.1 software. The ESI parameters such as declustering potential (DP), entrance potential (EP), collision energy (CE) and cell exit potential (CXP) were manually tuned for all the metabolites are listed in Table 2.3. All the results report the total production of aromatic amino acids in mg of total aromatic amino acid/ L media.

Table 2.3 Q1/Q3, RT and ESI parameters for detection of metabolites using mass spectrometer in negative ion mode

Metabolite	Retention time (min)	Q1	Q3	DP(V)	EP(V)	CE(V)	CXP(V)
Phe	2.76	164	147	-60	-10	-15	-6
Tyr	1.75	180	163	-102	-7	-16	-15.5
Trp	4.04	203	116	-160	-5	-20	-20
p-fluoro-Phe	3.5	182	165	-30	-12	-17	-6

2.3.8 Shikimate Pathway profiling

Two different methods, acidic and neutral were modified and used to profile the shikimate pathway that were previously developed in our lab by Robin Wheeler. Metabolites were extracted from cells and the cell extracts were divided into two parts to be analyzed by the LC-MS/MS methods. The samples for the neutral method were derivatized by equal volume addition of o-Phthaldialdehyde (OPA) reagent few minutes prior to injection.

The acidic method uses 1 mM tributylamine (TBA) and 5 mM acetic acid (pH ~ 4.6) as solvent A whereas the neutral method uses 2 mM TBA, 4 mM acetic acid and 13 mM ammonium acetate with pH adjusted to 7 using ammonium hydroxide. Both the methods use 100% methanol as solvent B. The gradient for used for the acidic method was as follows: 2% B (*v/v*) for 2 min, 2-

8% over 3 min, 8-20% B over 6 min, 20-60% B over 3 min, 60-90% B over 6 min followed by holding at 90% for 3 min and the back to 2% in 1 min followed by a 3 min hold for a total run time of 27 min. The gradient used for the neutral method was as follows: 5% B (*v/v*) for 1 min, 5-30% over 9 min, 30-80% over 5 min, 80-95% over 1 min followed by holding at 95% for 3 min and drop to 5% over 1 min followed by a 5 min hold for total run time of 25 min. The MS parameters are listed in Table 2.4.

Table 2.4 Q1/Q3, RT and ESI parameters for detection of metabolites using mass spectrometer in negative ion mode for acidic and neutral methods

Metabolite	RT(min) pH 4.6	RT(min) pH 7	Q1	Q3	DP(V)	EP(V)	CE(V)	CXP(V)
E4P	15.6	-	199	97	-215	-10	-40	-50
PEP	14.6	-	167	79	-140	-5	-30	-35
DHQ	5.9	-	189	171	-165	-5	-25	-10
DHS	7.4	-	171	127	-160	-6	-30	-10
SHK	3.5	-	173	93	-190	-3	-30	-10
ANT	13.9	-	136	92	-180	-5	-40	-25
Trp	6.1	-	203	116	-160	-5	-20	-20
PRE	-	9.8	225	181	-60	-6	-7	-50
HPP	14.1	-	179	107	-75	-12	-20	-12
PPY	16.2	-	163	91	-170	-10	-25	-25
Tyr	2	-	180	163	-140	-10	-30	-10
Phe	3.9	-	164	147	-220	-5	-35	-20
OPA-Trp	-	16	379	335	-60	-5	-20	-15
OPA-Tyr	-	15.5	356	312	-80	-10	-15	-20
OPA-Phe	-	16.5	340	192	-60	-5	-15	-20
OPA-ARO	-	16.3	402	384	-50	-5	-10	-30
CHR	-	9.3	225	163	-35	-9	-5	-8
S3P	14	-	253	97	-100	-5	-35	-20

2.3.9 Whole genome sequencing and SNP/indel analysis

Genomic DNA was extracted using a modified procedure (Englund et al., 2015). While cultures were in exponential phase, cells were pelleted and resuspended in 0.034 volumes of lysis buffer (25% sucrose in 50 mM Tris-HCl, pH 8, 10 mM disodium EDTA) and lysozyme was added to a final concentration of 2 mg/ml. Cells were then incubated at 37°C for 45 minutes. Proteinase K (0.4% v/v) and sarkosyl (1% v/v) was added to the cell lysis solution before incubation at 55°C for 30 minutes. The lysis solution was centrifuged, and DNA was extracted by chloroform-isoamyl alcohol extraction followed by extraction with equilibrated phenol and again by chloroform-isoamyl alcohol.

DNA sequencing was performed on the Illumina MiSeq platform (2x150) at the Purdue University Genomics Core Facility. The raw paired end data was trimmed using Trimmomatic (Bolger et al., 2014) to remove low quality reads and known adaptor sequences. Filtered paired end reads were then mapped to reference genomes for *Synechocystis* sp. PCC 6803 substrain GT-I as well as SYNY3 using Bowtie2 (Langmead & Salzberg, 2012). SNPs and indels were called using Genome Analysis Toolkit (GATK) UnifiedGenotyper (McKenna et al., 2010) after indel realignment. Ploidy for SNP and indel calls was set to 15 for *Synechocystis* (Zerulla et al., 2016). SNPs and indels with read depths less than 5 or greater than 200 (two times the average read depth) or quality scores lower than 20 were filtered out of the call set. Functional effects of SNPs were annotated using SnpEff (Cingolani et al., 2012).

2.3.10 Protein expression vector

The vector chosen for protein expression was pET-16b for N-terminal 6x histidine tagged protein expression induced by isopropyl-β-D-thiogalactopyranoside (IPTG). pET-16b_CM(WT) and pET-16b_CM(V52F) expression vectors were developed by cloning genes coding the CM and CM^{V52F} into pET-16b vector by GenScript, Piscataway, NJ, USA. Successful construction of the expression vectors was confirmed by both gel electrophoresis and sanger sequencing.

2.3.11 Protein expression strains and transformation

The expression host chosen for wild type and mutant chorismate mutase protein production was the *E. coli* strain BL21(DE3)pLysS [F– *ompT* $hsdS_B(r_B– \ m_B–)$ *gal dcm trxB*15::kan

(DE3)pLysS] and was obtained from Novagen, Madison, WI, USA. This strain is a high-stringency expression host which means that the strain carries the plasmid pLysS, a pET-compatible plasmid that produces T7 lysozyme which reduces the basal expression of target genes. The pLysS plasmid includes a cassette for chloramphenicol resistance. pET-16b, pET-16b_CM(WT), pET-16b_CM(V52F) expression vectors were successfully transformed into BL21(DE3)pLysS by standard heat shock transformation to develop BL21(DE3)pLysS_EV, BL21(DE3)pLysS_CM(WT) and BL21(DE3)pLysS_CM(V52F) respectively. Briefly, 50 µL of competent cells were thawed on ice for 20 mins followed by addition of 2-3 µL of 100 ng/µL of plasmid. Tubes were placed on ice for 15 mins followed by heat shock treatment by placing in a water bath at 42°C for 2 mins. Tubes were then returned to ice for 2 mins and 800 µL Luria-Bertani (LB) broth was added. Tubes were shaken at 37°C, 200 rpm for 40 mins and the transformation mixture was plated onto LB agar plate containing 25 µg/mL chloramphenicol and 100 µg/mL ampicillin and incubated overnight to isolate single colonies. Successful transformation was confirmed by PCR and gel electrophoresis.

2.3.12 Protein expression and purification

For protein expression, a modified strategy was used (Rosano & Ceccarelli, 2014). Briefly, expression strains were precultured to OD_{630} ~0.6 at 25°C in LB broth supplemented with 10% glycerol, 1% (w/v) glucose and 3% ethanol. The culture was then subjected to a cold shock treatment on ice at 4°C for 10 mins before the addition of 0.1 mM IPTG and incubated overnight at 16°C. Modifications were made after several optimizations to address leaky expression and the formation of inclusion bodies.

Following expression, cells were pelleted at 4°C and washed with cold 20 mM Tris-HCl (pH 8) with 1% lysozyme. The cell pellets were storage at -80°C until further use. Proteins were extracted using 1.5 mL B-PER complete bacterial protein extraction solution (Thermo Fisher Scientific) with 1 mM Ethylenediamine tetraacetic acid (EDTA) and 0.5% Tween 20. The soluble protein was measured using a BCA Protein Assay kit (Thermo Fisher Scientific) with bovine serum albumin (BSA) ladder and 6x His tag based protein purification was performed using HisPur Ni-NTA Spin Purification Kit (Thermo Fisher Scientific) using manufacturer's protocol. The purified protein elutes were then run on SDS gels for confirmation (Laemmli, 1970) and the concentration of the purified proteins was determined by BCA assay (Walker, 1994).

2.3.13 Chorimate mutase enzyme assay

Mutant (CM^{V52F}) and wild type CM activity was measured by modifying a previously described procedure (Kim et al., 2006; Qian et al., 2019). Briefly, activity assays were carried out in 50 µL reactions containing 20 mM Tris-HCl (pH 8), 1 mM EDTA, ten different levels of substrate upto 3 mM, and 5 ng enzyme. Pure chorismate was used as the substrate which was available in our lab previously and stored at -80°C. The reaction was started by the addition of the enzyme and incubated at 30°C for 30 mins. The reaction was terminated by the addition of 50 µL of 1 N HCl followed by incubation at 37°C for 20 mins to convert prephenate to phenylpyruvate. Finally, 150 µL of 2.5 N NaOH was added before monitoring phenylpyruvate by measuring absorbance at 320 nm. No enzyme controls were used as blanks. LC-MS/MS based confirmation was performed for products prephenate.

To test the activation or inhibition effects of aromatic amino acids on CM activity, the assay was performed as previously described with a substrate concentration of 0.5 mM and 10 ng of the enzyme. The aromatic amino acids were added to the reaction mixture at two different concentrations of 0.5 mM and 1 mM.

2.3.14 Statistical analysis

Data are presented as mean ± SE (biological replicates). Pairwise comparison and Tukey's test for multiple comparison were done using either SAS (SAS Institute) or Origin 2019b (OriginLab). A p value of <0.05 was considered statistically significant.

2.3.15 Data Availability

The raw data from the genome sequencing were deposited to GenBank and are accessible under accession numbers SAMN 12364542 (https://www.ncbi.nlm.nih.gov/) for the WT (SYNY3) and SAMN 12364543-5 for SYNY3-JV1-3 respectively. All the data are under BioProject:PRJNA556701. The sequencing data for SYNY3-JV4-6 is not yet available publicly.

2.4 Results

2.4.1 Rational engineering of wild type *Synechocystis* sp. PCC 6803 (SYNY3)

The enzymes DAHPS and AS are in general subject to feedback inhibition by phenylalanine and tryptophan respectively in cyanobacteria (Figure 2.1). To overcome the feedback regulation of the shikimate pathway by these end products, we expressed $aroG^{fbrL175D}$ and $trpE^{fbrS40F}$ from *E. coli* individually and in combination. The gene(s) were expressed after integration by homologous recombination of a plasmid with a light driven promoter as listed in Table 2.2. Both the intracellular and extracellular aromatic amino acid concentrations were measured, and the final titer was calculated for different strains (Figure 2.5). The major fraction of aromatic amino acids were obtained in the extracellular component and the contribution of the intracellular accumulation to the total was minimal (data not shown). The total titer of Phe was significantly increased in strains containing feedback resistant DAHPS (SYN3-AD2, SYN3-AD4), while Tyr was largely unaffected (Figure 2.7).

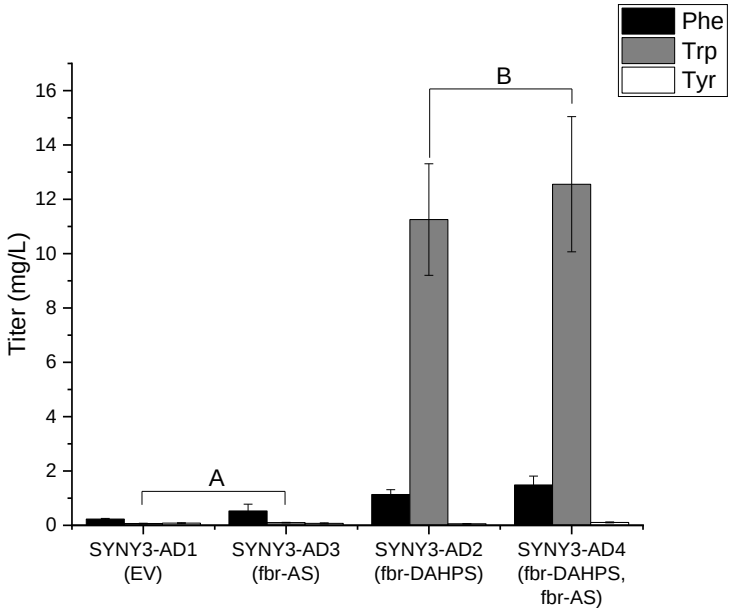

Figure 2.5 Aromatic amino acid production by rationally engineered *Synechocystis* strains after 168 hours under atmospheric CO_2, 240 µmol/m^2/s light at 30°C and 200 rpm. Error bars indicate standard error (n=3, biological replicates). Multiple comparison using Tukey's test (α=0.05) shows two distinct groups for Trp production, A and B.

The overexpression of the feedback resistant DAHPS alone and in combination with feedback resistant AS resulted in elevated tryptophan titers, however the individual overexpression of *trpE*^{fbr} (AS) showed no significant difference with respect to the empty vector control (Figure 2.5). The strain SYNY3-AD4 expressing both feedback resistant genes showed a 190 fold increase in the mean tryptophan production with a mean titer of 12.6 mg/L compared to the empty vector control. Multiple comparison was performed using the Tukey's test (α=0.05) which grouped the tryptophan production by these rationally engineered strains into two distinct groups, the higher titer value group contained a feedback resistant DAHPS. It was interesting to note that the expression of *aroG*^{fbr} resulted in greater accumulation of Trp compared to Phe. The growth rate of the engineered SYNY3 strains above mentioned (SYNY3-AD1-4) did not differ when compared to WT or empty vector controls according to Tukey's test (α=0.05) (Table 2.5). This result shows that relieving the allosteric inhibition at DAHPS is a crucial first step in aromatic amino acid overproduction and results in greater flux to the shikimate pathway.

Table 2.5 Specific growth rates of different strains at 240 µmol/m^2/s at 30°C and 200 rpm. Errors represent standard deviation of cultures in triplicates

Strain	Specific Growth Rate
SYNY3	0.069±0.002
SYNY3-AD1	0.067±0.001
SYNY3-AD2	0.072±0.004
SYNY3-AD3	0.068±0.003
SYNY3-AD4	0.069±0.003
SYNY3-JV1	0.074±0.002
SYNY3-JV4	0.072±0.005
SYNY3-AD5	0.071±0.002
SYNY3-AD6	0.074±0.002
SYNY3-AD7	0.075±0.001
SYNY3-AD8	0.075±0.004

2.4.2 Random mutagenesis of wild type *Synechocystis* sp. PCC 6803 (SYNY3)

Random mutagenesis was performed using MMS as the chemical mutagen which alters the DNA by causing mainly GC to TA or TA to GC transversions (Tillich et al., 2012). Several tryptophan and phenylalanine overproducing strains were selected using 5-fluoro-DL-tryptophan and 3-(2-thienyl)-DL-alanine as analogs respectively. Amino acid analogs are effectors that can

bind allosteric inhibition sites of enzymes in the shikimate pathway (Denenut & Demain, 1981). They also may inhibit growth by incorporating into protein resulting in lesser or non-functional proteins or by competitive inhibition of protein synthesis (Richmond, 1962). The strain SYNY3-JV1, the highest Trp producer among the randomly mutagenized strains produced 17.2 ± 1.5 mg/L of tryptophan, which is significantly higher than wild type 0.041 ± 0.003 mg/L. However, the other aromatic amino acids, Phe and Tyr were unchanged (Figure 2.6). The highest Phe producer, SYNY3-JV4 produced 35.1 ± 3.1 mg/L of Phe compared to 0.64 ± 0.17 mg/L by the wild type. Trp and Tyr titers were also significantly improved (Figure 2.6). Similar to the rationally engineered strains, a majority of the aromatic amino acid was extracellular. Interestingly, both the mutant SYNY3-JV1 and SYNY3-JV4 grew at a slightly higher rate than parent SYNY3 strain ($p < 0.05$) (Table 2.5). An additional electron sink could result in increased photosynthetic activity and growth as seen previously in *Synechocystis* sp. PCC 6803 (Grund et al., 2019). Similar observations were made with 2,3-butanediol and sucrose overproducing S. elongatus strains (Ducat et al., 2012; Oliver et al., 2013).

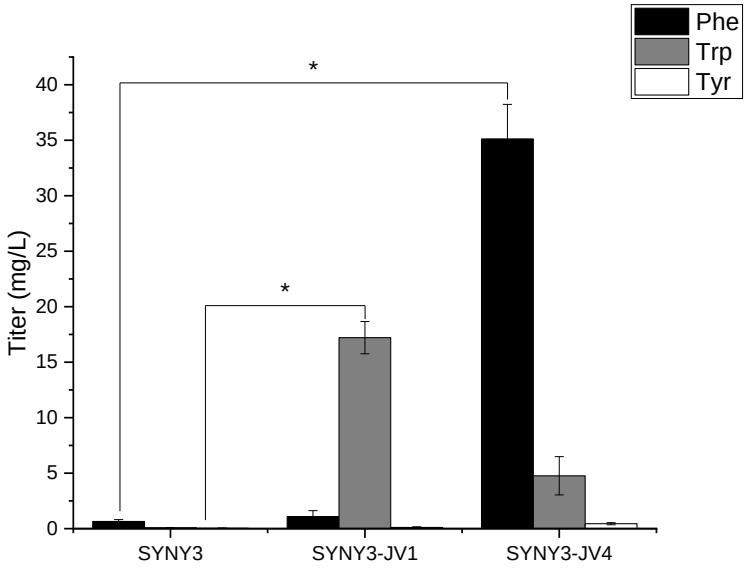

Figure 2.6 Aromatic amino acid production by randomly engineered Synechocystis strain SYNY3-JV1 and SYNY3-JV4 after 168 hours under atmospheric CO2, 240 µmol/m^2/s light at 30°C and 200 rpm. Error bars indicate standard error (n=3, biological replicates). * indicates $p<0.05$ using t-test.

To identify the mutations that led to the improved phenotype, we sequenced the genomic DNA from multiple isolated strains (SYNY3-JV1-JV6). Mutations were identified in these overproducing strains with respect to the re-sequenced SYNY3 as reference. In each case, the number of single nucleotide polymorphisms (SNPs) was less than 0.1% of the genome (3.6 Mb). SYNY3-JV1-6 showed 3189, 1718, 3000, 3653, 2096 and 1369 SNPs respectively which included missense, silent and non-sense mutations. No indels were identified in the variant calling pipeline. Because *Synechocystis* is polyploid, not all mutations observed were identified on all copies of the genome if they didn't completely segregate (Zerulla et al., 2016). Several SNPs were identified in the shikimate pathway in the overproducing strains developed however not all were fully segregated. Table 2.6 shows fully segregated mutations in the shikimate pathway while all the other mutations observed in this pathway are shown in table 2.7 (Trp overproducers) and table 2.8 (Phe overproducers).

Table 2.6 Summary of SNPs in aromatic amino acid overproducing strains developed using random mutagenesis. Note that only the fully segregated mutation are shown

	Strain	Mutation	Enzyme
Trp Overproducing	SYNY3-JV1	V52F	CM
Strains	SYNY3-JV2	F50V	CM
	SYNY3-JV3	I64N	CM
Phe Overproducing	SYNY3-JV4	V66E	DAHPS
Strains	SYNY3-JV5	L41S	DAHPS
	SYNY3-JV6	G43R	DAHPS

Table 2.7 List of SNPs observed in the shikimate pathway in randomly mutagenized Trp overproducers

Strain	Gene Product	Mutation	% Segregation
SYNY3-JV1	CM	V52F	100
	CS	V209G	35
		V210G	20
		V209G & V210G	14
	AS Subunit I	E448*	21
SYNY3-JV2	CM	F50V	100
	DAHPS	C242F	50
	Indole-3-glycerol phosphate synthase	Q45H	14.2
	AS Subunit I	D357G	18.1
	EPSP	R31M	11.1
SYNY3-JV3	CM	I64N	100
	DHQS	S322R	10.7
	Transketolase	P646T	9.5
	DAHPS	A192D	10
	AS Subunit I	S274N	6.25
	SK	L143*	6.25
	TRPS alpha chain	L149*	6.06
	TRPS beta chain	G129A	6.45
	PD	I97S	6.67
		L77R	9.67
		I97S & L77R	0.89

Table 2.8 List of SNPs observed in the shikimate pathway in randomly mutagenized Phe overproducers

Strain	Gene Product	Mutation	% Segregation
SYNY3-JV4	DAHPS	V66E	100
		I188N	9
		N238H	14
	AS Subunit I	E448*	19
		Y438H	22
		E448* & Y438H	12
SYNY3-JV5	DAHPS	L41S	100
	CS	T321P	20
	N-(5'phosphoribosyl) anthranilate isomerase	F63C	16.67
	PD	A118S	15.38
SYNY3-JV6	DAHPS	G43R	100
	PD	I155F	25
	AS Subunit I	I457V	13.33
	CS	D43E	11.7
	DHQS	V316L	25
	SK	L143*	6.25
	TRPS beta chain	V401A	14.28

All the Trp overproducing randomly mutagenized strains SYNY3-JV1, SYNY3-JV2 and SYNY3-JV3 showed fully segregated mutations in the gene *aroH* which encodes for CM. All the mutations identified were in the same region. Thus, the mutations observed likely result in a mutated CM that results in redirection of flux to the Trp branch. Surprisingly, no fully segregated mutations were observed in either DAHPS or AS in our randomly mutagenized tryptophan overproducing strains. Thus, our random mutagenesis strategy led to the identification of novel mutations in CM that lead to improved Trp accumulation. However, it is difficult to explain the overall greater flux into the shikimate pathway only as a result of a mutant CM. In order to understand this, we further mined our genome sequencing data for highly segregated mutations outside the shikimate pathway. Interestingly, we found that all the three Trp overproducing strains SYNY3-JV1-3 showed the same SNP V70G in the gene *pdhB* which codes for pyruvate dehydrogenase E1 subunit which were 85.12%, 70% and 68.42% segregated. Pyruvate dehydrogenase is responsible for conversion of pyruvate, which is derived from PEP to Acetyl-

Coenzyme A. This SNP could potentially result in greater availability of the shikimate pathway precursor PEP if it results in a less active enzyme. We could test this hypothesis by a crude PDH enzyme assay as part of the future work.

On the other hand, as expected all the Phe overproducers showed mutations to the gene coding DAHPS. This could result in mutant DAHP synthases which are resistant to feedback inhibition and thus result in greater flux into the shikimate pathway. Surprisingly, no mutations were found in *aroH*, the gene coding for CM. This result suggests that chorismate mutase in SYNY3 might not regulated by Phe.

Table 2.9 shows the other fully segregated mutations identified. Two of the three Trp overproducers sequenced, interestingly, showed mutations in the gene encoding ATP synthase subunit c (*atpH*).

Table 2.9 Fully segregated mutations in Trp overproducers identified outside the shikimate pathway

Strain	Gene	Mutation	Enzyme
SYNY3-JV1	*atpH* (ssl 2615)	L74F	ATP synthase subunit c
SYNY3-JV2	*kaiC2*	D261N	Circadian clock protein kinase like protein 2
SYNY3-JV3	*atpH*	L74F	ATP synthase subunit δ
	ndhB	Y311H	NAD(P)H-quinone oxidoreductase subunit 2
SYNY3-JV4	*ndhA*	L234P	NAD(P)H-quinone oxidoreductase subunit 1
	slr0753	P114L	Uncharacterized transporter protein
SYNY3-JV5	*Slr0825*	E604D	Serine type peptidase activity

2.4.3 CM^{V52F} mutation in the chorismate mutase redirects flux to tryptophan branch

All SYNY3 Trp overproducers developed using random mutagenesis revealed fully segregated mutations in CM. Furthermore, the mutations in all the Trp overproducers lay close to

each other (table 2.6). The *aroH* gene in *Synechocystis* sp PCC 6803 encodes a small protein of 127 amino acids (uniprot/Q55869). This is type of CM protein which belongs to type I or aroH class of CM represents a monofunctional, non-allosteric enzyme where we mapped the CM mutations (listed in table 2.6) on similar CM protein of aroH class such as *Bacillus subtillis*, which is the closest CM protein with a pdb structure available (Ladner et al., 2000), we found that the mutation resides in the substrate binding region (figure 2.7). However, neither the crystal structure nor the kinetics for CM in *Synechocystis* sp PCC 6803 is known. We hypothesized that CM mutations identified in overproducing mutants occur in CM substrate binding site and thus redirect flux to the tryptophan branch by reduction in its substrate affinity. We tested this hypothesis by analyzing the enzyme kinetics of the purified wild type and mutant CM (CM^{V52F}) proteins *in vitro*.

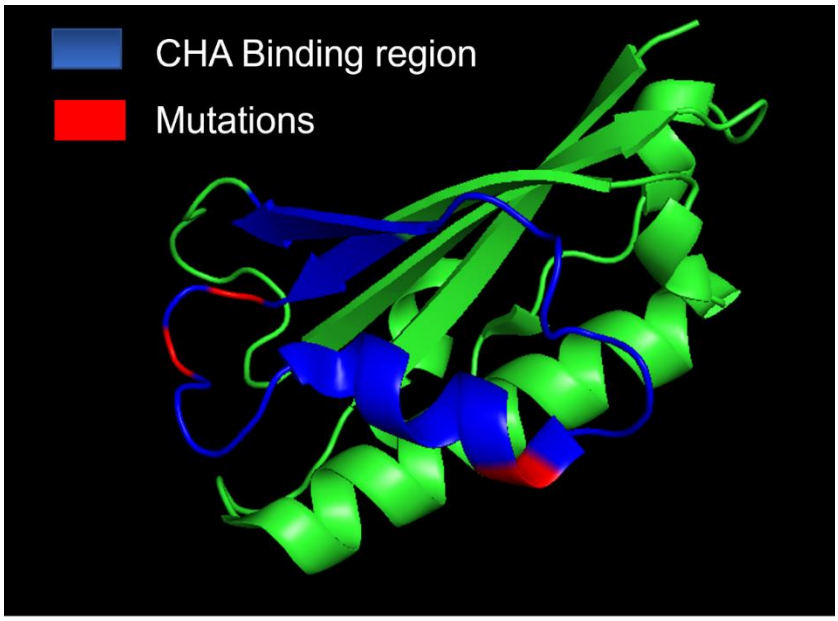

B. subtilis CM

Figure 2.7 CM mutations identified in Phe overproducing mutants (red) mapped onto the B. subtillis CM structure (Ladner et al., 2000). The blue region denotes the substrate (chorismate) binding region

First, we expressed and purified the wild type CM and mutant CM^{V52F} (figure 2.8A) and performed enzyme activity assays (figure 2.8B) with varying substrate concentration as outlined in the methods section.

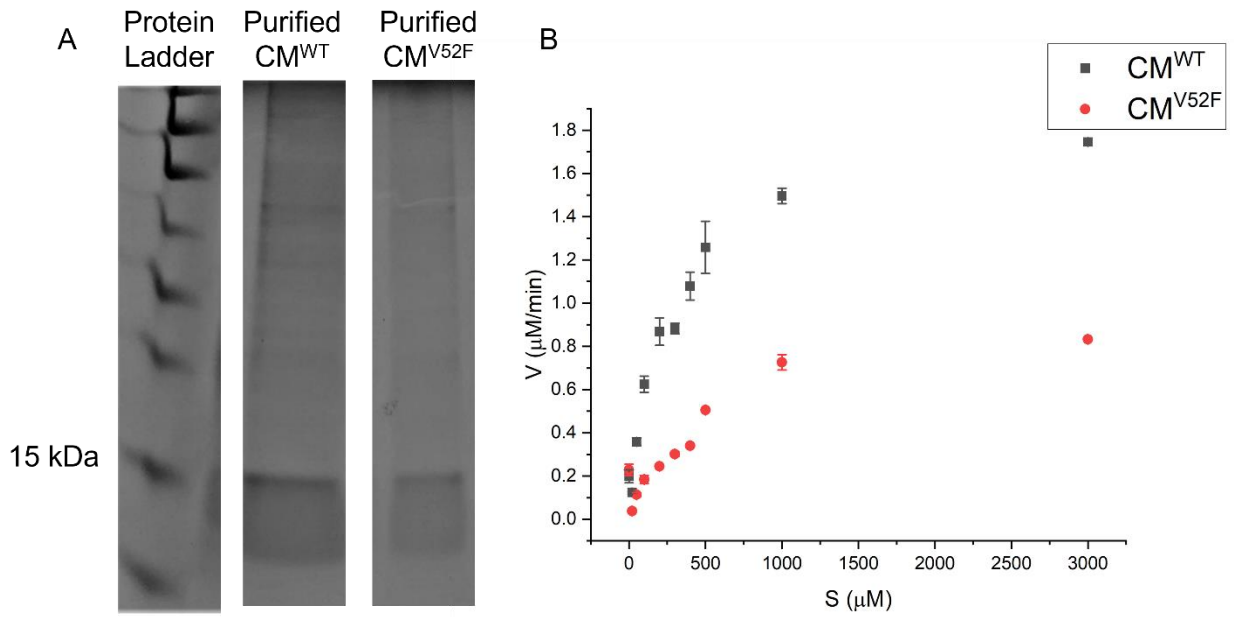

Figure 2.8 (A) SDS page gel showing WT and mutant CM enzymes post purification on Ni-NTA spin columns (B) Plot of enzyme rate and substrate concentration for CM^{WT} and CM^{V52F}

Kinetic parameters listed in table 2.10 were derived from the Lineweaver-Burk plots (data not shown). As expected, we found a 2.3-fold increase in the K_m in the mutant. Since K_m represents the concentration of substrate at which the enzyme can operate at half of the V_{max}, our results support our hypothesis that the mutation V52F affects substrate binding and thus has a reduced chorismate affinity compared to the WT. However, to our surprise, we also observed a reduction the maximum rate (V_{max}) of the mutant enzyme.

Table 2.10 Kinetic parameters of CM^{WT} and CM^{V52F} enzymes from *Synechocystis* PCC 6803

Kinetic parameter	CM^{WT}	CM^{V52F}
V_{max} (µmol/min/mg)	38.5±1.1	20.4±0.8
K_m (µM)	263.8±20.3	610.0±40.1
K_{cat} (1/s)	9.23±1	4.9±0.5
K_{cat}/K_m	34987±453	8022±1014

Since the native protein is predicted to be non-allosteric, we hypothesize that the activity of neither the wild type nor the mutant enzyme will be affected by the end products of the shikimate pathway. Our data shows that the presence of Trp, Phe, or Trp does not have a significant effect on the activity of the CM enzyme (figure 2.9).

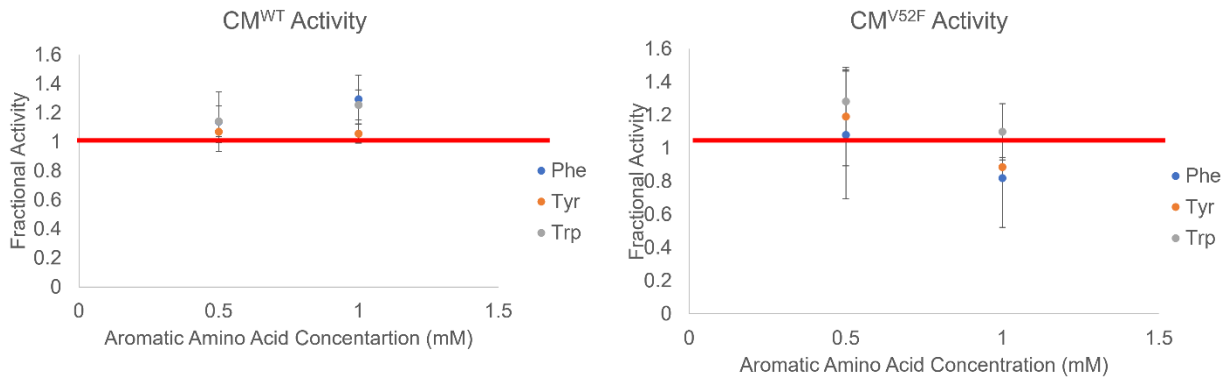

Figure 2.9 Effect of aromatic amino acids on enzymatic activity of CM^{WT} and CM^{V52F}

2.4.4 Combining random and rational approaches for tryptophan overproduction

The randomly mutagenized strain with highest tryptophan titer, SYNY3-JV1, was chosen for further rational metabolic engineering. The feedback resistant enzyme coding genes *aroG*^{fbr} (DAHPS) and *trpE*^{fbr} (AS) were overexpressed both individually and in combination to determine the effect on tryptophan production with the pEERM derived plasmids used earlier in the study (Table 2.2). All the newly engineered strains (SYNY3-AD5-8) grew equally well compared to SYNY3-JV1 (Table 2.5).

These strains (SYNY3-AD6-8) performed better than the empty vector control in best Trp producer obtained from random mutagenesis (SYNY3-AD5), as well as the wild type strain overexpressing both *aroG*^{fbr} and *trpE*^{fbr} (SYNY3-AD4) (Figure 2.10). The best strain SYNY3-AD8 containing both feedback resistant DAHPS and AS produced 46.1 mg/L of tryptophan which is ~2.5 fold of the SYNY3-AD5 (Figure 2.10) and ~3.5 fold the wild type overexpressing *aroG*^{fbr} and *trpE*^{fbr} (SYNY3-AD4). This result shows that a combination of random mutagenesis and rational engineering is superior to either approach alone. We analysed the other aromatic amino acids, Phe and Tyr, produced by SYNY3-AD4-8 and found that Phe and Tyr were not changed (data not shown).

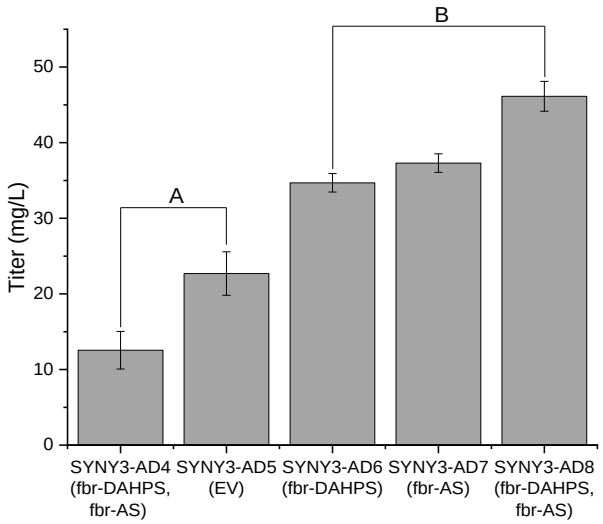

Figure 2.10 Trp production by a combination of randomly mutagenized and rationally engineered *Synechocystis* strains after 168 hours under atmospheric CO_2, 240 µmol photons/m^2/s light at 30°C and 200 rpm. Error bars indicate standard error (n=3). Multiple comparison using Tukey's test (α=0.05) showed two distinct groups A and B for Trp production.

The best Trp overproducer developed using a combination of random and rational approaches, SYNY3-AD8 was then chosen to be cultivated in enhanced conditions. Cultures were inoculated with a starting OD ~0.2 and grown photoautotrophically for 10 days in an incubator at 3% (v/v) CO_2 and 30° under 240 µE (µmol photons/m^2/s) light. The elevated CO_2 levels coupled with higher staring density and growth time led to Trp titer of 211.6±23.2 mg/L. The Phe and Tyr titers were 18.6±1.5 mg/L and 6.7±2.2 mg/L respectively. The growth under enhanced CO_2 is shown in figure 2.11.

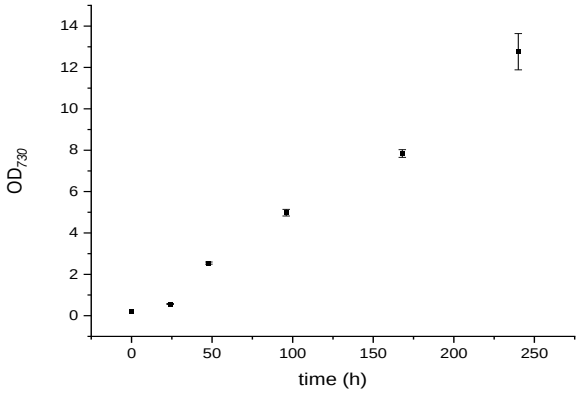

Figure 2.11 Growth curve of SYNY3-AD8 grown under 3% (v/v) CO_2, 240 µmol/m^2/s light at 30°C and 200 rpm. The cultures were inoculated at OD ~0.2. Error bars indicate standard error (n=3).

2.4.5 Shikimate feeding coupled with metabolite profiling to identify other pathway bottlenecks

Shikimate is an intermediate which can be uptaken by cyanobacteria. Shikimate feeding coupled with metabolite profiling could be used to identify if further bottlenecks in the pathway lie upstream or downstream of shikimate. Cultures (SYNY3, SYNY3-JV1 and SYNY3-JV4) were fed shikimate (final concentration 29 mM in media) 2 days after inoculation at OD~0.05. Samples were extracted 2 days after introduction of shikimate to investigate intracellular metabolite profiles and the media was tested to quantify aromatic amino acid titers. It was found that the shikimate was successfully uptaken by all the three strains (Figure 2.12a). However, there were no changes in the total aromatic amino acid production after feeding shikimate in SYNY3-JV1 and SYNY3-JV4 whereas SYNY3 showed elevated levels of Trp (Figure 2.12b and 2.12c). This result suggests that there are further bottlenecks in the randomly engineered strains downstream of shikimate (SYNY3-JV1 and SYNY3-JV4). SYNY3 showed elevated Trp titers which indicates that a bottleneck upstream of shikimate in the wild type is relieved. This result is also in agreement with the elevated Trp titers seen in SYNY3-AD2 where expression of feedback resistant DAHPS resulted in elevated Trp titers. These results indicate that increased flux to chorismate is redirected to the Trp branch. In case of SYNY3-JV1 and SYNY3-JV4, the shikimate uptaken did not result in accumulation of pathway intermediates downstream of shikimate (Figure 2.12d). This could be due to a potential bottleneck enzyme shikimate kinase which is responsible for the conversion of

shikimate to S3P which prevents the uptaken shikimate to be successfully converted to the aromatic amino acid end products. It is unclear if the *Synechocystis* sp. PCC 6803 shikimate kinase is allosterically regulated and this would have to be tested in the future. It might be possible to overcome this limitation by expression of genes from other organisms such as *E. coli* and this should be tested in the future.

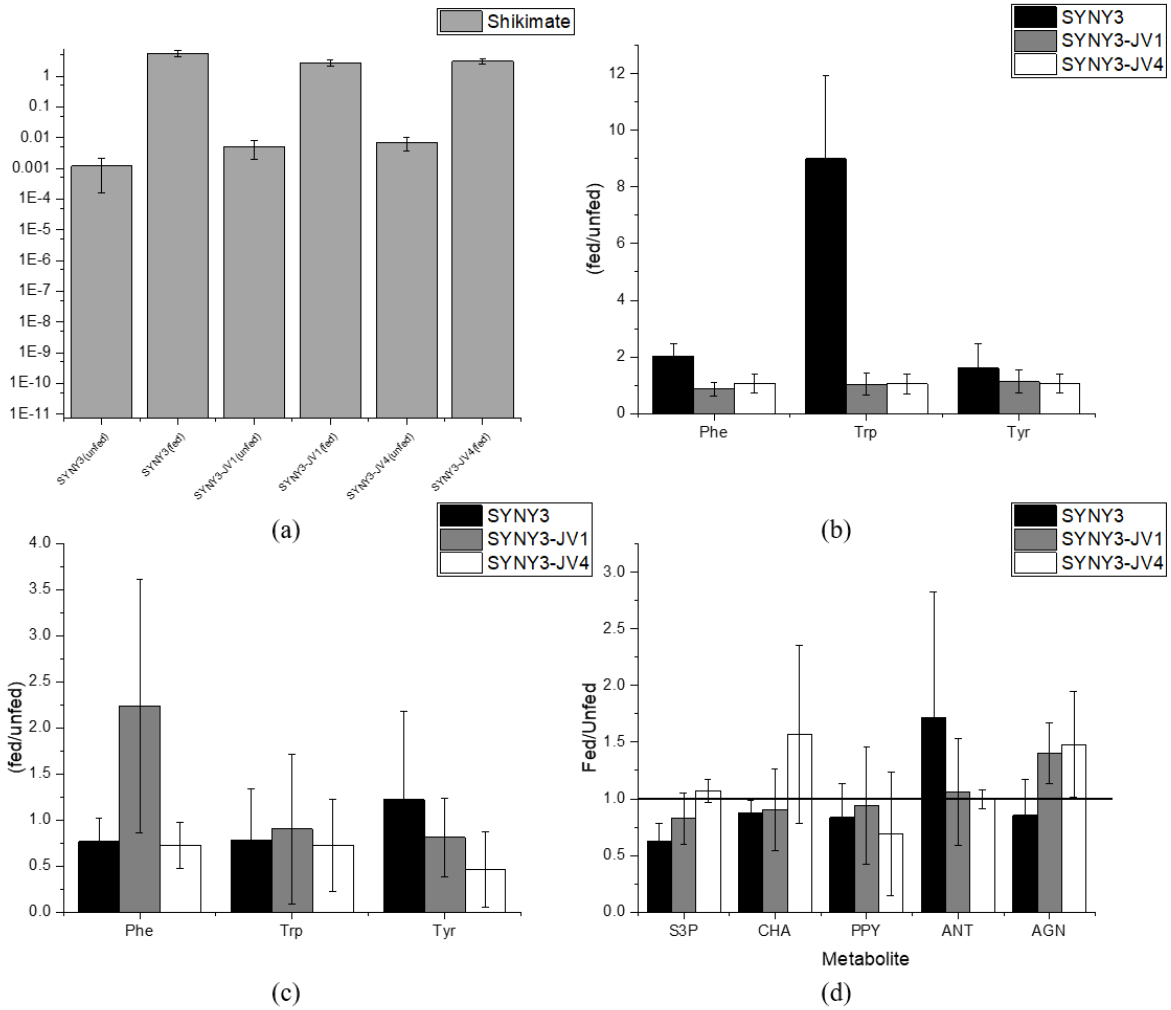

Figure 2.12 (a) Intracellular shikimate concentration in SYNY3 strains. (b) Ratio of intracellular aromatic amino acid concentration in SYNY3 strains fed and not fed shikimate. (c) Ratio of extracellular aromatic amino acid concentration in SYNY3 strains fed and not fed shikimate. (d) Ratio of intracellular shikimate pathway metabolite concentrations in SYNY3 strains fed and not fed shikimate

2.4.6 N depletion as a tool to alter flux splits in the shikimate pathway

In order to understand how nutrient depletion could be potentially used to produce aromatic amino acids and their derivatives, N depletion was tested. Previously it had been shown that N depletion in *E. coli* and *S. cerevisiae* resulted in drastic reduction in glutamine levels while glutamate levels were not altered significantly (Brauer et al., 2006). This could be utilised to divert flux from the Trp branch to the Phe/Tyr branch since Trp uses glutamine as the amine donor whereas Phe and Tyr use glutamate. In order to test this, SYNY3 and SYNY3-AD8 were grown in 3% (v/v) CO_2 in regular BG-11 media for 5 days. Cells were then pelleted by centrifugation and resuspended in media with either with BG-11 in the control group (no N depletion) or with BG-11 without sodium nitrate in the N depletion group. The cultures were then incubated for 2 days after which metabolites were extracted as described previously. Figure 2.13 shows the fold change in shikimate pathway metabolites post N depletion. It was seen that several intermediate pools decreased such as SHK, ANT, PPA and S3P whereas there was an increase in PPY in SYNY3-AD8. Phe levels increased modestly whereas Tyr levels showed a drastic increase. Trp, which uses glutamine as the amine donor saw a drastic fall especially in the Trp overproducer SYNY3-AD8 with flux possibly redirected diverted Tyr. Similar changes in aromatic amino acid levels were observed by Brauer et al. during N depletion in *E. coli* and *S. cerevisiae* (Brauer et al., 2006).

This result shows that N depletion post exponential cell growth can be a useful approach to divert flux at the chorismate branch point and towards Phe/Tyr which can be particularly useful for overproduction of phenylpyruvate, Phe, Tyr as well as their derivatives such as 2-phenylethanol.

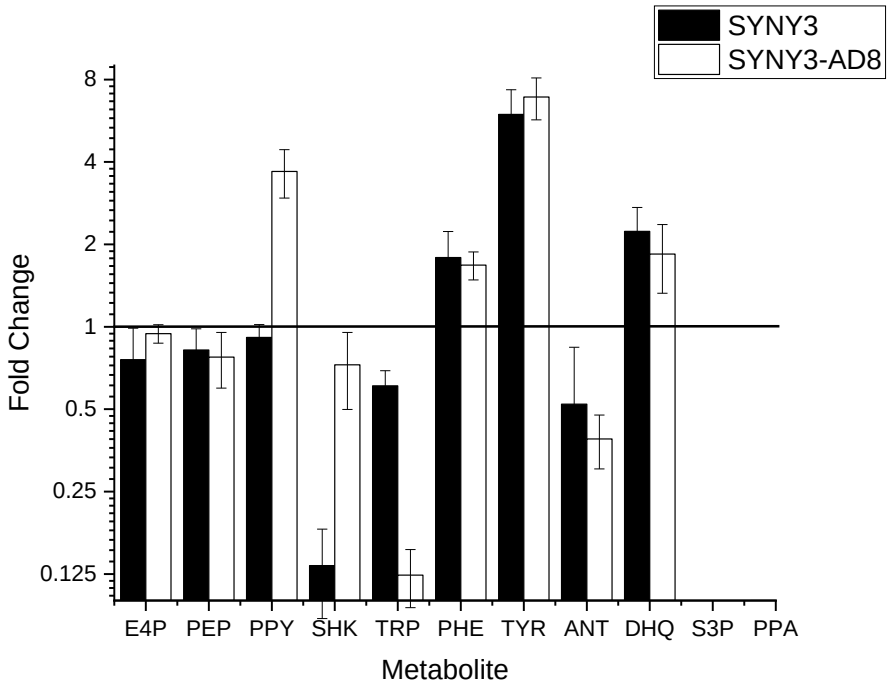

Figure 2.13 Fold change in shikimate pathway metabolites 2 days post N depletion. Error bars indicate SEM (n=3). S3P and PPA were not detectable in the case of N depletion.

2.5 Discussion

This study shows that the combination of random mutagenesis and rational engineering is superior to either of the approaches alone for the biosynthesis of tryptophan. Our results show that alleviating feedback inhibition by the end products is a crucial first step in the overproduction of aromatic amino acids, consistent with previous work (Ikeda, 2006). In this work, we found that overexpressing fbr-DAHPS can significantly increase the overall flux to the shikimate pathway by alleviating feedback inhibition at DAHPS (Figure 2.5). This is consistent with the work done in other organisms such as *E. coli* where genes coding feedback resistant DAHPS and AS are overexpressed to engineer Trp overproducing strains (Bongaerts et al., 2001; Ikeda, 2006). Recent studies have also shown to successfully increase the flux to the shikimate pathway to improve Phe accumulation by transgenic expression of $aroG^{fbr}$ and $pheA^{fbr}/tyrA^{fbr}$ from *E. coli* in *Synechococcus elongatus* (Ni et al., 2018) and *Synechocystis* sp. PCC 6803 (Brey et al., 2020).

Random mutagenesis coupled with amino acid analog selection has been previously shown to be successful in selecting amino acid overproducing mutants (Hall et al., 1982, 1983; Hall & Jensen, 1980). *Synechocystis* sp. PCC 6803 typically contains multiple copies of its genome

depending on the phase of growth (Zerulla et al., 2016) and thus selecting mutants requires multiple rounds of re-streaking under selection. The independently obtained strains from random mutagenesis, SYNY3-JV1, SYNY3-JV2 and SYNY3-JV3, all had fully segregated mutations in *aroH* which codes for CM and all had increased production of Trp. The mutations observed (Table 2.6) have lowered the activity of CM thereby redirecting flux to the tryptophan biosynthesis branch. This was also observed in Phe and Tyr bradytrophs in *Anabaena* sp PCC 7119 (Hall et. al, 1981). However, although the flux split was altered, the flux towards Phe and Tyr was not altered significantly. All the three strains showed mutations in the region of CM between amino acids 50 and 64. *Synechocystis* sp. PCC 6803 has a single CM enzyme that belongs to the type I or aroH class (Chook et al., 1993). This is a monofunctional CM protein similar to *Bacillus subtilis* CM that is a non-allosteric homotrimeric enzyme (Chook et al., 1993) and for which a crystal structure is available (Ladner et al., 2000). We mapped the mutations listed in CM mutations listed in table 2.6 onto the crystal structure of the CM protein in *Bacillus subtilis* [http://dx.doi.org/10.2210/pdb1DBF/pdb] and found that all the mutations lie in the chorismate binding site. This potentially means that the mutant CM has its activity reduced due to reduced binding of chorismate. We tested this and confirmed that the V52F mutation in the CM enzyme leads to reduced affinity for chorismate. This is similar to the results in *B. subtillis* where mutations in the chorismate binding region at position 51 reduced affinity to substrate (Kim et al., 2006). Thus, it is possible that larger chorismate pools are available to be used by the competing enzyme AS. Moreover, this could be the reason why overexpression of $trpE^{fbr}$ only increases Trp accumulation in the background with our CM mutation. Future work will aim to express and purify the WT and mutant CM proteins which will then be tested *in vitro* to see if the mutant CM shows reduced activity compared to the WT. However, it is interesting that the randomly mutagenized strain did not possess a fbr-DAHPS but showed greater flux into the shikimate pathway as seen by elevated Trp titers which cannot be attributed to mutant CM. We think that the highly segregated (85.12%) V70G SNP in pdhB might result in greater PEP availability by reducing the enzyme activity.

Our work also shows the importance of sequencing the genome of randomly mutagenized strains to avoid redundant targeting of the same genes. Since fully segregated mutations to genes coding feedback sensitive DAHPS and AS were not observed in the genome sequence of SYNY3-JV1, SYNY3-JV2 and SYNY3-JV3, we chose to overexpress feedback resistant DAHPS and AS

from *E. coli*. Overexpression of feedback resistant DAHPS improved tryptophan titers which shows that the total flux into the pathway is a limiting factor in SYNY3-JV1. Overexpression of feedback resistant AS too improved the tryptophan titers indicating that relieving the feedback inhibition at AS is also crucial. The overexpression of feedback resistant forms of DAHPS and AS complement the mutated CM that likely redirects flux to the Trp branch by possibly lowering its affinity for chorismate.

We report Trp titer and productivity of 212±23 mg/L and 0.88±0.09 mg/L.h that is the highest reported in a photoautotrophic system to the best of our knowledge. This is smaller compared to productivities of heterotrophic systems with reported titers up to 1.85 g/L (shake-flask, 38.5 mg/L.h), 50 mg/L (shake flask, 2 mg/L.h) and 50 g/L (fed-batch, 0.625 g/L.h) in *E. coli* (Liu et al., 2016), *S. cerevisiae* (Prasad et al., 1987) and *C. glutamicum* (Ikeda & Katsumata, 1999) respectively. However, heterotrophic systems suffer from low sugar yields, typically less than 20-25% (Ikeda & Katsumata, 1999; Liu et al., 2016; Prasad et al., 1987) whereas photoautotrophs can be grown on CO_2 and light which are readily available.

In order to further develop cyanobacteria for aromatic amino acid production, significant enhancements of yield and productivity are needed. After removing the allosteric feedback inhibitions, improving the flux requires identifying rate-limitations. One strategy to overcome the rate limiting enzymes employed combinatorial overexpression of all the shikimate pathway enzymes which successfully led to greater titers of aromatic amino acids in *E. coli* and *S. cerevisiae*, respectively (Lütke-Eversloh & Stephanopoulos, 2008; Rodriguez et al., 2015). Targets that have shown success in other organisms are primary metabolism enzymes that provide the precursors of the shikimate pathway (Draths et al., 1992). Transketolase, which catalyzes the formation erythrose-4-phoshate (E4P), was shown to be a limiting factor for synthesis of DAHP in *E. coli* with a feedback resistant DAHP synthase (Draths et al., 1992). Transketolase may additionally improve carbon fixation, further increasing aromatic amino acid production, because of its central position in the Calvin cycle (Liang & Lindblad, 2016; Yu King Hing et al., 2019). Interestingly, we observed one partially segregated mutation in transketolase (tkt) in SYNY3-JV1, but the effect due to this mutation has not been examined in separate experiments.

Strain improvement could continue by using other means of mutagenesis such as UV irradiation or chemical mutagens that explore other types of nucleotide conversions (Packer & Liu, 2015). Taking advantage of reduced costs for genome sequencing allows one to learn from strains

selected for improved production of metabolite after random mutagenesis. As shown in this work, combining traits from randomly mutated strains with rational engineering targets has the potential to significantly outperform results from either approach alone.

2.6 Acknowledgements

This work was supported by the U.S. Department of Energy (DE-SC0008628). We declare no conflicts of interest. I would like to acknowledge Jeremiah Vue, an alumnus of our lab for laying the groundwork for much of this work and providing me the background to get started with this study. I would also like to mention Robin Wheeler whose LC-MS/MS methods I have modified for use in this study for profiling the shikimate pathway metabolites. I also would like to thank Anna Pretschner, a visiting student in our lab who performed several preliminary studies on optimizing the protein expression conditions which proved to be a great help to me in determining the final expression conditions. I would also like to thank both the Liu lab and the Dudareva lab that provided me with the protein gel electrophoresis cell for my experiments.

I would like to acknowledge Applied and Environmental Microbiology for publishing parts of this work and granting the authors the right to use the material with proper credit given. Parts of this chapter are included in the publication “Deshpande A, Vue J, Morgan J. 2020. Combining random mutagenesis and metabolic engineering for enhanced tryptophan production in *Synechocystis* sp. strain PCC 6803. Appl Environ Microbiol 86:e02816-19. https://doi.org/10.1128/AEM .02816-19.”. The copyright to some of this work are: "Copyright © American Society for Microbiology, Applied and Environmental Microbiology. 86:e02816-19. https://doi.org/10.1128/AEM .02816-19".

2.7 References

Bolger, A. M., Lohse, M., & Usadel, B. (2014). Trimmomatic: A flexible trimmer for Illumina sequence data. *Bioinformatics*, *30*(15), 2114–2120. https://doi.org/10.1093/bioinformatics/btu170

Bongaerts, J., Krämer, M., Müller, U., Raeven, L., & Wubbolts, M. (2001). Metabolic engineering for microbial production of aromatic amino acids and derived compounds. In *Metabolic Engineering* (Vol. 3, Issue 4, pp. 289–300). Academic Press Inc. https://doi.org/10.1006/mben.2001.0196

Bose, J. L. (2016). Chemical and UV Mutagenesis. In J. L. Bose (Ed.), *The Genetic Manipulation of Staphylococci: Methods and Protocols* (pp. 111–115). Springer New York. https://doi.org/10.1007/7651_2014_190

Brauer, M. J., Yuan, J., Bennett, B. D., Lu, W., Kimball, E., Botstein, D., & Rabinowitz, J. D. (2006). *Conservation of the metabolomic response to starvation across two divergent microbes*. www.pnas.org/cgi/content/full/

Brey, L. F., Włodarczyk, A. J., Bang Thøfner, J. F., Burow, M., Crocoll, C., Nielsen, I., Zygadlo Nielsen, A. J., & Jensen, P. E. (2020). Metabolic engineering of Synechocystis sp. PCC 6803 for the production of aromatic amino acids and derived phenylpropanoids. *Metabolic Engineering*, *57*, 129–139. https://doi.org/10.1016/j.ymben.2019.11.002

Chook, Y. M., Ket, H., & Lipscomb, W. N. (1993). Crystal structures of the monofunctional chorismate mutase from BaciUus subtilis and its complex with a transition state analog (x-ray crystaflography/shil imate pathway/daisen gement). In *Proc. Natl. Acad. Sci. USA* (Vol. 90).

Cingolani, P., Platts, A., Wang, L. L., Coon, M., Nguyen, T., Wang, L., Land, S. J., Lu, X., & Ruden, D. M. (2012). A program for annotating and predicting the effects of single nucleotide polymorphisms, SnpEff: SNPs in the genome of Drosophila melanogaster strain w1118; iso-2; iso-3. *Fly*, *6*(2), 80–92. https://doi.org/10.4161/fly.19695

Denenut, E. 0, & Demain, A. L. (1981). Enzymatic Basis for Overproduction of Tryptophan and Its Metabolites in Hansenula polymorpha Mutants. *Applied and Environmental Microbiology*. https://journals.asm.org/journal/aem

Draths, K. M., Pompliano, D. L., Conley, D. L., Frost, J. W., Berry, A., Disbrow, G. L., Staversky, R. J., & Lievense, J. C. (1992). Biocatalytic synthesis of aromatics from D-glucose: the role of transketolase. *Journal of the American Chemical Society*, *114*(10), 3956–3962. https://doi.org/10.1021/ja00036a050

Ducat, D. C., Avelar-Rivas, J. A., Way, J. C., & Silvera, P. A. (2012). Rerouting carbon flux to enhance photosynthetic productivity. *Applied and Environmental Microbiology*, *78*(8), 2660–2668. https://doi.org/10.1128/AEM.07901-11

Englund, E., Andersen-Ranberg, J., Miao, R., Hamberger, B., & Lindberg, P. (2015). Metabolic Engineering of Synechocystis sp. PCC 6803 for Production of the Plant Diterpenoid Manoyl Oxide. *ACS Synthetic Biology*, *4*(12), 1270–1278. https://doi.org/10.1021/acssynbio.5b00070

Grund, M., Jakob, T., Wilhelm, C., Bühler, B., & Schmid, A. (2019). Electron balancing under different sink conditions reveals positive effects on photon efficiency and metabolic activity of Synechocystis sp. PCC 6803. *Biotechnology for Biofuels*, *12*(1). https://doi.org/10.1186/s13068-019-1378-y

Hall, G., Flick, M., Gherna, R., & Jensen, R. (1982). Biochemical diversity for biosynthesis of aromatic amino acids among the cyanobacteria. *Journal Of Bacteriology*, *149*(1), 65-78. doi: 10.1128/jb.149.1.65-78.1982

Hall, G., Flick, M., & Jensen, R. (1983). Regulation of the aromatic pathway in the cyanobacterium Synechococcus sp. strain Pcc6301 (Anacystis nidulans). *Journal Of Bacteriology*, *153*(1), 423-428. doi: 10.1128/jb.153.1.423-428.1983

Hall, G., & Jensen, R. (1980). Enzymological Basis for Growth Inhibition by l -Phenylalanine in the Cyanobacterium Synechocystis sp. 29108. *Journal Of Bacteriology*, *144*(3), 1034-1042. doi: 10.1128/jb.144.3.1034-1042.1980

Hall, G.C., Jensen, R.A. Isolation of cyanobacterial auxotrophs by direct selection of regulatory-mutant phenotypes. *Current Microbiology* **6,** 189–194 (1981). https://doi.org/10.1007/BF01642397

Hu, C., Jiang, P., Xu, J., Wu, Y., & Huang, W. (2003). Mutation analysis of the feedback inhibition site of phenylalanine- sensitive 3-deoxy-D-arabino-heptulosonate 7-phosphate synthase of Escherichia coli. *Journal of Basic Microbiology*, *43*(5), 399–406. https://doi.org/10.1002/jobm.200310244

Ikeda, M. (2006). Towards bacterial strains overproducing L-tryptophan and other aromatics by metabolic engineering. In *Applied Microbiology and Biotechnology* (Vol. 69, Issue 6, pp. 615–626). https://doi.org/10.1007/s00253-005-0252-y

Ikeda, M., & Katsumata, R. (1999). Hyperproduction of Tryptophan by Corynebacterium glutamicum with the Modified Pentose Phosphate Pathway. *Applied and Environmental Microbiology* (Vol. 65, Issue 6). https://journals.asm.org/journal/aem

Kim, S. K., Reddy, S. K., Nelson, B. C., Vasquez, G. B., Davis, A., Howard, A. J., Patterson, S., Gilliland, G. L., Ladner, J. E., & Reddy, P. T. (2006). Biochemical and structural characterization of the secreted chorismate mutase (Rv1885c) from Mycobacterium tuberculosis H37Rv: An *AroQ enzyme not regulated by the aromatic amino acids. *Journal of Bacteriology*, *188*(24), 8638–8648. https://doi.org/10.1128/JB.00441-06

Ladner, J. E., Reddy, P., Davis, A., Tordova, M., Howard, A. J., & Gilliland, G. L. (2000). Biological Crystallography The 1.30 A Ê resolution structure of the Bacillus subtilis chorismate mutase catalytic homotrimer. *Acta Cryst*.

Laemmli, U. K. (1970). Cleavage of Structural Proteins during the Assembly of the Head of Bacteriophage T4. *Nature*, *227*(5259), 680–685. https://doi.org/10.1038/227680a0

Langmead, B., & Salzberg, S. L. (2012). Fast gapped-read alignment with Bowtie 2. *Nature Methods*, *9*(4), 357–359. https://doi.org/10.1038/nmeth.1923

Leuchtenberger, W., Huthmacher, K., & Drauz, K. (2005). Biotechnological production of amino acids and derivatives: Current status and prospects. In *Applied Microbiology and Biotechnology* (Vol. 69, Issue 1, pp. 1–8). https://doi.org/10.1007/s00253-005-0155-y

Liang, F., & Lindblad, P. (2016). Effects of overexpressing photosynthetic carbon flux control enzymes in the cyanobacterium Synechocystis PCC 6803. *Metabolic Engineering*, *38*, 56–64. https://doi.org/10.1016/j.ymben.2016.06.005

Liu, L., Duan, X., & Wu, J. (2016). Modulating the direction of carbon flow in Escherichia coli to improve l-tryptophan production by inactivating the global regulator FruR. *Journal of Biotechnology*, *231*, 141–148. https://doi.org/10.1016/j.jbiotec.2016.06.008

Lütke-Eversloh, T., & Stephanopoulos, G. (2008). Combinatorial pathway analysis for improved L-tyrosine production in Escherichia coli: Identification of enzymatic bottlenecks by systematic gene overexpression. *Metabolic Engineering*, *10*(2), 69–77. https://doi.org/10.1016/j.ymben.2007.12.001

McKenna, A., Hanna, M., Banks, E., Sivachenko, A., Cibulskis, K., Kernytsky, A., Garimella, K., Altshuler, D., Gabriel, S., Daly, M., & DePristo, M. A. (2010). The genome analysis toolkit: A MapReduce framework for analyzing next-generation DNA sequencing data. *Genome Research*, *20*(9), 1297–1303. https://doi.org/10.1101/gr.107524.110

Nelms, J., Edwards, R. M., Warwick, J., & Fotheringhaml, I. (1992). Novel Mutations in the pheA Gene of Eschenichia coli K-12 Which Result in Highly Feedback Inhibition-Resistant Variants of Chorismate Mutase/Prephenate Dehydratase. *Applied and Environmental Microbiology* (Vol. 58, Issue 8). https://journals.asm.org/journal/aem

Ni, J., Liu, H., Tao, F., Wu, Y., & Xu, P. (2018). Remodeling of the Photosynthetic Chain Promotes Direct CO 2 Conversion into Valuable Aromatic Compounds . *Angewandte Chemie*, *130*(49), 16222–16226. https://doi.org/10.1002/ange.201808402

Oliver, J. W. K., Machado, I. M. P., Yoneda, H., & Atsumi, S. (2013). Cyanobacterial conversion of carbon dioxide to 2,3-butanediol. *Proceedings of the National Academy of Sciences of the United States of America*, *110*(4), 1249–1254. https://doi.org/10.1073/pnas.1213024110

Packer, M. S., & Liu, D. R. (2015). Methods for the directed evolution of proteins. In *Nature Reviews Genetics* (Vol. 16, Issue 7, pp. 379–394). Nature Publishing Group. https://doi.org/10.1038/nrg3927

Prasad, R., Niederberger, P., & Hütter, R. (1987). Tryptophan accumulation in Saccharomyces cerevisiae under the influence of an artificial yeast TRP gene cluster. *Yeast*, *3*(2), 95–105. https://doi.org/https://doi.org/10.1002/yea.320030206

Qian, Y., Lynch, J. H., Guo, L., Rhodes, D., Morgan, J. A., & Dudareva, N. (2019). Completion of the cytosolic post-chorismate phenylalanine biosynthetic pathway in plants. *Nature Communications*, *10*(1). https://doi.org/10.1038/s41467-018-07969-2

Ramos, I., & Downs, D. M. (2003). Anthranilate synthase can generate sufficient phosphoribosyl amine for thiamine synthesis in Salmonella enterica. *Journal of Bacteriology*, *185*(17), 5125–5132. https://doi.org/10.1128/JB.185.17.5125-5132.2003

Rao, N. S., Shakila, T. M., & Bagchi, S. N. (1995). De-regulated assimilation and over-production of amino acids in analogue-resistant mutants of a cyanobacterium, Phormidium uncinatum. *World Journal of Microbiology & Biotechnology* (Vol. 11).

Riccardi, G., de Rossi, E., & Milano, A. (1989). Amino acid biosynthesis and its regulation in cyanobacteria. *Plant Science*, *64*(2), 135-151. doi: 10.1016/0168-9452(89)90018-6

Richmond M. H. (1962). The effect of amino acid analogues on growth and protein synthesis in microorganisms. *Bacteriological reviews*, *26*(4), 398–420. https://doi.org/10.1128/br.26.4.398-420.1962

Rippka, R., Stanier, R., Deruelles, J., Herdman, M., & Waterbury, J. (1979). Generic Assignments, Strain Histories and Properties of Pure Cultures of Cyanobacteria. *Microbiology*, *111*(1), 1-61. doi: 10.1099/00221287-111-1-1

Rodriguez, A., Kildegaard, K. R., Li, M., Borodina, I., & Nielsen, J. (2015). Establishment of a yeast platform strain for production of p-coumaric acid through metabolic engineering of aromatic amino acid biosynthesis. *Metabolic Engineering*, *31*, 181?188-188. https://doi.org/10.1016/j.ymben.2015.08.003

Rosano, G. L., & Ceccarelli, E. A. (2014). Recombinant protein expression in Escherichia coli: Advances and challenges. In *Frontiers in Microbiology* (Vol. 5, Issue APR). Frontiers Research Foundation. https://doi.org/10.3389/fmicb.2014.00172

Song, J., Bonner, C. A., Wolinsky, M., & Jensen, R. A. (2005). The TyrA family of aromatic-pathway dehydrogenases in phylogenetic context. *BMC Biology*, *3*. https://doi.org/10.1186/1741-7007-3-13

Sprenger, G. A. (2007). From scratch to value: Engineering Escherichia coli wild type cells to the production of L-phenylalanine and other fine chemicals derived from chorismate. In *Applied Microbiology and Biotechnology* (Vol. 75, Issue 4, pp. 739–749). https://doi.org/10.1007/s00253-007-0931-y

Tillich, U. M., Lehmann, S., Schulze, K., Dühring, U., & Frohme, M. (2012). The Optimal Mutagen Dosage to Induce Point-Mutations in Synechocystis sp. PCC6803 and Its Application to Promote Temperature Tolerance. *PLoS ONE*, *7*(11). https://doi.org/10.1371/journal.pone.0049467

Walker, J. M. (1994). The Bicinchoninic Acid (BCA) Assay for Protein Quantitation. In J. M. Walker (Ed.), *Basic Protein and Peptide Protocols* (pp. 5–8). Humana Press. https://doi.org/10.1385/0-89603-268-X:5

Yu King Hing, N., Liang, F., Lindblad, P., & Morgan, J. A. (2019). Combining isotopically non-stationary metabolic flux analysis with proteomics to unravel the regulation of the Calvin-Benson-Bassham cycle in Synechocystis sp. PCC 6803. *Metabolic Engineering*, *56*, 77–84. https://doi.org/10.1016/j.ymben.2019.08.014

Zerulla, K., Ludt, K., & Soppa, J. (2016). The ploidy level of synechocystis sp. PCC 6803 is highly variable and is influenced by growth phase and by chemical and physical external parameters. *Microbiology (United Kingdom)*, *162*(5), 730–739. https://doi.org/10.1099/mic.0.000264

3. ENGINEERING OF FAST-GROWING CYANOBACTERIA *SYNECHOCOCCUS ELONGATUS* SP PCC 11801 FOR PHENYLALANINE AND 2 PHENYLETHANOL PRODUCTION

3.1 Abstract

Cyanobacteria as microbial factories are being increasingly explored due to their ability to directly convert CO_2 to useful bio-chemicals. However, initial engineering efforts have resulted in low productivity and titers primarily due to slow growth. Recently, a robust fast-growing strain resistant to abiotic stresses, *Synechococcus elongatus* sp. PCC 11801 (hereafter PCC 11801) was discovered with growth rate comparable to yeasts. Due to the limited availability of synthetic biology tools, we utilize ultraviolet (UV) irradiation-based mutagenesis coupled with amino acid analog selection for the development of phenylalanine (Phe) overproducers. Mutants resistant to 3-(2-thienyl)-DL-alanine were characterized for Phe production to identify the best producer M14, which was subjected to a second round of UV mutagenesis and selection to isolate M14.2, which can produce 1.2 ± 0.1 g/L of Phe in 3 days under 3% CO_2. We also report a nutrient feeding strategy that increased Phe titer to 3 g/L in a fifteen day culture. Additionally, selected mutants show no growth reduction compared to wild type but show a 30% increase in carbon productivity. This is the highest productivity and titer for Phe overproduction by a photosynthetic organism and highlights the advantages of using fast growing cyanobacteria as systems for biochemical production.

The strains developed are good candidates for the production of Phe derived compounds due to the high flux to Phe. 2-PE is a natural aromatic valuable in the fragrance industry as well as a promising oxygenate for fuel that is derived from Phe. Thus, we attempt to engineer Phe overproducing strains developed to produce Phe derivative 2-phenylethanol (2-PE) by the introduction of the Ehrlich pathway and the phenylacetaldehyde synthase (PAAS) pathway. Our efforts show the successful production of 2-PE, however productivity and titer remain low. Our work highlights the need to further develop synthetic biology tools specialized for PCC 11801 for engineering of heterologous biochemical production.

3.2 Introduction

Cyanobacteria are photosynthetic prokaryotes with the capability of fixing CO_2 and converting it into valuable biochemicals (Singh et al., 2018). One such valuable biochemical is Phenylalanine (Phe), an aromatic amino acid synthesized by the shikimate pathway with applications in the food, feed, and pharmaceutical industries (Bongaerts et al., 2001). Typically, heterotrophs such as *E. coli* convert plant derived sugars into Phe via fermentation constituting a two-step process that suffers from poor yield on sugar (Y. Liu et al., 2018). Recently, cyanobacteria have been engineered to produce aromatic amino acids such as Phe and tryptophan (Trp) and their derivatives including phenylpropanoids and 2-PE, but the productivities and titers have remained low partially due to slow growth (Brey et al., 2020; Deshpande et al., 2020; Ni et al., 2018a). Engineering of newly discovered fast growing strains can overcome limitations of slow growth to enable higher productivities (Jaiswal et al., 2018). This is especially true in the production of growth coupled products such as amino acids. Recently, it was shown that using a fast growing cyanobacteria strain UTEX 2973 improved lysine production using the same strategy when compared to *Synechococcus elongatus* sp PCC 7942 (Dookeran & Nielsen, 2021). One such strain Synechococcus elongatus PCC 11801 (hereafter PCC 11801) is an ideal choice for engineering due to its low doubling time, resistance to abiotic stressors such as salt and temperature, and ability to grow under high light (Jaiswal et al., 2018). These attributes are of particular importance since a production strain in a commercial scale implementation necessitates a robust response to abiotic stressors. In this study, we use PCC 11801 to engineer strains for Phe overproduction directly from CO_2 and solar energy.

The flux towards Phe biosynthesis is tightly regulated in cyanobacteria (Riccardi et al., 1989). The key rate limiting steps are catalyzed by 3-deoxy-D-arabino-heptulosonate-7-synthase (DAHPS) and prephenate dehydratase (PD), which are typically feedback regulated by the end products of the shikimate pathway, Phe and Tyr (Hall et al., 1982; Hall & Jensen, 1980; Riccardi et al., 1989). Although chorismate mutase (CM) has been shown to be regulated by Phe and Tyr in a few cyanobacterial strains, it is unlikely to be the case in PCC 11801 as CM in this strain is only 130 amino acids long and is unlikely to contain a Phe binding site (UniProt entry: A0A3G6X0V1). To enable aromatic amino acid overproduction, random mutagenesis followed by amino acid analog selection is a promising first step (Deshpande et al., 2020). As synthetic biology tools for PCC 11801 emerge (A. Sengupta et al., 2020; S. Sengupta et al., 2020), metabolic

engineering techniques can be combined to achieve further improvements in Phe overproduction Herein, we utilized methylmethanesulfonate (MMS) and ultraviolet (UV) irradiation as mutagens followed by selection on Phe analog 3-(2-thienyl)-dl-alanine. Mutants resistant to analogs can overcome potential feedback regulation leading to overproduction (Hall & Jensen, 1980). Phe analogs can bind to feedback inhibition sites in the shikimate pathway enzymes (e.g. DAHPS) and inhibit biosynthesis of aromatic amino acids essential for growth, thus mutants that can tolerate Phe analog are likely to be insensitive to feedback inhibition by Phe. Multiple rounds of mutagenesis, especially with different mutagens can be crucial to improving the phenotype that is being selected for, as different mutagens can explore independent mutation spaces (Bose, 2016; Packer & Liu, 2015). Thus, multiple rounds of mutagenesis and selection were tested as part of this work to develop a Phe overproducing strain M14.2 with a photosynthetic Phe productivity as high as ~400 mg/L/day. The Phe overproducer development strategy is shown in figure 3.1.

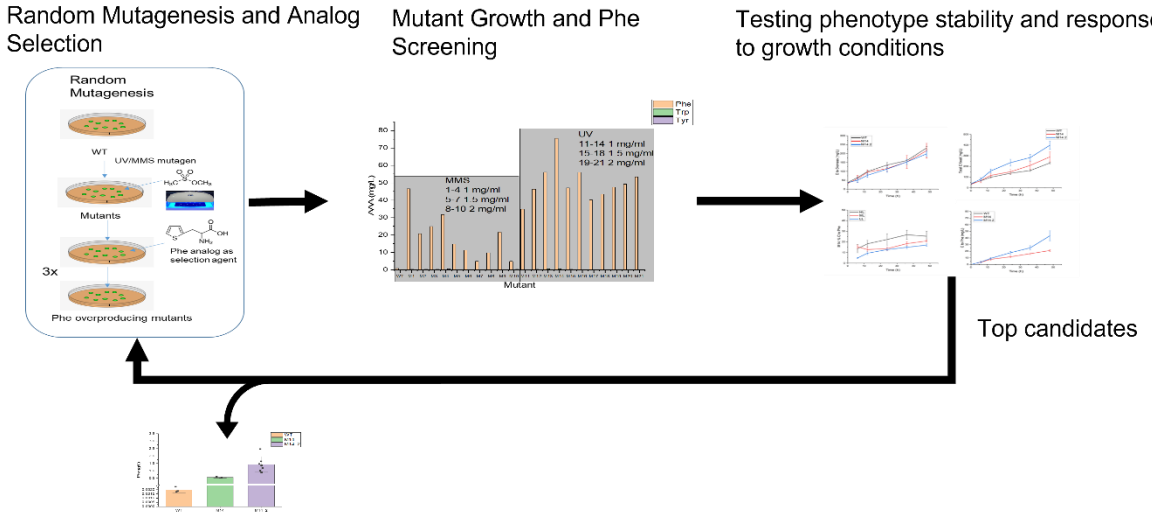

Figure 3.1 Phe overproducer development strategy using multiple rounds of random mutagenesis coupled with amino acid analog selection

The strains developed using this strategy are ideal candidates to serve as hosts for the further engineering efforts directed towards the production of Phe derived compounds. One such compound 2-phenylethanol (2-PE) is a natural aromatic with a distinctive “rose-like” odor and is valuable in the fragrance and flavoring industry (Etschmann et al., 2002). In addition to this, 2-PE is a promising candidate as an oxygenate alternative to ethanol for petroleum derived fuels due to its higher energy density, lower volatility, and lower hygroscopicity (Atsumi et al., 2008).

However, most of the 2-PE produced is synthetically derived from Friedel-Crafts reaction of ethylene oxide and benzene with aluminum chloride as a catalyst (Etschmann et al., 2002). Chemical synthesis is low cost but suffers from several drawbacks such as use of strong acids, toxic byproducts, petroleum derived precursors and require high temperature and pressure. Further, poor separation from byproducts in the chemical synthesis result in odors that significantly reduces its value and applicability in the cosmetics and fragrance industry (Wang et al., 2019a). 2-PE derived from natural sources is thus very valuable in the cosmetics industry ($5/kg synthetically derived vs $1000/kg naturally derived) and thus harnessing the ability of microorganisms to produce 2-PE is important (Wang et al., 2019a).

Microorganisms including bacteria (H. Zhang et al., 2014), filamentous fungi (M. M. W. Etschmann et al., 2015; Wani et al., 2010) and yeast such as *Saccharomyces cerevisiae*, *Pichia pastoris* and *Yarrowia lipolytica* (Wang et al., 2019b) have the ability and gene set to naturally produce 2-PE. Several routes exist for the biosynthesis of 2-PE: phenylethylamine (PEA) pathway, phenylacetaldehyde synthase (PAAS) pathway or the Ehrlich pathway as shown in figure 3.2. The Ehrlich pathway uses phenylpyruvate as the precursor and is utilized in industrial fermentations in engineered heterotrophs, such as yeasts, typically overexpressing phenylpyruvate decarboxylase and alcohol dehydrogenases (ADHs) (Hassing et al., 2019). The major known pathway in plants such as rose and petunia is the PAAS pathway that directly uses Phe as a precursor. PAAS is a bi functional enzyme that catalyzes the deamination and decarboxylation of Phe to phenylacetaldehyde which is subsequently reduced to 2-PE by different alcohol dehydrogenases (Sakai et al., 2007). However, most studies employ the use of heterotrophic microorganisms that are either fed plant derived glucose/sugars or even more expensive precursor Phe (Wang et al., 2019a). There has been only one attempt to photosynthetically produce 2-PE in cyanobacteria in *Synechococcus elongatus* sp PCC 7942 (Ni et al., 2018). In this work, we aim to build on this study by utilizing fast growing Phe overproducing strains to directly produce 2-PE from CO_2 and sunlight using the PAAS and Ehrlich pathways.

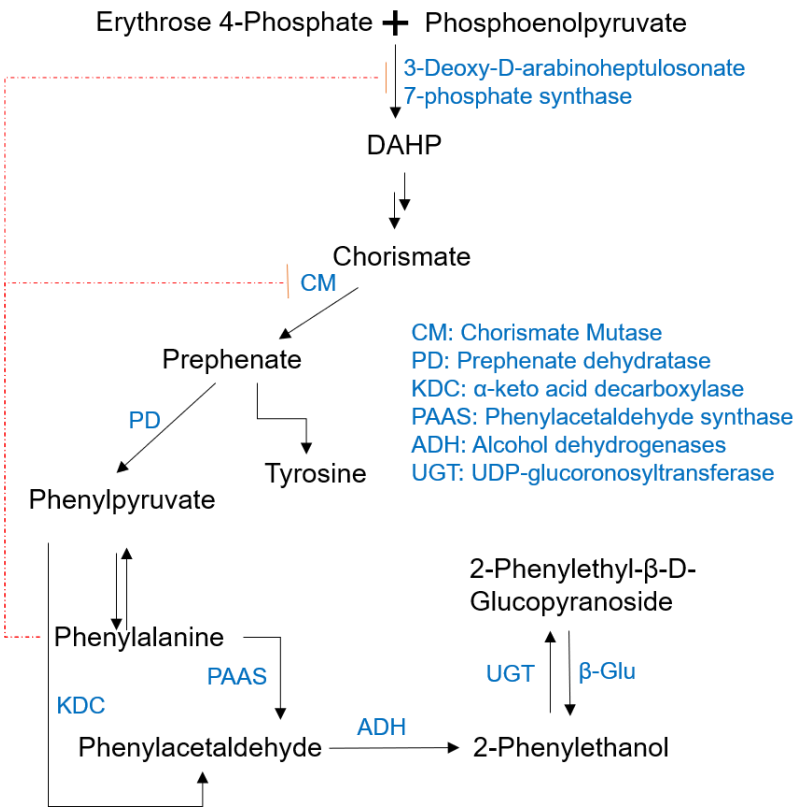

Figure 3.2 Biosynthetic pathways for 2-PE. Dashed red lines depict feedback inhibition.

3.3 Materials and Methods

3.3.1 Construction of plasmids for gene expression

The wild-type strain used is *Synechococcus elongatus* sp. PCC 11801 (Jaiswal et al., 2018) (PCC 11801), procured from Dr. Wangikar, Indian Institute of Technology, Bombay. The wild type and all the strains developed were routinely cultured in a modified BG-11 media (hereafter BG-11M) in 250 mL Erlenmeyer flasks with a culture volume 50 mL at constant temperature 38°C, 240 or ~1000 µmol-photons/m^2/s light, 200 rpm with supply of air or 3% CO_2 enriched air in an incubator shaker (Infors HT Minitron) or a warm room. BG-11M media was prepared by supplementing BG-11 (Rippka et al., 1979) with an additional 1 g/L sodium nitrate, 20 mg/L magnesium sulfate heptahydrate, 40 mg/L potassium phosphate, 10 mg/L ammonium chloride and 1 mL of A5 trace metal solution. The growth of the cultures was determined by measuring either the optical density at 730 nm (OD_{730}) using a Beckman DU Series 500 spectrophotometer or measuring the dry cell weight. The relationship between the dry cell weight and the OD_{730} was

determined to be 0.40 g (dry cell weight)/L/OD_{730}. A summary of all the strains that are part of this work is shown in table 3.1.

Table 3.1 List of strains used in this study

Strains		Characteristic	Source
PCC 11801		*Synechocystis* sp. PCC 6803 substrain GT-I	Dr. Pramod Wangikar
M1-M10		MMS mutant Phe overproducers	This work
M11-M21, M14.2		UV mutant Phe overproducer	This work
Strain	Parent Strain	Integrative Plasmid	Source
M14 EV	M14	pSYN6	This work
M14 PAAS	M14	pSYN6_PAAS	This work
M14 KDC	M14	pSYN6_KDC	This work
M14.2 EV	M14.2	pSYN6	This work
M14.2 PAAS	M14.2	pSYN6_PAAS	This work
M14.2 KDC	M14.2	pSYN6_KDC	This work

3.3.2 Random mutagenesis, selection, and Phe characterization

Random mutagenesis was performed by modifying a previously described protocol (Bose, 2016; Deshpande et al., 2020; Tillich et al., 2012) with methylmethanesulfonate (MMS) and ultra-violet (UV) irradiation as the mutagens. Cells were prepared for random mutagenesis by pelleting exponentially growing cultures (OD ~0.6-1) of PCC 11801 and resuspending in 1mL of fresh BG-11M media. For MMS mutagenesis, 1% (v/v) MMS (Sigma-Aldrich, St. Louis, MO) was added, and the reaction quenched by addition of 5% (w/w) sodium thiosulfate solution to yield a ~85-95% kill rate. For UV mutagenesis, the culture was subjected to different times of UV irradiation (302nm peak, UVP Transilluminator) to attain a kill rate of ~90%. The amount of irradiation could not be determined.

The mutagenized cultures were incubated at 38°C overnight in the dark before selection. To select for overproducers, concentrations ranging from 0.5-2 mg/ml Phe analog 3-(2-thienyl)-dl-alanine (Sigma-Aldrich, St. Louis, MO) on BG-11M agar plates were applied. The parent strain and mutagenized cultures were diluted and spread on BG-11M (to test kill rate) or BG-11M analog containing plates and incubated at 38°C until colonies appeared. Colonies that successfully grew

on analog selection plates were picked and re-streaked on selection plates for at least 3 rounds to enable complete segregation of mutations. After transfer to liquid cultures, aromatic amino acid titers were quantified in the supernatant using LC-MS/MS as previously described (Deshpande et al., 2020).

3.3.3 2-PE and 2-PE glucopyranoside toxicity

2-PE and 2-PE glucopyranoside was added exogenously at different concentrations to the cultures inoculated at OD_{730} 0.2 and grown under constant illumination (240 µmol-photons/m^2/s) at 38°C, 3% CO_2 and shaken at 200 rpm. The growth was measured by monitoring the OD_{730} and the final biomass accumulation calculated by measuring the gDCW/L at the end of 3 days in culture.

3.3.4 Plasmid and strain construction

The base plasmid pSYN6 that has been widely used in Synechococcus elongatus sp PCC 7942 was used as the starting point and was procured from Life Technologies Corporation, California, USA. To engineer the PAAS pathway, the *paas* gene from *R. damascena* was codon optimized for cyanobacteria and cloned into the pSYN6 plasmid using NdeI/NdeI restriction sites through GenScript, Piscataway, NJ, USA to develop pSYN6_PAAS. Similarly, to engineer the Ehrlich pathway, the *kivD* gene from *L. lactis* was codon optimized for cyanobacteria and cloned into the pSYN6 plasmid using NdeI/NdeI restriction sites to develop pSYN6_KDC. Cloning was verified using PCR, gel electrophoresis and sequencing. The plasmids were transformed into *E. coli* DH5α for propagation and purified using plasmid miniprep kit (Thermo Fisher Scientific) prior to transformation of cyanobacteria. A list of primers used in this study is shown in table 3.2.

3.3.5 Transformation

Transformation was performed as previously described for PCC 11801 (Sengupta et al., 2020). PCC 11801 can take up DNA naturally, so natural transformation was attempted (Jaiswal et al., 2018). Briefly, 10 mL of culture at OD_{730}~0.6-1 was centrifuged, washed with fresh medium and subsequently resuspended in 200 µL of fresh BG-11M medium. 500 ng to 1 µg of plasmid was added and the mixture was mixed and incubated in the dark at 38°C overnight. The culture was then diluted in BG-11M containing 10 µg/L spectinomycin and incubated for 5 days followed

by transfer to 50 mL media containing 100 µg/L spectinomycin before transfer to 100 µg/L spectinomycin BG-11M plates to obtain single colonies. Alternatively, cultures incubated overnight were directly transferred to 10 µg/L spectinomycin plates followed by at least 3-4 rounds of streaking onto 100 µg/L spectinomycin BG-11M plates to isolate single colonies. Transformation was confirmed by PCR amplification and gel electrophoresis as described previously (Deshpande et al., 2020). The list of primers used for PCR amplification are listed in table 4.2 and the list of strains developed are shown in table 4.1. Two sets of neutral site I (NSI) primers were tested since the primers were designed for *Synechococcus elonagtus* PCC 7942 but since PCC 11801 shares ~83% identity.

Table 3.2 List of primers used in this study

Primer	Sequence	Source
PAAS forward	TGCAAGAGATTGCCTCTAGCC	Invitrogen
PAAS reverse	TGCACGACATTCCAAGCCTC	Invitrogen
KDC forward	CGCCTGCATGAACTCGGTAT	Invitrogen
KDC reverse	GCCAGGATCAGTTCAATCCA	Invitrogen
NS1 forward	CTGACTGTTGAAGGCGTTGC	Invitrogen
NS1 reverse	TCGTACAGCCAGGGTTGAAT	Invitrogen
NS1_2 forward	AAATGACAAGATCACGGCCC	Invitrogen
NS1_2 reverse	TTCAGCTGCTTTAGGCCCAC	Invitrogen

3.3.6 GC-MS analysis of 2-PE and phenylacetaldehyde

Cells were pelleted by centrifugation and the supernatant was separated. Both the cell pellet and supernatant were extracted using ethyl acetate with naphthalene as internal standard. The extracts were concentrated under a gentle stream of N_2 and the 2-PE and phenylacetaldehyde content was analyzed using Agilent 7890A gas chromatograph coupled with 5975C inert MSD quadrupole mass spectrometer using a HP5-MS column (0.25 mm x 30m x 0.25µm, Agilent, Santa Clara, CA). The temperature program used was as follows: 40°C maintained for 2 min and raised from 40 to 150°C at 10°C/min, then from 150 to 250°C at 20°C/min with a final holding time of 2 min. Injector and detector temperatures were set at 250 and 230°C, respectively, 2-PE and phenylacetaldehyde were quantified based on known m/z values, and quantified based on calculated response factors relative to the internal standard naphthalene.

3.3.7 Statistical Analysis

Data are presented as mean ± SE (biological replicates). Pairwise comparison was performed using student's t-test with either SAS (SAS Institute) or Origin 2019b (OriginLab). A p value of <0.05 was considered statistically significant.

3.4 Results and Discussion

3.4.1 UV and MMS random mutagenesis to develop Phe overproducers

In our previous work to develop aromatic amino acid overproducers, we successfully utilized MMS based mutagenesis as outlined in Chapter 2. In this work, we utilized MMS and UV irradiation as mutagens followed by selection on Phe analog 3-(2-thienyl)-dl-alanine. Mutants resistant to analogs can overcome potential feedback regulation leading to overproduction (Hall & Jensen, 1980). We screened 21 mutants resistant to 1, 1.5, and 2 mg/mL 3-(2-thienyl)-dl-alanine for Phe production as shown in figure 3.3. It was found that almost all the Phe (>95%) was excreted and obtained extracellularly in the media. In general, we observed that mutants created by UV mutagenesis had higher levels of Phe accumulation compared to mutants created by MMS.

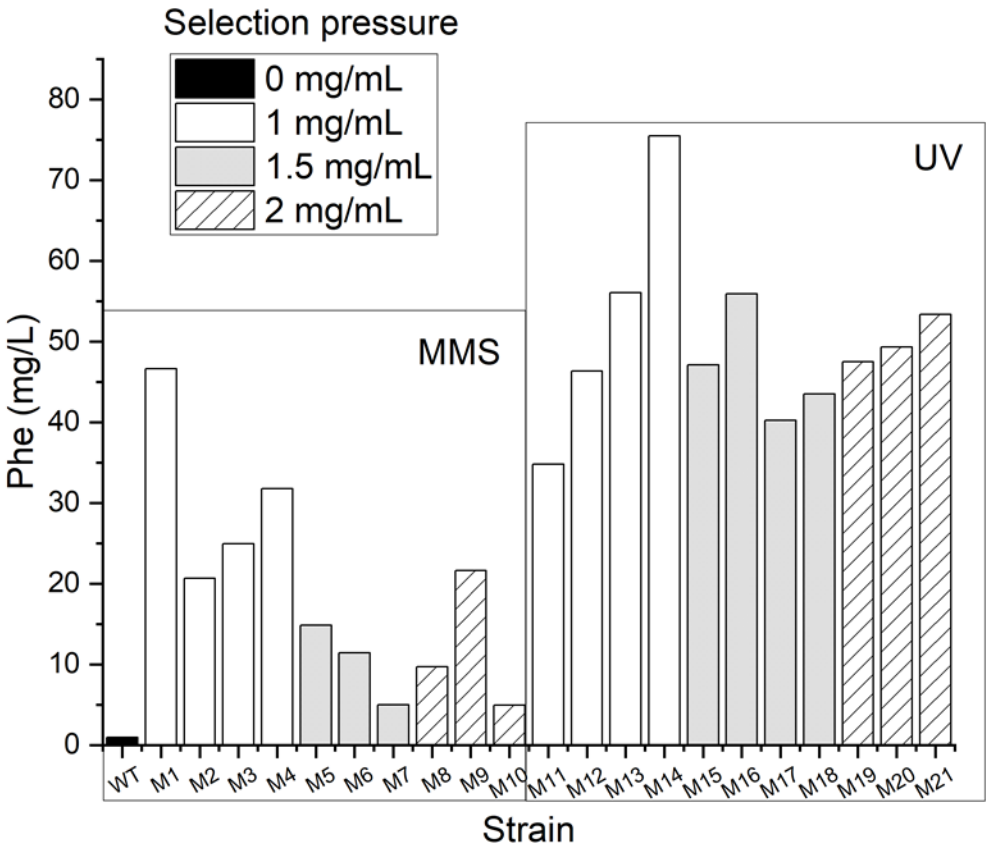

Figure 3.3 Phenylalanine accumulation after 3 days in the supernatant from selected mutant cyanobacteria. The strains were grouped by the mutagen from which they were derived; MMS (M1-M10) and ultraviolet irradiation (M11-M21). Growth conditions were 240 µmol/m^2/s

Interestingly, mutants selected on the highest selection pressure could not outcompete mutants selected on lower analog concentration. This might be primarily due to reduced growth as seen in mutants screened at 2 mg/L analog concentration. We speculate that resistance to higher analog pressure might select for strains with higher mutation counts that negatively affect growth. It could also be the case that a significant fraction of cellular resources are directed towards enabling resistance to high analog concentration that competes with growth.

The top 3 MMS (M1, M4, and M9) and UV mutants (M14, M17, and M21) were further screened in triplicate for Phe production and growth to ensure stable phenotype after removal of selection pressure (figure 3.4). Only M9 lost its phenotype after removal of analog pressure as it possible that it was not fully segregated, since cyanobacteria have multiple copies of its genome

(Zerulla et al., 2016). M14 proved to be the best strain and can accumulate 200±40 mg/L Phe in the supernatant after 5 days in culture at 240 µmol $m^{-2}s^{-1}$ under ambient CO_2.

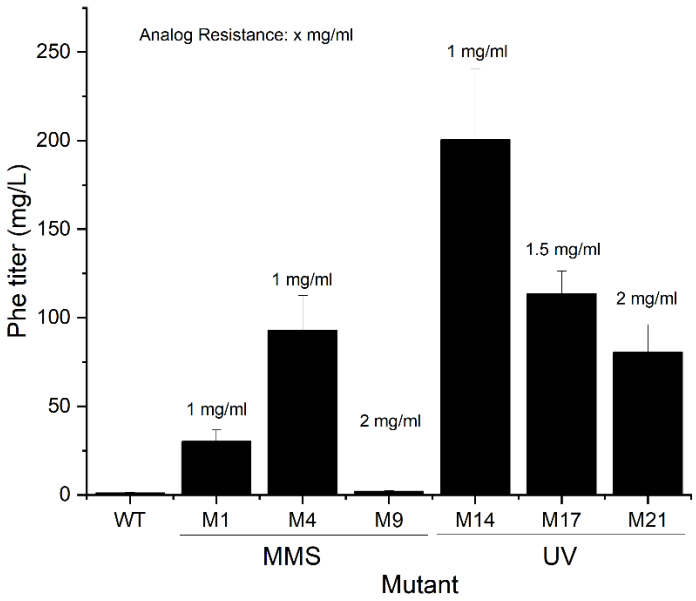

Figure 3.4 Phe production of MMS and UV mutants without analog selection pressure after 5 days in culture at 240 µmol/m^2/s under ambient CO_2. Analog resistance in the figure indicates the originally concentration on selection plates and does not indicate that the media contained analog. Error bars indicate the standard deviation from 3 biological replicates.

3.4.2 Second round of mutagenesis for the development of M14.2

To improve Phe overproduction, M14 was selected for further mutagenesis as it was the best strain from the first round of random mutagenesis. Random mutagenesis using UV irradiation and 1% MMS (v/v) exposure was tested independently to achieve ~90-95% kill rate coupled with selection on plates containing 1.5,2, 2.5, and 3 mg/ml of the Phe analog, 3-(2-thienyl)-dl-alanine. After screening several resistant colonies as described previously, only 1 colony was found to outcompete the parent strain M14 for Phe production. This colony was a result of UV exposure and selection on 1.5 mg/mL analog. This mutant denoted as M14.2, accumulated roughly 2-fold more Phe in the media, a significant improvement over M14 (data not shown). It is interesting that a second round of UV but not MMS mutagenesis resulted in an improvement in the Phe overproduction. It was expected that since MMS targets different base changes (Sikora et al., 2010) (such as GC → AT, AT → GC, AT → TA) compared to UV mutagenesis, a UV + MMS mutant

would show an improvement when compared to two rounds of UV mutagenesis. This indicates that the first round of UV mutagenesis and selection was unable to target all bottlenecks that can be addressed by inducing cytosine (C) → thymine (T) and CC → TT mutations (Ikehata & Ono, 2011).

3.4.3 Phe production under physiologically relevant conditions

Scaling up and testing cyanobacteria cultures outdoors requires a robust performance under stressors such as high light and day-night cycles (Schipper et al., 2021). Since our strain development, segregation and Phe characterization studies have been performed under continuous illumination of 240 µmol-photons/m^2/s, we decided to test the performance of our mutant strains under 12h:12h diurnal cycle, and separately at a higher light intensity closer to what might be expected in outdoor culture conditions. Both M14 and M14.2 were adapted to at least one subculture under diurnal cycle before being tested for Phe production (figure 3.5) and biomass accumulation. The Phe productivity normalized to time under illumination for M14 and M14.2 in a 12h:12h diurnal cycle was comparable to continuous illumination. The biomass accumulation for both the mutant strains was comparable to wild type. Our result suggests that it is unlikely that Phe is uptaken under dark to be used as either a nitrogen or carbon source. To determine strain performance under high light conditions, we used 1045±45 µmol-photons/m^2/s continuous illumination. Due to higher availability and greater penetration of light at higher cell density, M14.2 was able to accumulate 287±28 mg/L Phe in 3 days. The resultant productivity 95±9 mg/L/d Phe is the highest reported in cyanobacteria under ambient CO_2.

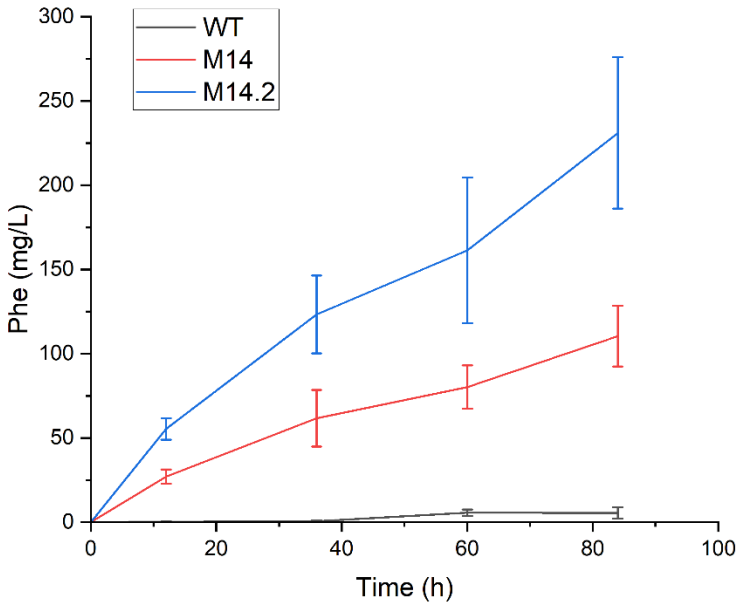

Figure 3.5 Phe production under a 12h light (240 µmol/m^2/s) and 12h dark cycle under ambient CO_2. Error bars indicate standard deviation of three biological replicates.

3.4.4 Engineering strategies to improve Phe production

Enhancing the dissolved concentration of CO_2 has been shown to increase not only the growth rate but also the final culture density of PCC 11801 (Jaiswal et al., 2018). Previously aromatic amino acid production was found to be enhanced under the supply of CO_2 enriched air (Brey et al., 2020; Deshpande et al., 2020). To improve final product and biomass titer and productivities, we decided to test the effect of 3% CO_2 supply. Figure 3.6A shows the Phe titers of mutant strains. To ensure stability of the most productive strain M14.2, the experiment was repeated three times and it was seen that M14.2 had a consistent phenotype with a Phe titer 1.24±0.13 g/L in 3 days. Figure 3.6B shows the total accumulation of two major sink products, biomass and Phe. We define carbon productivity as the sum of carbon in biomass and secreted extracellular Phe. Therefore, we measured the % carbon in biomass of WT, M14 and M14.2 using isotope ratio mass spectrometry and found no significant difference (Chapter 4, Table 4.1). Interestingly, both M14 and M14.2 showed higher carbon productivities compared to wild type by nearly 14% and 28%, although only M14.2 was statistically significant at $p<0.05$. There was no significant difference in biomass accumulation, composition, or chlorophyll a content (data not

shown) of the wild type and mutants. The mutant M14.2 has 9.23±0.44 µg carotenoids/mgDCW and showed a small but significant increase compared to the WT content of 7.7±0.5 µg carotenoids/mgDCW. The effect of increased carotenoids on Phe secretion will need further investigation. Phe production was instead enhanced by increasing the carbon productivity. This indicates that under 3% CO_2 supply PCC 11801 is sink limited and that the introduction of a strong sink for Phe relieves this limitation to enable improved carbon productivity. This phenomenon has also been observed in other cyanobacteria where strains engineered for production of sucrose (Santos-Merino et al., 2021), 2-phenylethanol (Ni et al., 2018b), or 2,3-butanediol (Oliver et al., 2013) showed increase carbon fixation. Moreover, this work demonstrates that directed engineering can be a faster alternative to adaptive laboratory evolution (ALE) to improve CO_2 fixation. M14.2 showed a 28% increase in carbon fixation productivity whereas similar increases take several years with ALE approaches (B. Zhang et al., 2021).

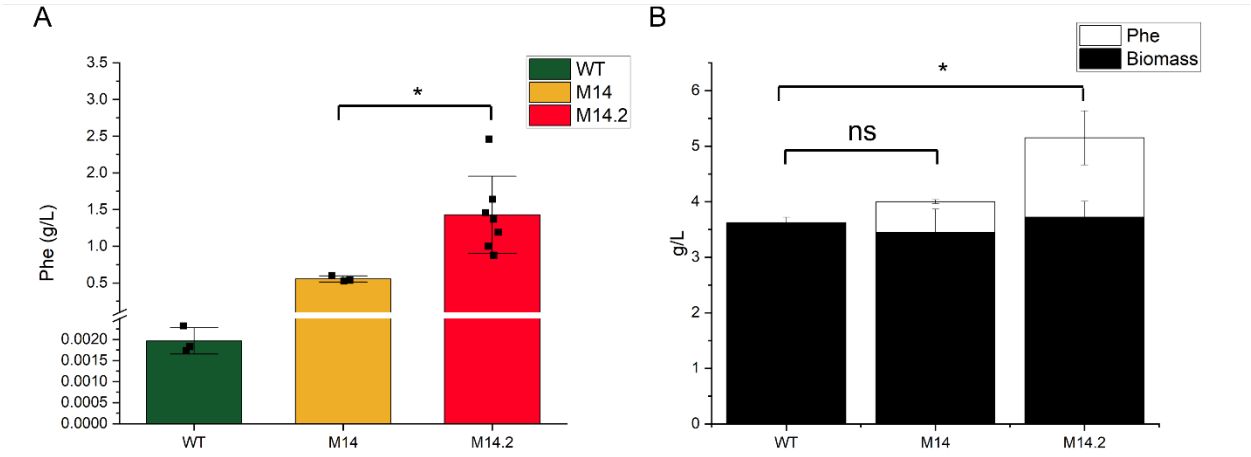

Figure 3.6 (A) Phe titer of wild type and mutants when cultured for 3 days at 240 µmol/m^2/s under 3% CO2. (B) Total capacity of biomass and Phe sinks. * indicates $p<0.05$ using a two tailed two sample t-test.

Improving biomass accumulation is vital to increase the titer of growth associated products such as Phe. Recently, the biomass accumulation of *Synechocystis* sp. PCC 6803 and *Synechococcus* sp. PCC 11901 were improved by alleviating nutrient limitations (van Alphen et al., 2018; Włodarczyk et al., 2020). We tested optimizing the contents of BG-11M by further optimizing levels of nitrates, phosphates, sulfates as well as nutrient replete 5x BG-11M (data not shown). Interestingly, none of these resulted in improved performance compared to BG-11M

media. This may be due to multiple nutrient limitations that cannot be removed by optimization of nutrients one at a time or in the case of 5x BG-11M, toxicity due to high cation concentration. We next tested addition of complete BG-11M nutrients every 3 days using a concentrated solution to minimize volume changes. This strategy enabled increasing the biomass and Phe accumulation to nearly 7 g DCW/L and 3 g/L respectively in 15 days under 240 µmol-photons/m^2/s light and 3% CO_2 as shown in Figure 3.7. This result also outlines a strategy that can be easily implemented at higher scales to reduce the number of batches.

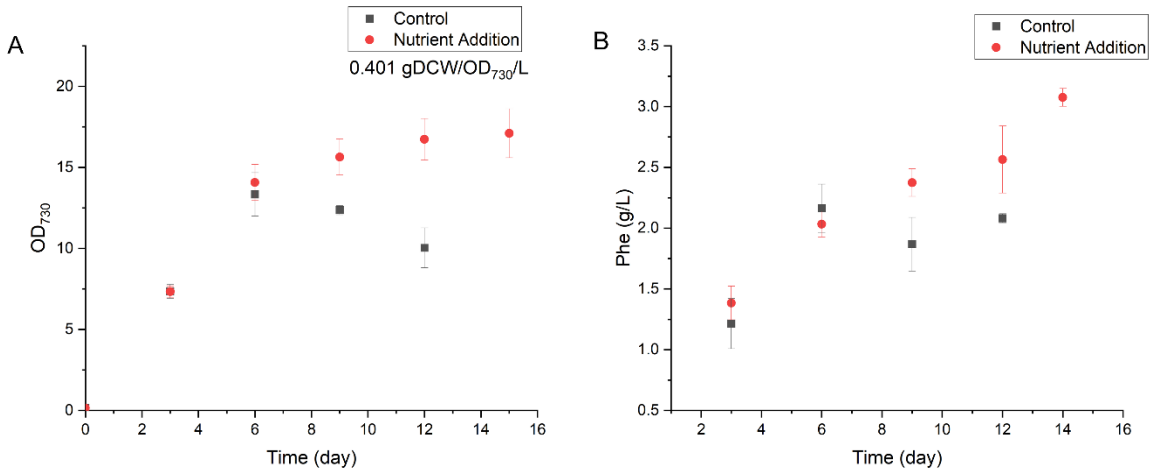

Figure 3.7. (A) Growth (OD730) and (B) Phe titer of Phe overproducing mutant M14.2 with and without a nutrient supplementation strategy (addition of complete BG-11M nutrients at day 3, 6, 9, and 12 using a concentrated solution to minimize volume change) when cult cultivated under 3% CO_2 and 240 µmol/m^2/s.

In this work, we have used random mutagenesis on PCC 11801 to develop Phe overproducing strains that can accumulate 3 g/L Phe, the highest reported titer in cyanobacteria. Figure 3.8A compares the Phe productivity in cyanobacteria engineered for production of Phe and its derivatives. Our strain M14.2, shows a higher productivity under both ambient and 3% CO_2 conditions with a maximum productivity about 400 mg/L/d Phe under a 3 day cultivation cycle. Further, total carbon sink productivity is one of the highest reported in cyanobacteria and comparable to other fast growing cyanobacteria strains under high CO_2 as shown in figure 3.8B. The comparison with heterotrophs is not a direct one. Heterotrophic Phe producers such as *E. coli* need to utilize sugars such as glucose and suffer from low yields on glucose, typically lower than 50% of the maximum theoretical yield of 0.55 g/g (X. Liu et al., 2019). Thus, we compare the two-

step process of sugar production by crops and subsequent conversion to Phe by heterotrophs with the single step cyanobacterial process using space-time yield as previously described (Brandenburg et al., 2021). The current best Phe producing bacterial strain accumulates roughly 72 g/L Phe in the media with a yield of 0.26 mol/mol in glucose (X. Liu et al., 2019). Assuming the average yield for sugarcane over the last 10 years (70.63 tfw/ha/annum) and a sugar content of 15% (FAO, 2020), the space time yield for the two-step process is nearly 7 kgPhe/ha/d. In case of cyanobacterial photoautotrophic Phe production, we assume commercial photobioreactors of scale 500,000 L/ha that operate can reach the same cell density and with productivity 21% compared to shake flasks. This results in a space time yield of nearly 22 kgPhe/ha/d, about 3 fold more efficient than the current heterotrophic process.

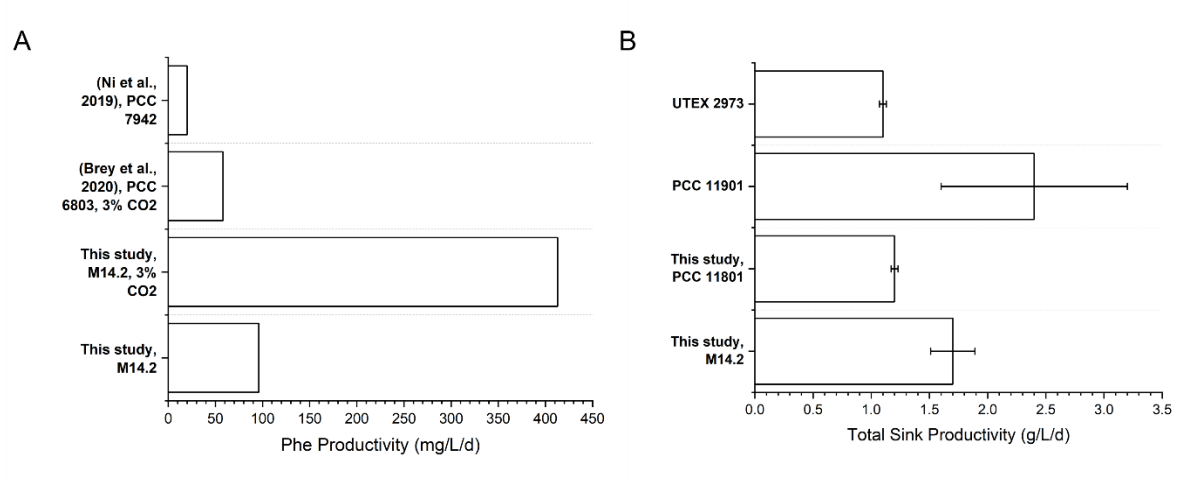

Figure 3.8 (A) Comparison of Phe productivity in engineered cyanobacteria and (B) total carbon sink productivities in cyanobacteria.

3.4.5 Effect of diurnal cycle on Phe

In our previous study on the effect of the 12h:12h diurnal cycle, we only measured Phe and biomass at 24-hour intervals after a complete diurnal cycle. Although this experiment provided crucial data that shows that the Phe and biomass productivity under continuous light and diurnal cycle is not significantly different after normalizing to the total time under illumination, these measurements did not elucidate the fate of Phe and growth in the dark. Currently, there is no evidence in cyanobacteria that shows that Phe can be uptaken to be used as a carbon source or nitrogen source for proliferation. However, cyanobacteria are known to possess non-specific nat family of transporters that are involved in the uptake of Phe (Luz Montesinos et al., 1997).

Synechococcus elongatus PCC 7942, a close relative of PCC 11801 was shown to uptake several amino acids with Phe uptake rate of 4.18 nmol/mg Chl/min when 10 µM Phe was supplemented in the media under illumination (Luz Montesinos et al., 1997). However, the dynamics and fate of Phe under dark in overproducing mutants is unclear and remains to be investigated. Under dark it is unlikely that Phe is produced since it is a growth coupled product. Thus, we hypothesized that Phe could be uptaken under dark with the activity of nat family of transporters. To test this, acclimatized the WT and Phe overproducing mutants to a 12h:12h diurnal cycle (240 µmol/m^2/s) prior to the inoculation of cultures in triplicate at a starting OD_{730} ~ 0.2. Growth and Phe were monitored every 12 hours as shown in figure 4.9.

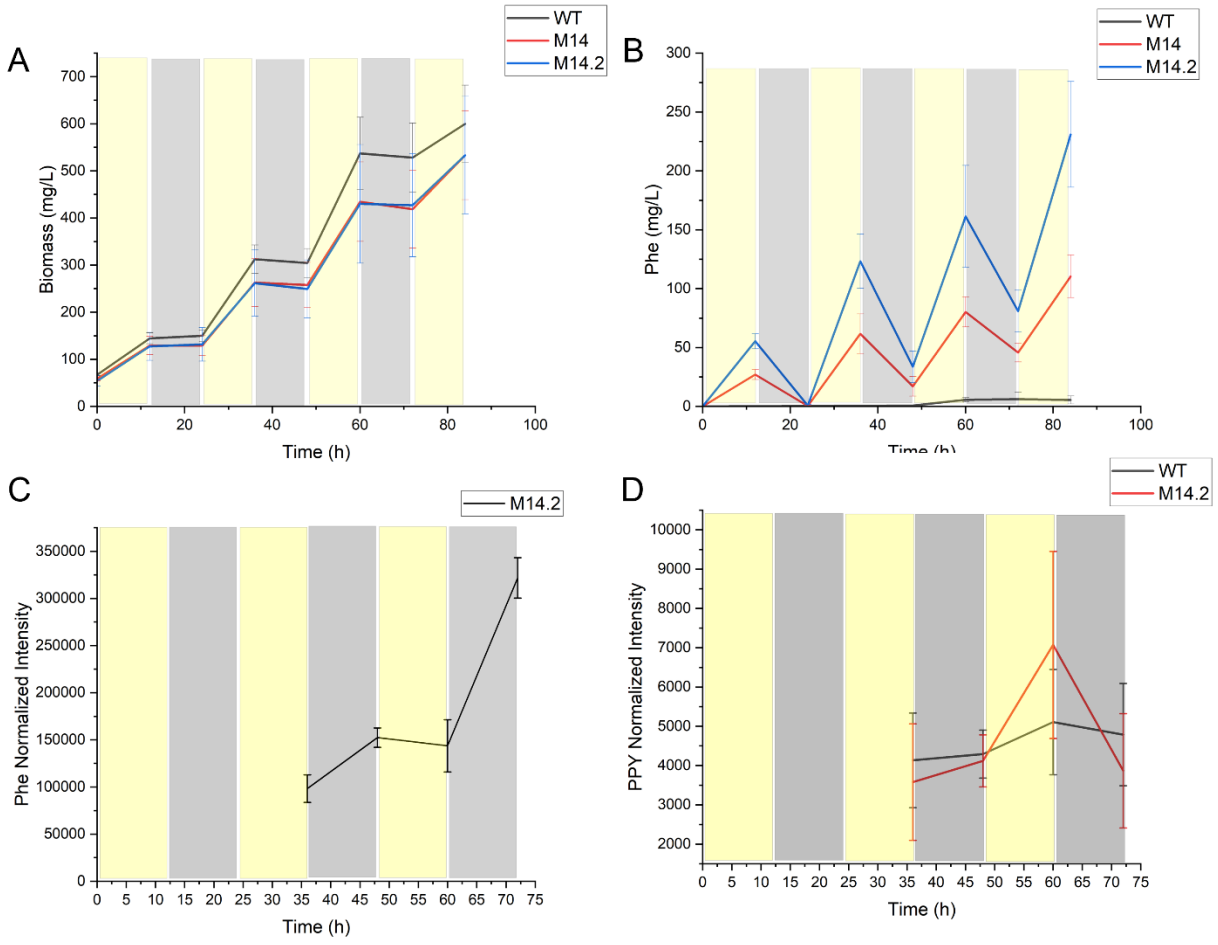

Figure 3.9 (A) Biomass accumulation, (B) Phe accumulation in the media, (C) Intracellular Phe accumulation, (D) Intracellular phenylpyruvate (PPY) accumulation under a 12h:12h diurnal cycle. The yellow regions indicate illumination whereas the grey regions indicate dark.

We find that under dark conditions, there is a decrease in the Phe content in the media (figure 3.9B). This indicates that under dark conditions, Phe is uptaken possibly by the activity of nat family of transporters (Luz Montesinos et al., 1997). This is also supported by the intracellular free Phe content normalized to the biomass as shown in figure 3.9C. However, the role of Phe uptake under dark remains unclear. Phe is not used as carbon source as can be seen by no increase in biomass accumulation under dark (figure 3.9A). Furthermore, the data points that there is no loss of Phe productivity normalized to time under illumination. This indicates that the uptaken Phe is exported back into the media. One hypothesis is that the uptaken Phe is used as a N source, where the Phe uptaken is converted to phenylpyruvate by reversible amino transferase activity. Thus, phenomenon could result in shuttling of the N in Phe to different metabolites and result in the accumulation of phenylpyruvate since phenylpyruvate cannot be catabolized using native cyanobacterial enzymes. We tried to test this hypothesis by testing if there is phenylpyruvate buildup in the dark. However, our data does not support this since the intracellular phenylpyruvate levels show no significant change under dark (figure 3.9D). The cause of this intriguing effect needs to be investigated further. One hypothesis is that expression of nat family of transporters is highly upregulated under dark resulting in a significant uptake of the large pool of Phe available under dark while the biosynthesis and export remains inactive.

3.4.6 Effect of 2-PE and 2-PE-glucopyranoside on growth

2-PE is naturally toxic to microbes as it can interfere with the bacterial membrane and result in leakage of ions and uptake of nutrients (Stark et al., 2002). Previously, 2-PE was shown to affect growth in *Synechococcus elongatus* PCC 7942 (Ni et al., 2018), and thus it is important to determine the tolerance of PCC 11801 to 2-PE and its glucopyranoside derivative before engineering the strains for the production of 2-PE. 2-PE was added at concentrations upto 2 g/L and 2-PE glucopyranoside was added upto 10 g/L exogenously to test the inhibition on growth as shown in figure 3.10. It is seen exogenous addition of 2-PE at the start of the culture severely inhibits growth, with complete inhibition at 1.5 g/L. However, when 0.8 g/L and 1 g/L 2-PE is added after one day of growth (~ 1 gDCW/L), there is only 14% and 20% and reduction in accumulation of biomass at the end of 3 days. Since our best Phe overproducer produces about 1 g/L Phe at the end of 3 days (figure 3.6), it seems that the current strain should have fair tolerance

to 2-PE and thus the strains developed should serve as good starting points for developing 2-PE producers.

Our results also show the promise of the novel strategy of engineering tolerance to 2-PE production by engineering its subsequent conversion to 2-PE glucopyranoside. Exogenous addition of 2-PE glucopyranoside only completely inhibits growth when added at 10 g/L at the start of the culture whereas there is no effect on growth when added at 1 g/L at the end of one day of growth (data not shown).

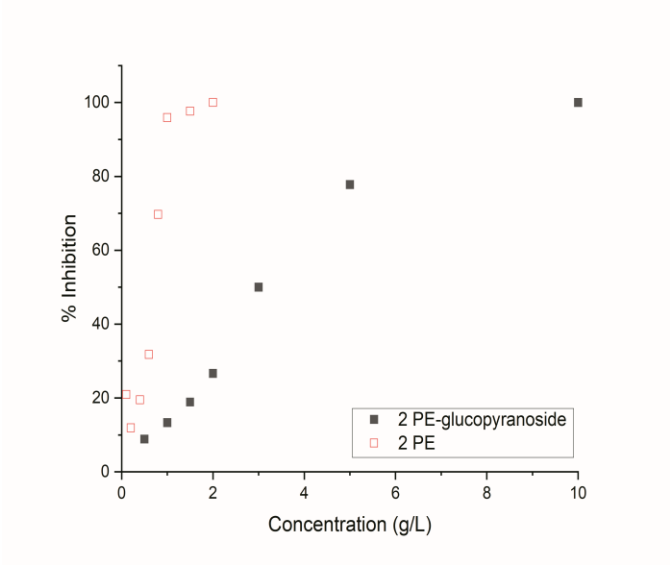

Figure 3.10 Determination of the growth inhibition of 2PE and 2PE-glucopyranoside on PCC 11801

3.4.7 Metabolic engineering of 2-PE production in Phe overproducers M14 and M14.2

M14 and M14.2 are ideal candidates for further engineering efforts to directed towards production of Phe derived products due to the high flux to Phe. Previously, photosynthetic 2-PE production was achieved in *Synechococcus elongatus* PCC 7942 by the expression of the PAAS and the Ehrlich pathways (Ni et al., 2018). We hypothesized that utilizing a faster growing strain could improve production of 2-PE, especially when engineering high Phe flux strains M14 and M14.2. We adopted a similar strategy by utilizing the *paas* gene from *R. damascena* and the *kivD* gene from *L. lactis* for the engineering of the PAAS and Ehrlich pathways in M14 and M14.2.

Since PCC 11801 was only recently discovered in 2018, there is a lack of dedicated synthetic biology tools for metabolic engineering. However, since PCC 11801 shares ~83% identity with well-studied *Synechococcus elongatus* PCC 7942, we tried to implement plasmids developed for

PCC 7942 for the engineering of PCC 11801. This was previously also attempted by the only other study till date that has metabolically engineered PCC 11801 for succinic acid production. We utilize the pSYN6 plasmid as the backbone to express the *paas* and *kivD* genes. pSYN6 has integration site NS1 which shares ~83% identity with PCC 11801, while the promoter used is the strong light inducible PpsbA native to PCC 7942. However, how well the promoters native to PCC 7942 work in PCC 11801 needs to be investigated further.

Transformation of attempted at least 5 times, however only M14_PAAS and M14.2_PAAS could be isolated and maintained. M14_PAAS and M14.2_PAAS which expressed the *paas* gene were analyzed and the Phe, 2-PE, and phenylacetaldehyde titers were measured in a three-day experiment. Cultures were inoculated at OD_{730} 0.2 and maintained at 3% CO_2, 38°C, 200 rpm, and 240 µmol-photons/m^2/s light intensity. At the end of three days, the 2-PE accumulation was only 19±4.5 mg/L and 17±5.2 mg/L in M14_PAAS and M14.2 PAAS respectively. To determine if export of Phe competes with the PAAS enzyme, we quantified Phe excreted. Surprisingly, M14_PAAS accumulated only 3±1 mg/L Phe whereas M14.2_PAAS showed a significant accumulation, 800±23 mg/L. Phenylacetaldehyde accumulation in the cell pellet was measured and showed significant buildup (figure 4.10B, absolute not quantified) whereas no peaks were detected in the WT which was used as a control. Figure 3.11 shows a pictorial representation of metabolic engineering of the PAAS pathway and 2-PE production.

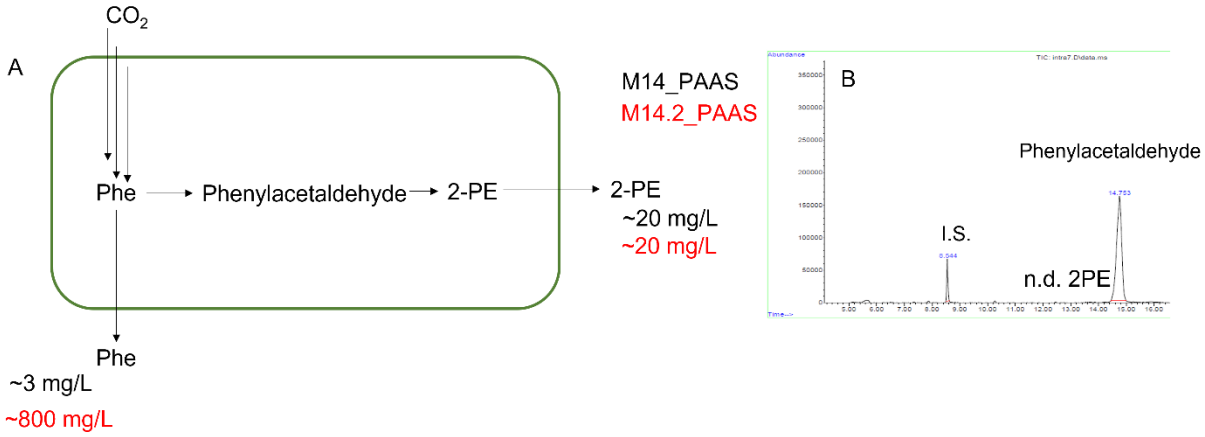

Figure 3.11 (A) Phe and 2-PE accumulation in the media by M14_PAAS (black) and M14.2_PAAS (red). (B) Gas chromatograph showing Phenylacetaldehyde accumulation in the cell pellet, 2-PE is not detectable

It is seen that there is a phenylacetaldehyde accumulation in both M14_PAAS and M14.2_PAAS which indicates that native ADHs are not sufficient to drive 2-PE production or might also result from toxicity to phenylacetaldehyde. This was also a bottleneck in 2-PE production in PCC 7942 where introduction of heterologous ADHs relieved the accumulation of phenylacetaldehyde (Ni et al., 2018). Furthermore, the total flux to the shikimate pathway in the engineered strains is lower than the parents. This indicates that either 2-PE production or phenylacetaldehyde accumulation has a negative effect on flux to the shikimate pathway and could be involved in its regulation. A similar observation was made in the case of lysine overproduction where introduction of genes to engineer lysine derivatives impacted the total flux into the lysine biosynthetic pathway significantly (Dookeran & Nielsen, 2021). The effect of toxicity at low 2-PE accumulation does not seem to be significant (figure 3.10).

Although M14_KDC, M14.2_KDC, M14_EV, and M14.2_EV were isolated from antibiotic plates, they quickly lost their resistance to spectinomycin and 2-PE production could not be quantified. The difficulty in transforming and segregation was not surprising since the tools used were not optimized for PCC 11801 and although PCC 7942 tools are amenable, they did not transfer well. Instability of metabolically engineered PCC 11801 was also observed previously in the Wangikar lab (personal communication, Vivek Mishra). Genetic instability in cyanobacteria is more common than is reported and there have only been a few reports that investigate this issue (Jones, 2014) . Further development of specialized synthetic biology tools is necessary for the metabolic engineering of this promising organism.

3.5 Conclusions and future work

In this work, we have successfully used random mutagenesis coupled with analog selection for development of Phe overproducing strains. To the best of our knowledge, this work reports the highest productivity for Phe production under ambient as well as elevated CO_2. Future work will target further increasing flux to Phe. Previously, it has been shown that nearly 50% of CO_2 fixed can be directed to Phe (Brey et al., 2020) which indicates that there is further room for improvement. This can be addressed by sequencing and identification of mutations that enable Phe overproduction which can then be combined with metabolic engineering approaches as previously described for tryptophan production (Deshpande et al., 2020). Our study highlights the advantages and potential of using random mutagenesis as an initial engineering approach with fast growing

cyanobacterial strains for the sustainable production of valuable biochemicals using CO_2 and sunlight.

Interestingly, under diurnal conditions we observed that the Phe secreted during the day was depleted in the extracellular media. Although we show that some of the Phe is uptaken, it does not completely account for the loss in the media. One possibility is that during the night, Phe is converted extracellularly into a different product by the action of a secreted protein. Future work could be directed at analyzing the extracellular metabolite content since our methods only quantify the aromatic amino acids. However, it is also possible that Phe is converted intracellularly to a different product. Recently, dynamic metabolomics analysis of PCC 11801 during diurnal cycle has shown accumulation of gamma glutamyl dipeptides of phenylalanine in the dark phase and suggested that this is one of the potential reservoirs of these amino acids (Jaiswal et al., 2022; Jaiswal & Wangikar, 2020). Further investigation is required to determine if this is still the case for the Phe overproducing mutants M14 and M14.2. Diurnal Phe labelling experiments can be performed to investigate this where just before dark, media is switched to Phe labelled media and cells are subsequently harvested just prior to illumination for untargeted metabolomics. If so, future work should investigate the role of gamma glutamyl dipeptides of Phenylalanine in Phe overproducing strains.

From a commercial perspective, uptake of product under dark, such as Phe in our study is not ideal to maximize productivity. Since our work selected strains under continuous illumination and subsequently adapted our strains to diurnal conditions, it will be interesting to understand if selection under diurnal conditions also results in the same phenotype or if strains that do not uptake Phe under dark can be identified.

However, our development of strains for the production of 2-PE highlights the challenges in metabolic engineering of PCC 11801. Although some successful transformants were identified, their genetic instability led loss of 2-PE production phenotype. Further, bottlenecks in 2-PE production were highlighted such as native alcohol dehydrogenases that result in the accumulation of phenylacetaldehyde. Further work in development of synthetic biology tools specialized for PCC 11801 is needed for addressing genetic instability and well as improving the transformation efficiency.

Commercial scale deployment of cyanobacteria will require further increases in titer and productivity as well as process engineering for economical scale up. We lay a foundation for

further development of fast-growing strains for Phe production using metabolic engineering as more synthetic biology tools emerge.

3.6 Acknowledgements

I would like to thank the National Biodiversity Authority of India for approval in the procurement of the strain *Synechococcus elongatus* sp PCC 11801 from Dr. Wangikar's lab at Indian Institute of Technology, Bombay, India. I would also like to thank Dr. Pramod Wangikar and his lab for providing the strain as well as protocols related to cultivation of the strain. I would also like to thank the Purdue Research Foundation and the Office of Technology Commercialization for all their assistance and guidance in filing a US provisional patent application that contains parts of this chapter.

3.7 Conflict of Interest

I report that part of this work is included in an US provisional patent application No. 63219691 filed by Purdue Research Foundation with inventors listed as the Arnav Deshpande and Dr. John A. Morgan.

3.8 References

Atsumi, S., Hanai, T., & Liao, J. C. (2008). Non-fermentative pathways for synthesis of branched-chain higher alcohols as biofuels. *Nature*, *451*(7174), 86–89. https://doi.org/10.1038/nature06450

Bongaerts, J., Krämer, M., Müller, U., Raeven, L., & Wubbolts, M. (2001). Metabolic engineering for microbial production of aromatic amino acids and derived compounds. *Metabolic Engineering* (Vol. 3, Issue 4, pp. 289–300). Academic Press Inc. https://doi.org/10.1006/mben.2001.0196

Bose, J. L. (2016). Chemical and UV Mutagenesis. In J. L. Bose (Ed.), *The Genetic Manipulation of Staphylococci: Methods and Protocols* (pp. 111–115). Springer New York. https://doi.org/10.1007/7651_2014_190

Brandenburg, F., Theodosiou, E., Bertelmann, C., Grund, M., Klähn, S., Schmid, A., & Krömer, J. O. (2021). Trans-4-hydroxy-L-proline production by the cyanobacterium Synechocystis sp. PCC 6803. *Metabolic Engineering Communications*, *12*. https://doi.org/10.1016/j.mec.2020.e00155

Brey, L. F., Włodarczyk, A. J., Bang Thøfner, J. F., Burow, M., Crocoll, C., Nielsen, I., Zygadlo Nielsen, A. J., & Jensen, P. E. (2020). Metabolic engineering of *Synechocystis* sp. PCC 6803 for the production of aromatic amino acids and derived phenylpropanoids. *Metabolic Engineering*, *57*, 129–139. https://doi.org/10.1016/j.ymben.2019.11.002

Deshpande, A., Vue, J., & Morgan, J. (2020). Combining Random Mutagenesis and Metabolic Engineering for Enhanced Tryptophan Production in *Synechocystis* sp. Strain PCC 6803. https://doi.org/10.1128/AEM

Dookeran, Z. A., & Nielsen, D. R. (2021). Systematic Engineering of Synechococcus elongatus UTEX 2973 for Photosynthetic Production of l-Lysine, Cadaverine, and Glutarate. *ACS Synthetic Biology*, *10*(12), 3561–3575. https://doi.org/10.1021/acssynbio.1c00492

Etschmann, M., Bluemke, W., Sell, D., & Schrader, J. (2002). Biotechnological production of 2-phenylethanol. In *Applied Microbiology and Biotechnology* (Vol. 59, Issue 1, pp. 1–8). https://doi.org/10.1007/s00253-002-0992-x

Etschmann, M. M. W., Huth, I., Walisko, R., Schuster, J., Krull, R., Holtmann, D., Wittmann, C., & Schrader, J. (2015). Improving 2-phenylethanol and 6-pentyl-α-pyrone production with fungi by microparticle-enhanced cultivation (MPEC). *Yeast*, *32*(1), 145–157. https://doi.org/https://doi.org/10.1002/yea.3022

Hall, G., Flick, M., Gherna, R., & Jensen, R. (1982). Biochemical diversity for biosynthesis of aromatic amino acids among the cyanobacteria. *Journal Of Bacteriology*, *149*(1), 65-78. doi: 10.1128/jb.149.1.65-78.1982

Hall, G., & Jensen, R. (1980). Enzymological Basis for Growth Inhibition by l -Phenylalanine in the Cyanobacterium Synechocystis sp. 29108. *Journal Of Bacteriology*, *144*(3), 1034-1042. doi: 10.1128/jb.144.3.1034-1042.1980

Hassing, E. J., de Groot, P. A., Marquenie, V. R., Pronk, J. T., & Daran, J. M. G. (2019). Connecting central carbon and aromatic amino acid metabolisms to improve de novo 2-phenylethanol production in Saccharomyces cerevisiae. *Metabolic Engineering*, *56*, 165–180. https://doi.org/10.1016/j.ymben.2019.09.011

Ikehata, H., & Ono, T. (2011). The mechanisms of UV mutagenesis. In *Journal of Radiation Research* (Vol. 52, Issue 2, pp. 115–125). Oxford University Press. https://doi.org/10.1269/jrr.10175

Jaiswal, D., Sengupta, A., Sohoni, S., Sengupta, S., Phadnavis, A. G., Pakrasi, H. B., & Wangikar, P. P. (2018). Genome Features and Biochemical Characteristics of a Robust, Fast Growing and Naturally Transformable Cyanobacterium Synechococcus elongatus PCC 11801 Isolated from India. *Scientific Reports*, *8*(1). https://doi.org/10.1038/s41598-018-34872-z

Jones, P. R. (2014). Genetic instability in cyanobacteria - An elephant in the room? *Frontiers in Bioengineering and Biotechnology*, *2*(MAY). https://doi.org/10.3389/fbioe.2014.00012

Liu, X., Niu, H., Li, Q., & Gu, P. (2019). Metabolic engineering for the production of l-phenylalanine in Escherichia coli. *3 Biotech*, *9*(3), 85. https://doi.org/10.1007/s13205-019-1619-6

Liu, Y., Xu, Y., Ding, D., Wen, J., Zhu, B., & Zhang, D. (2018). Genetic engineering of Escherichia coli to improve L-phenylalanine production. *BMC Biotechnology*, *18*(1). https://doi.org/10.1186/s12896-018-0418-1

Montesinos, M., Herrero, A., & Flores, E. (1997). Amino acid transport in taxonomically diverse cyanobacteria and identification of two genes encoding elements of a neutral amino acid permease putatively involved in recapture of leaked hydrophobic amino acids. *Journal Of Bacteriology*, *179*(3), 853-862. doi: 10.1128/jb.179.3.853-862.1997

Ni, J., Liu, H., Tao, F., Wu, Y., & Xu, P. (2018). Remodeling of the Photosynthetic Chain Promotes Direct CO 2 Conversion into Valuable Aromatic Compounds . *Angewandte Chemie*, *130*(49), 16222–16226. https://doi.org/10.1002/ange.201808402

Oliver, J. W. K., Machado, I. M. P., Yoneda, H., & Atsumi, S. (2013). Cyanobacterial conversion of carbon dioxide to 2,3-butanediol. *Proceedings of the National Academy of Sciences of the United States of America*, *110*(4), 1249–1254. https://doi.org/10.1073/pnas.1213024110

Packer, M. S., & Liu, D. R. (2015). Methods for the directed evolution of proteins. In *Nature Reviews Genetics* (Vol. 16, Issue 7, pp. 379–394). Nature Publishing Group. https://doi.org/10.1038/nrg3927

Riccardi, G., de Rossi, E., & Milano, A. (1989). Amino acid biosynthesis and its regulation in cyanobacteria. *Plant Science*, *64*(2), 135-151. doi: 10.1016/0168-9452(89)90018-6

Rippka, R., Stanier, R., Deruelles, J., Herdman, M., & Waterbury, J. (1979). Generic Assignments, Strain Histories and Properties of Pure Cultures of Cyanobacteria. *Microbiology*, *111*(1), 1-61. doi: 10.1099/00221287-111-1-1

Sakai, M., Hirata, H., Sayama, H., Sekiguchi, K., Itano, H., Asai, T., Dohra, H., Hara, M., & Watanabe, N. (2007). Production of 2-phenylethanol in roses as the dominant floral scent compound from L-phenylalanine by two key enzymes, a PLP-dependent decarboxylase and a phenylacetaldehyde reductase. *Bioscience, Biotechnology and Biochemistry*, *71*(10), 2408–2419. https://doi.org/10.1271/bbb.70090

Santos-Merino, M., Torrado, A., Davis, G. A., Röttig, A., Bibby, T. S., Kramer, D. M., & Ducat, D. C. (2021). *Improved photosynthetic capacity and photosystem I oxidation via heterologous metabolism engineering in cyanobacteria*. *118*(11). https://doi.org/10.1073/pnas.2021523118/-/DCSupplemental

Schipper, K., Das, P., al Muraikhi, M., AbdulQuadir, M., Thaher, M. I., al Jabri, H. M. S. J., Wijffels, R. H., & Barbosa, M. J. (2021). Outdoor scale-up of Leptolyngbya sp.: Effect of light intensity and inoculum volume on photoinhibition and -oxidation. *Biotechnology and Bioengineering*, *118*(6), 2368–2379. https://doi.org/10.1002/bit.27750

Sengupta, S., Jaiswal, D., Sengupta, A., Shah, S., Gadagkar, S., & Wangikar, P. P. (2020). Metabolic engineering of a fast-growing cyanobacterium Synechococcus elongatus PCC 11801 for photoautotrophic production of succinic acid. *Biotechnology for Biofuels*, *13*(1). https://doi.org/10.1186/s13068-020-01727-7

Sikora, A., Mielecki, D., Chojnacka, A., Nieminuszczy, J., Wrzesiński, M., & Grzesiuk, E. (2010). Lethal and mutagenic properties of MMS-generated DNA lesions in Escherichia coli cells deficient in BER and AlkB-directed DNA repair. *Mutagenesis*, *25*(2), 139–147. https://doi.org/10.1093/mutage/gep052

Singh, A. K., Kishore, G. M., & Pakrasi, H. B. (2018). Emerging platforms for co-utilization of one-carbon substrates by photosynthetic organisms. In *Current Opinion in Biotechnology* (Vol. 53, pp. 201–208). Elsevier Ltd. https://doi.org/10.1016/j.copbio.2018.02.002

Stark, D., Münch, T., Sonnleitner, B., Marison, I. W., & von Stockar, U. (2002). Extractive bioconversion of 2-phenylethanol from L-phenylalanine by Saccharomyces cerevisiae. *Biotechnology Progress*, *18*(3), 514–523. https://doi.org/10.1021/bp020006n

Tillich, U. M., Lehmann, S., Schulze, K., Dühring, U., & Frohme, M. (2012). The Optimal Mutagen Dosage to Induce Point-Mutations in Synechocystis sp. PCC6803 and Its Application to Promote Temperature Tolerance. *PLoS ONE*, *7*(11). https://doi.org/10.1371/journal.pone.0049467

van Alphen, P., Abedini Najafabadi, H., Branco dos Santos, F., & Hellingwerf, K. J. (2018). Increasing the Photoautotrophic Growth Rate of Synechocystis sp. PCC 6803 by Identifying the Limitations of Its Cultivation. *Biotechnology Journal*, *13*(8). https://doi.org/10.1002/biot.201700764

Wang, Y., Zhang, H., Lu, X., Zong, H., & Zhuge, B. (2019a). Advances in 2-phenylethanol production from engineered microorganisms. In *Biotechnology Advances* (Vol. 37, Issue 3, pp. 403–409). Elsevier Inc. https://doi.org/10.1016/j.biotechadv.2019.02.005

Wang, Y., Zhang, H., Lu, X., Zong, H., & Zhuge, B. (2019b). Advances in 2-phenylethanol production from engineered microorganisms. In *Biotechnology Advances* (Vol. 37, Issue 3, pp. 403–409). Elsevier Inc. https://doi.org/10.1016/j.biotechadv.2019.02.005

Wani, M. A., Sanjana, K., Kumar, D. M., & Lal, D. K. (2010). GC – MS analysis reveals production of 2 – Phenylethanol from Aspergillus niger endophytic in rose. *Journal of Basic Microbiology*, *50*(1), 110–114. https://doi.org/https://doi.org/10.1002/jobm.200900295

Włodarczyk, A., Selão, T. T., Norling, B., & Nixon, P. J. (2020). Newly discovered Synechococcus sp. PCC 11901 is a robust cyanobacterial strain for high biomass production. *Communications Biology*, *3*(1). https://doi.org/10.1038/s42003-020-0910-8

Zerulla, K., Ludt, K., & Soppa, J. (2016). The ploidy level of synechocystis sp. PCC 6803 is highly variable and is influenced by growth phase and by chemical and physical external parameters. *Microbiology (United Kingdom)*, *162*(5), 730–739. https://doi.org/10.1099/mic.0.000264

Zhang, B., Wu, J., & Meng, F. (2021). Adaptive Laboratory Evolution of Microalgae: A Review of the Regulation of Growth, Stress Resistance, Metabolic Processes, and Biodegradation of Pollutants. *Frontiers in Microbiology* (Vol. 12). Frontiers Media S.A. https://doi.org/10.3389/fmicb.2021.737248

Zhang, H., Cao, M., Jiang, X. *et al*. *De-novo* synthesis of 2-phenylethanol by *Enterobacter*sp. CGMCC 5087. *BMC Biotechnol* **14,** 30 (2014). https://doi.org/10.1186/1472-6750-14-30

4. EFFECT OF PHENYLALANINE SINK IN SYNECHOCOCCUS ELONGATUS PCC 11801 ON PHOTOSYNTHESIS

4.1 Abstract

Cyanobacteria are a promising chassis that can utilize CO_2 and sunlight to produce valuable biochemicals in a sustainable manner. However, low productivity is a major bottleneck to the economical scale up of cyanobacteria. Recent studies have shown that introduction of a heterologous sink, such as sucrose, 2,3 butanediol, and 2-phenyl ethanol, improves carbon fixation by relieving the "sink" limitation of photosynthesis. However, behavior of this sink-derived enhancement in carbon fixation and the effect on ATP/NADPH ratio is not well understood under different light conditions. In this study, we utilize engineered *Synechococcus elongatus* PCC 11801 phenylalanine (Phe) overproducing strains to show the effect of different light conditions on total carbon fixation. We find that low light condition results in competition between biomass and Phe sink whereas under excess light, the high flux of fixed carbon is directed solely to the Phe sink. We further show that the introduction of the Phe sink improves the quantum yield of photosystem I and II with a concomitant increase in the total electron flow. An imbalance in the synthesis and consumption of ATP and NADPH can lead to inefficient photosynthesis. The introduction of new carbon sink can further affect the ATP to NADPH ratio. In this work, we use photosystem I re-reduction kinetics to show that cyclic electron flow is decreased with the introduction of the Phe sink so as to decrease the ATP/NADPH ratio. Our data highlight the importance of light in controlling the sink-derived enhancement in carbon fixation, the role of CEF to balance the source-sink demand for ATP and NADPH, and that introduction of even homologous overflow sinks can improve carbon fixation.

4.2 Introduction

Cyanobacteria are promising hosts for engineering due to their ability to use sunlight and CO_2 to produce biochemicals and biofuels sustainably (Knoot et al., 2018). However, industrial application of cyanobacteria requires addressing several barriers which are not limited to economical scale up and improving product titers (Q. Huang et al., 2017). Improving the rate of carbon fixation, and thus the productivity of growth associated bio-products can improve the

feasibility of cyanobacteria in industrial applications (Jaiswal et al., 2022). Approaches to improve carbon fixation by improving the photosynthetic efficiency have been directed at engineering of ribulose-1,5-bisphosphate carboxylase/oxygenase (RuBisCO) (Whitney et al., 2011) (Liang et al., 2018), enabling greater light penetration, for example by engineering reduction in antenna size (Kirst et al., 2014), or engineering the Calvin Benson-Bassham (CBB) cycle (Liang et al., 2018).

Recently, it has been shown that engineering the heterologous production of biochemicals ("sink engineering") in cyanobacteria has led to the unexpected result of increased carbon fixation (Zhang et al., 2017). Strains of cyanobacteria engineered to produce biochemicals such as sucrose (Abramson et al., 2016) (Santos-Merino, Torrado, et al., 2021a), 2,3-butendiol (Oliver & Atsumi, 2015), 2-phenylethanol (Ni et al., 2018), glycerol (Savakis et al., 2015), ethylene (Ungerer et al., 2012) have shown increased carbon fixation ability. However, neither the underlying mechanism nor the effect of light conditions is well understood. Investigating the dynamics of this source-sink dynamics is particularly important in evaluating and improving the feasibility of cyanobacteria in industrial applications where light conditions can vary substantially.

It has been previously hypothesized that under excess light, introduction of a heterologous sink can improve the utilization of the excess light energy (Grund et al., 2019). However, it was shown recently shown that a sucrose sink showed highest improvement in photosynthetic flux at low light whereas under high light, an electron sink, cytochrome P450 led to photosynthetic enhancement (Santos-Merino, Torrado, et al., 2021). Furthermore, the extent of photosynthetic enhancement was substantially lower compared to the enhancement achieved in carbon fixation (Santos-Merino, Torrado, et al., 2021).

Introduction of a heterologous sink can result in the change of adenosine triphosphate (ATP)/nicotinamide adenine dinucleotide phosphate (NADPH) ratio requirements, and it is an important factor to improve photosynthetic productivity (Kramer & Evans, 2011; Erdrich et al., 2014). Linear electron flow (LEF) through the photosystem II (PSII) and photosystem I (PSI) in cyanobacteria generates ATP/NADPH ratio of 1.38 whereas the CBB cycle requires ATP/NADPH ratio of 1.5. Alternate electron flow (AEF), one of which is cyclic electron flow (CEF) around PSI produces only ATP and can be a source to address this imbalance (Nogales et al., 2012) (Allen, 2003). However, the effect of heterologous sink on LEF and CEF under different light conditions remains unclear in cyanobacteria. Figure 4.1 shows the photosynthetic machinery, electron flow,

Phenylalanine (Phe) sink, ATP/NADPH production and demands as well as photosynthetic inhibitors used in this study.

In our previous work, we showed that even overproduction by a homologous Phe sink in the fast-growing cyanobacteria strain *Synechococcus elongatus* PCC 11801 can show increased C fixation (Chapter 3). This indicated that not only heterologous sinks but native products too can be used as efficient sinks to improve carbon fixation. In this work, we utilize Phe overproducing strains to study the effect of different light conditions on carbon sink performance by studying Phe and biomass productivity, PSII efficiency and non-photochemical quenching and PSI donor and acceptor side limitations. We also study the effect of the Phe sink on LEF and CEF, thus altering the ratio of ATP/NADPH production.

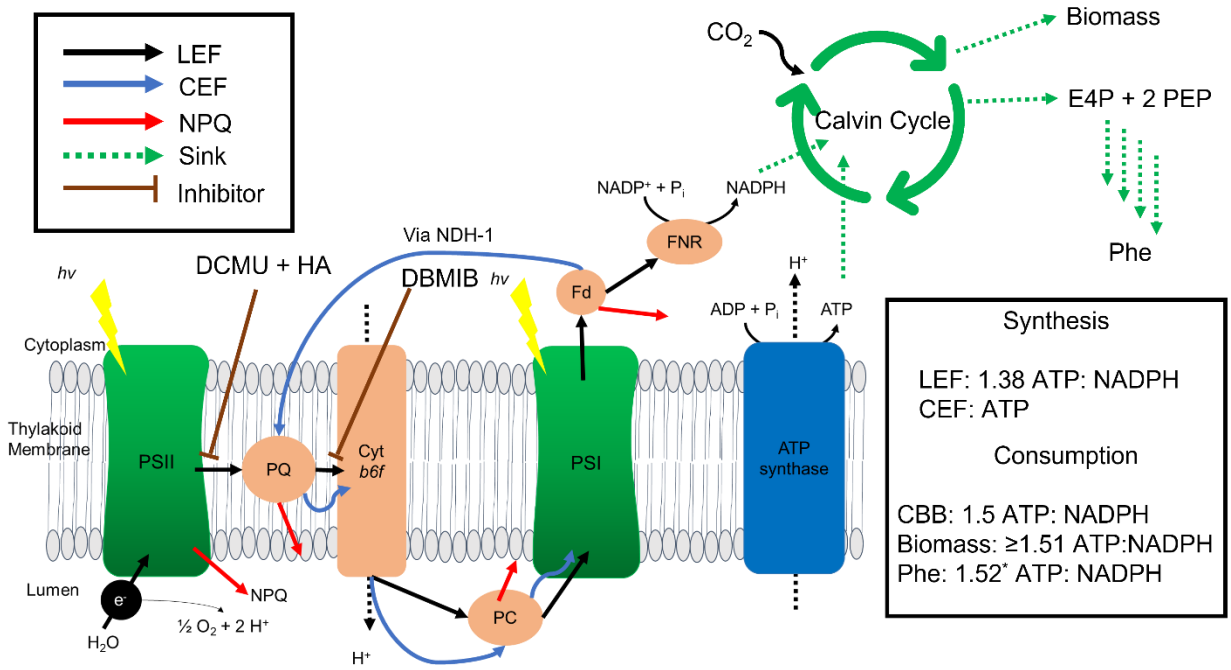

Figure 4.1 Schematic representation of photosynthetic machinery showing electron transfer pathways, non-photochemical quenching pathways, action of inhibitors, Calvin cycle, Biomass and Phe sinks, and ATP/NADPH production and consumption. * variable depending of N source, carbon uptake, amino acid re-uptake, C recycling etc.

Abbreviations: photosystem II (PSII), photosystem I (PSI), Plastoquinone (PQ), Plastocyanin (PC), Cytochrome *b6f* (Cyt *b6f*), Linear electron flow (LEF), Cyclic electron flow (CEF), Non-photochemical quenching (NPQ), Calvin Benson Bassham (CBB), Phenylalanine (Phe), Phosphoenolpyruvate (PEP), Erythrose-4-phosphate (E4P), Hydroxylamine (HA), 3-(3,4-dichlorophenyl)-1,1-dimethylurea (DCMU), Dibromothymoquinone (DBMIB), Ferridoxin $NADP^+$ oxidoreductase (FNR), Ferridoxin (Fd)

4.3 Materials and Methods

4.3.1 Strains and culture conditions

Synechococcus elongatus PCC 11801 (PCC 11801) was procured from Dr. Wangikar, Indian Institute of Technology, Bombay (Jaiswal et al., 2018). Phenylalanine overproducing mutants M14 and M14.2 were previously developed in our lab by ultraviolet (UV) irradiation induced random mutagenesis followed by selection using Phe analog 3-(2-thienyl)-dl-alanine (Chapter 3).

All the strains were cultured 250 mL Erlenmeyer flasks with a culture volume of 50 mL at 38°C, under ambient CO_2 and shaken at 200 rpm in modified BG-11 medium (BG-11M) in an incubator shaker (Infors HT Minitron) or in a warm room. BG-11 (Rippka et al., 1979) was modified by an additional 1 g/L sodium nitrate, 20 mg/L magnesium sulfate heptahydrate, 40 mg/L potassium phosphate, 10 mg/L ammonium chloride and 1 mL of A5 trace metal solution to develop the BG-11M media. Cultures were routinely maintained at a light intensity 240 µmol-photons/m^2/s or as otherwise specified.

4.3.2 Strains and culture conditions

The growth of cultures was measured using optical density at 730 nm (OD_{730}) using a Beckman DU Series 500 spectrophotometer. A linear relationship between the dry cell weight (DCW) and optical density was established to be 0.40 g (dry cell weight)/liter/OD_{730}. Briefly, cultures at different stages of growth were pelleted, washed with ultrapure water, and filtered onto pre-weighed 0.8 µm filters and dried at 65°C until weight remained constant. A linear fit was used to determine the relationship between DCW and OD_{730}.

Phenylalanine was quantified as previously described using LC-MS/MS (Deshpande et al., 2020). Briefly, 1 mL of culture was centrifuged to remove the supernatant, diluted to an appropriate volume, transferred to a glass vial and stored at -20°C for upto a week before injection into the LC-MS/MS.

4.3.3 Carbon (C) and Nitrogen (N) content of biomass

Cultures were grown in triplicates and biomass was dried at 65°C in clean glass vials until weight remained constant. 0.5 mg of samples were accurately weighed into tin capsules and the C and N fractions were analyzed using Sercon 20-22 elemental analyzer isotope ratio mass

spectrometer (EA-IRMS) by the Purdue Stable Isotope Facility. NIST 1547 was used as the standard reference material.

4.3.4 Measurement of Chlorophyll a, and carotenoid content

Chl a and carotenoid content was measured as previously described (Ritchie, 2006), (Porra, 1989). Briefly, cells were grown at different light intensities (40, 240, and 1000 µmol-photons/m^2/s) and harvested at 0.8-1 OD_{730}. 2 mL of culture was centrifuged at 4°C at 7000 rpm for 5 mins. Supernatant was removed and the cultures were resuspended in either chilled methanol or 80% acetone at 4°C and incubated on ice for 10-20 mins. Samples were centrifuged again, and the absorbance was measured using either Beckman DU Series 500 spectrophotometer or U-3900 Head-on PMT. For methanol extraction Chl a and carotenoids were quantified using equation 1 and 3 respectively and for 80% acetone extraction, Chl a was quantified using equation 2.

$$Chla\ \left(\frac{\mu g}{ml}\right) = 12.9447\ (A_{665} - A_{720}) \tag{1}$$

$$Chla\ \left(\frac{\mu g}{ml}\right) = 12.25\ (A_{663.6} - A_{750}) - 2.55\ (A_{646.6} - A_{750}) \tag{2}$$

$$Carotenoids\ \left(\frac{\mu g}{ml}\right) = [1000\ (A_{470} - A_{720}) - 2.86\ (Chla\left(\frac{\mu g}{ml}\right)]/221 \tag{3}$$

The whole cell absorption spectra was obtained for the wild type and M14.2 by measuring the absorbance spectra from 350 to 750 nm using Molecular Devices SpectraMax M2 spectrophotometer and normalizing it to the optical density OD_{730}.

4.3.5 Pulse Amplitude Modulated (PAM) fluorometry

Cultures were grown to OD_{730}~0.8 in triplicates under either 40, 240 or 1000 µmol-photons/m^2/s depending on the actinic light intensity to be tested using PAM measurements. All the cultures were centrifuged, and the cells resuspended in fresh BG-11M media prior to measurements. All PAM measurements were performed in a warm room maintained at 38°C using a Hansatech pulse amplitude modulated (PAM) fluorescence monitoring system (FMS1) (Norfolk, England) with an emitter-detector unit. A DW2/2 liquid phase electrode chamber (Hansatech Instruments) was used to hold 2 mL the sample. Different intensities of actinic light (40, 240 or 1000 µmol-photons/m^2/s) was provided by internal optics of FMS1. The samples were stirred using a micro magnetic stirrer. All samples were dark adapted for 3 mins prior to measurements

of which the last 30s were recorded to measure the minimum fluorescence F_0 with an illuminating light (≤ 0.01 µmol-photons/m^2/s). Maximum fluorescence for dark adapted state (F_M) was determined using 0.8 s pulse of white actinic light at 13,000 µmol-photons/m^2/s. Actinic light was then switched on with either 40, 240 or 1000 µmol-photons/m^2/s depending on the experiment. Six more saturating pulses were applied 60 s apart and the last one used for determination of F_m' when a steady fluorescence signal (F_s) had been obtained. Actinic light was subsequently switch off to determine F_0'. Finally, F_m^{DCMU} was determined by addition of 20 µM 3-(3,4-dichlorophenyl)-1,1-dimethylurea (DCMU) and switching on the actinic light (1000 µmol-photons/m^2/s) (Campbell et al., 1998). A typical trace obtained using our procedure is shown in figure 4.2.

Effective quantum yield; $\Phi_{PSII} = (F_m' - F_s)/F_m'$, Maximum quantum yield; $\Phi_{PSIImax} = (F_m^{DCMU} - F_0)/F_m^{DCMU}$, photochemical quenching; $q_P = (F_m' - F_s)/(F_m' - F_0')$, Estimate of fraction of open PSII centres; $q_L = (F_m' - F_s)/[(F_m' - F_0) \times (F_0'/F_s)]$, non-photochemical quenching; $NPQ = (F_m^{DCMU} - F_m')/F_m'$, relative electron transport rate through PSII; $rETR2 = \Phi_{PSII} \times PAR$, were calculated as previously described (Genty et al., 1989), (Ralph & Gademann, 2005), (Baker, 2008).

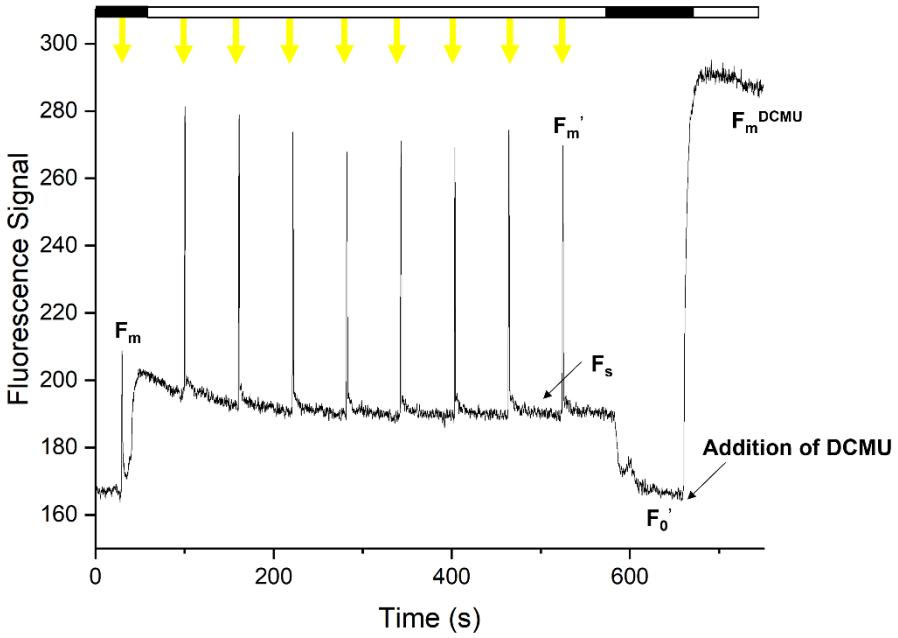

Figure 4.2 Typical PAM fluorescence trace obtained. The bar on the top represents the light condition. Black indicates dark whereas white indicates illumination with actinic light with intensity dependent on the individual experiment. The yellow arrows indicate a saturating light pulse. Addition of DCMU, and parameters are as indicated.

4.3.6 P700 Spectroscopy

Synechococcus cultures were grown in biological triplicates at 240 µmol photons m^{-2} s^{-1} white light until they reached mid-exponential growth phase. Chl concentrations were determined as outlined in Section 4.3.4. Samples were then centrifuged and resuspended in fresh BG-11M medium to a Chl concentration of 10 µg/mL. P700 absorbance measurements were made by a JTS-10 spectrophotometer (SpectroLogiX) using 630 nm actinic light and 705 nm measuring light. Samples were dark-adapted for 3 minutes and mixed by pipetting right before measurements were taken. Basal P700 absorbance after dark adaptation was monitored with the measuring light on for 10 s. Samples were subsequently treated for 10 s with a 720 nm far red light (200 µmol photons m^{-2} s^{-1}) to avoid acceptor-side limitation of PSI. Enabling the measurement, this background illumination also induces a donor-side limitation due to its preferential excitation of PSI over PSII. Interestingly, the far-red light, with a wavelength that overlaps slightly with the measuring light, causes a positive P700 absorption signal likely due to contamination of the detector unit. A 630 nm 250 ms-long saturating pulse (2600 µmol photons m^{-2} s^{-1}) was then applied at the end of the far-red light to determine P_m, the maximally oxidized P700 signal. Actinic light (45, 320, or 940 µmol photons m^{-2} s^{-1}) was immediately switched on for 5s to record the intermediately oxidized P700 signal denoted as P. A second saturating pulse was then applied at the end of the actinic light to determine P_m' and the dark rereduction of P700 was followed for 7 s. The stable P700 absorbance signal was noted as P_0. Interestingly we find our Pm values to be consistently lower than the P_m' values, an observation also noted by other cyanobacterial studies. We therefore estimated P_m in the presence of 40 µM DCMU and 2 mM hydroxylamine (HA) as previously described (Vega de Luna et al., 2020). The P700 absorbance signal was further corrected by the subtraction of a contaminating signal from chlorophyll fluorescence, as determined by the measurement of the sample under actinic illumination without the probe light. A representative trace is shown in figure 4.3. Each trace was an average of five runs. Photosystem I quantum yield $Y(I) = (P_m' - P)/(P_m - P_0)$, quantum yield of non-photochemical energy dissipation due to donor side limitation $Y(ND) = (P - P_0)/(P_m - P_0)$, and quantum yield of non-photochemical energy dissipation due to acceptor side limitation $Y(NA) = (P_m - P_m')/(P_m - P_0)$ were calculated as previously described (Klughammer & Schreiber, 1994). The sum of Y(I), Y(ND), and Y(NA) is 1. Relative electron transport rate through PSI is calculated as rETR1 = ΦPSI × PAR.

The percentage of cyclic electron flow and total relative electron flow are determined as described previously from P700 rereduction kinetics by fitting first order exponential decay equation to determine half times. P700 oxidation kinetics were also determined similarly by fitting a first order reaction model to determine the half times as previously described (Berla et al., 2015). To measure cyclic electron flow around PSI, linear electron transport was blocked by the addition of PSII-specific inhibitors 40 µM DCMU and 2 mM HA. Measurements were also carried out under 40 µM dibromothymoquinone (DBMIB), a cyt b6f complex-targeted inhibitor of both linear and cyclic electron transport pathways.

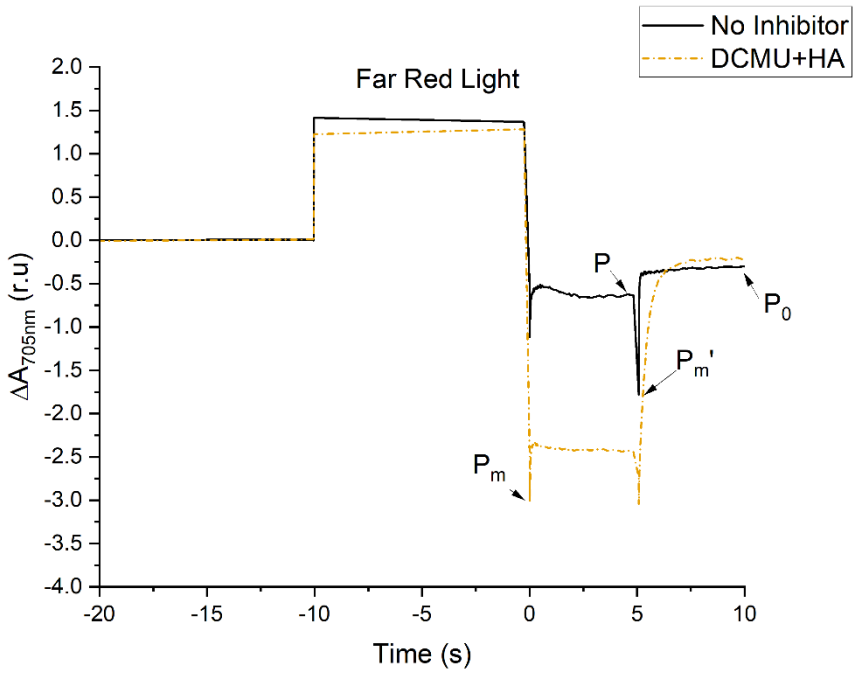

Figure 4.3 Typical P700 absorbance change trace obtained. The solid line represents trace obtained with no inhibitor whereas the dotted line represents the trace with inhibitor DCMU + HA. Trace with addition of DBMIB is not shown. PSI parameters used to estimate Y(I), Y(ND), and Y(NA) are shown. P_M, the maximum oxidation is determined by the addition of inhibitors as previously described in (Klughammer & Schreiber, 1994).

4.3.7 Statistical Analysis

All the data are shown as mean values with errors representing standard deviation of three or more biological replicates unless stated otherwise. Difference between measurements is compared by unpaired student's t-test unless stated otherwise. Statistical analyses were carried out

with either Microsoft Excel or by Origin 2021b (OriginLab). The criteria for statistical significance was set as $p<0.05$.

4.4 Results

Introduction of Phe sink enhanced carbon fixation (Chapter 3). In this work, we study two Phe overproducers M14 and M14.2, with increasing flux to the Phe sink as well as the wild type PCC 11801 which does not direct significant flux to Phe that is secreted.

In order to determine the effect of light conditions on enhancement in carbon fixation by the Phe sink, we decided to test three light intensities. Unless stated otherwise, low light (LL) was chosen as 40 µmol-photons/m^2/s to represent a light limited state whereas 240 µmol-photons/m^2/s was chosen as moderate light (ML) and 1000 µmol-photons/m^2/s as high light (HL) conditions.

4.4.1 Enhancement in C fixation by Phe sink is light dependent

Previously, it was hypothesized that engineering heterologous sinks could utilize excess light energy to achieve enhanced carbon fixation (Grund et al., 2019). We decided to test the effect of LL, ML, and HL conditions and hypothesized that under light (source)-limited condition, we would not see any enhancement of carbon fixation. We further hypothesized that the engineered Phe sink will affect biomass accumulation as it will compete for ATP and NADPH with anabolic pathways under light limited conditions. To minimize the effect of self-shading and the resultant change in light availability, all experiments were performed with low density cell cultures from early growth phase (see figure 4.4).

Figure 4.4 shows the contribution of Phe and biomass sink to the total carbon fixed under different light conditions in WT and Phe sink engineered strains M14 and M14.2. The total carbon fixed was calculated by determining the carbon content in the two sinks, biomass, and excreted Phe (C% = 65.43). To determine the carbon content in biomass of different strains, elemental analysis of biomass was performed and the C% and N% is shown in Table 4.1.

Table 4.1 Carbon and Nitrogen content of biomass in WT, M14 and M14.2. Each measurement represents the mean and standard deviation of three biological replicates grown at 38°C and 240 µmol photons $m^{-2}s^{-1}$ light intensity at ambient CO_2

Strain	Carbon (%)	Nitrogen (%)
WT	50.60±1.00	11.56±0.16
M14	47.4±1.06	11.38±0.21
M14.2	48.20±0.65	11.11±0.31

The mean C% and N% for both M14 and M14.2 were lower when compared to the WT, however these differences were not statistically significant ruling out the possibility that Phe overproduction was achieved by partially diverting carbon and nitrogen from the biomass to the Phe sink.

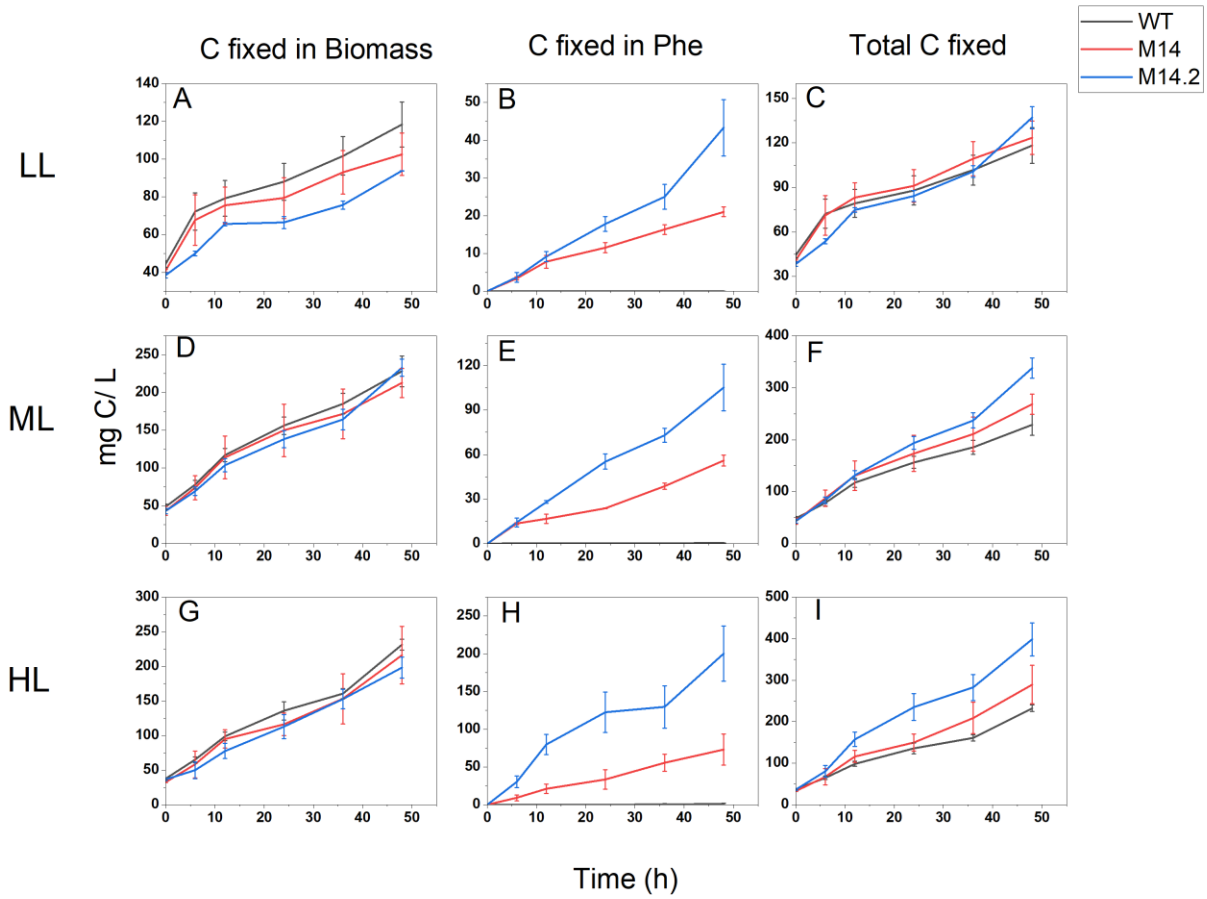

Figure 4.4 Distribution of photosynthetically fixed carbon to the biomass, Phe sink and their total (Biomass+Phe sink) in WT, M14 and M14.2 under LL (A-C), ML (D-F) and HL (G-I) conditions. Data represents mean and standard deviation of three biological replicates inoculated

Figure 4.4 continued

at the same density and cultured at 38°C and ambient CO_2. The x-axis represents time in hours and the y-axis represents carbon content in mg/L.

Figure 4.4 shows that the total carbon fixation increases with increase in light intensity as expected. All three strains show highest carbon fixation in the HL condition, which is the optimum light condition for PCC 11801 (Jaiswal et al., 2018). Under ML and HL, biomass production is not affected with the introduction of Phe sink (figure 4.4D and G), and the Phe production (figure 4.4 E and H) is achieved entirely by enhancing the carbon fixation. It should be noted that more than 95% of the overproduced Phe in M14 and M14.2 is excreted out of the cell into the growth media while the wild type cultures do not contain any measurable Phe in their growth media. It is likely that the enhancement of carbon fixation observed in Phe overproducing strains requires excretion of the new homologous carbon sink. Under LL (sink limitation), the Phe sink causes a reduction in the biomass accumulation (figure 4.4A) while the total carbon fixed is not affected in M14 (figure 4.5A). M14.2, interestingly, shows a minor increase in total carbon fixed (figure 4.5 A), likely due to contribution from Phe sink (figure 4.4B).

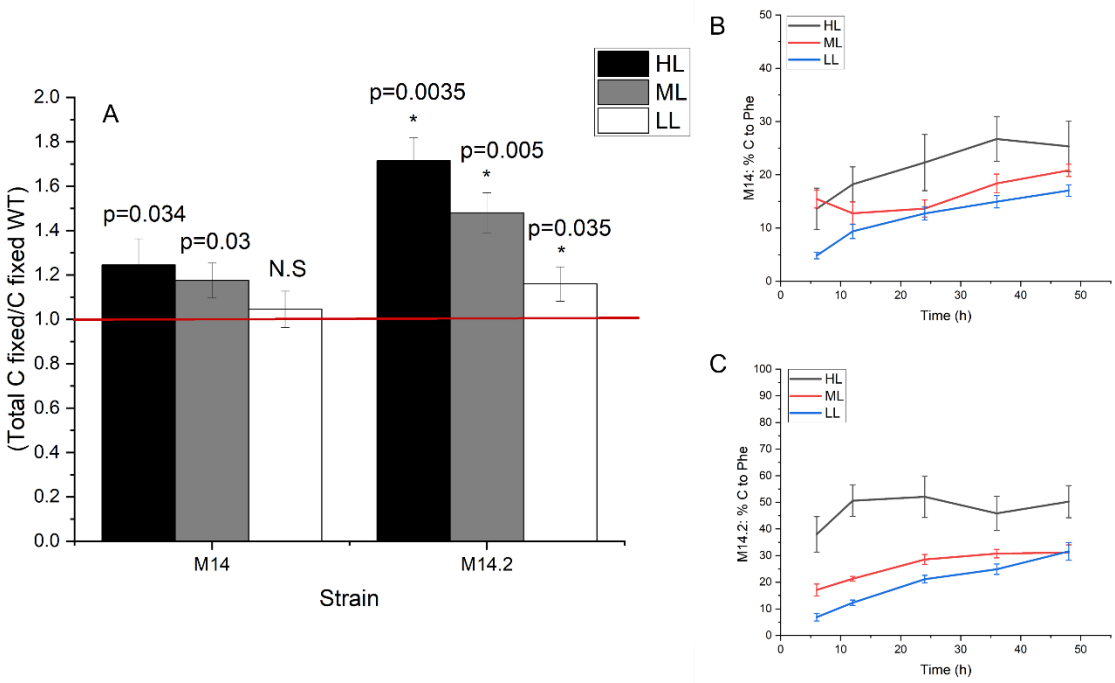

Figure 4.5 (A) Ratio of total carbon fixed by M14 and M14.2 with the WT at the end of 2 days. Statistical comparison was performed with a one sample t-test with the null hypothesis mean ≤ 1. Percentage of carbon that is diverted to the Phe sink under different light conditions in (B) M14 and (C) M14.2. Data represents mean and standard deviation of three biological replicates inoculated at the same density and cultured at 38°C and ambient CO_2.

Our results support the hypothesis that under light limited conditions, the biomass and Phe sinks compete for energy and reducing power. Our results also show that under excess light, the enhancement in total carbon fixation is dependent on the strength of the engineered sink. Under ML and HL, we observe a 17% and 24% improvement in total carbon fixation in M14 over the WT respectively whereas M14.2 shows a 47% and 70% improvement. Under excess light we did not find any significant improvement in biomass accumulation in the sink engineered strains (figure 4.4D and G). All the improvement in carbon fixation, instead, is directed to the engineered Phe sinks. The light condition thus directly affects the carbon partitioning (figure 4.5B and C).

4.4.2 Phe sink engineered strain shows improvement in PSII efficiency

To investigate the effect of the Phe sink on the photosynthetic efficiency, we chose to study M14.2, which shows a higher flux to Phe compared to M14. The effective quantum yield of PSII (Φ_{PSII}) and the relative linear electron flow rate through PSII (rETR2) were measured using PAM. Cultures were grown in triplicates under LL, ML and HL conditions to ensure that the chl fluorescence measurements were not affected by the growth light condition. As expected with increasing light intensity, we saw a significant reduction in the quantum yield of PSII in both the WT and Phe overproducer M14.2. We find that effect of the Phe sink on Φ_{PSII} is light dependent with a higher mean at all light levels although significant improvement over the WT was seen only at ML and HL (Figure 4.6).

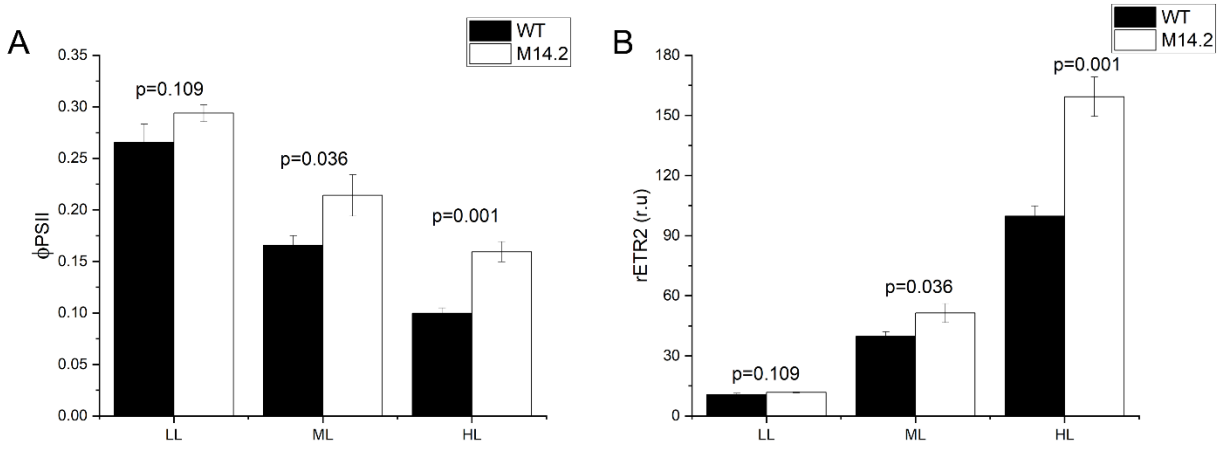

Figure 4.6 (A) Effective quantum yield of PSII and (B) relative electron transfer rate through PSII (linear electron flow) under different light intensities. Data are the mean and standard deviations of three biological replicates. Cultures were grown at different

With the introduction of the Phe sink under ML, both Φ_{PSII} and rETR2, which report on the linear electron flow, improved by ~30%, whereas a 59% improvement was observed under HL. This is comparable to the 47% and 70% enhancement observed in the carbon fixation under the same light conditions at the end of two days of growth. Since these measurements were performed on cultures with the same optical density, it is possible that M14.2 has a higher chl a content and therefore improved light utilization. However, we can rule this out as the chl a content of the WT and M14.2 is not significantly different under any of the light conditions (Figure 4.7).

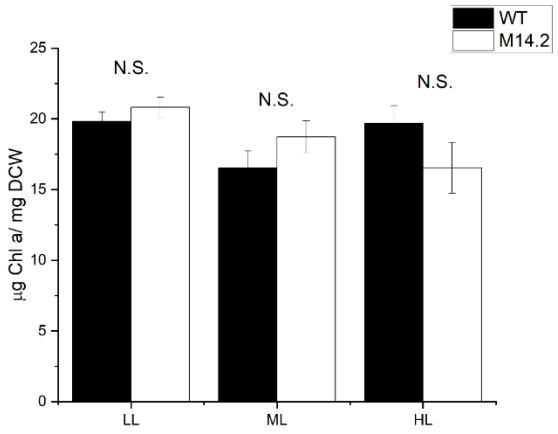

Figure 4.7 Chl a content of WT and M14.2 under different light conditions normalized to DCW. Data are the mean and standard deviation of three biological replicates grown at 38°C at ambient CO_2.

One pathway through which the quantum yield of PSII could be improved is by decreasing the thermal dissipatory loss of absorbed light energy as non-photochemical quenching. The introduction of the Phe sink in M14.2 might thus reduce non-photochemical quenching especially at high light conditions. However, we did not find a significant difference in NPQ between the WT and M14.2 at any light levels (Table 4.2). The qP and qL parameters, which reflect the fraction of oxidized Q_A electron acceptor of PSII, does not differ between WT and M14.2 at LL and ML but are 42 % and 46 % higher under high light conditions in M14.2. In general, both qP and qL decrease (Q_A becomes more reduced) with increase in light intensity, in turn decreasing the openness of PSII reaction centers. At high light, M14.2 has a significantly higher qP or qL compared to WT, as indicative of its higher fraction of open PSII reaction centers available for photochemistry at high light. Engineering of the Phe sink thus results in a greater PSII photochemical efficiency in M14.2 (Table 4.2).

Table 4.2 NPQ, q_p, 1-q_p, q_L, 1-q_L, and $\Phi_{PSIImax}$ in WT and M14.2. Each measurement represents the mean and standard deviation of three biological replicates.

Strain	WT			M14.2		
	LL	ML	HL	LL	ML	HL
NPQ	0.07±0.02	0.08±0.02	0.12±0.01	0.05±0.02	0.15±0.08	0.16±0.03
q_P	0.70±0.02	0.62±0.05	0.24±0.02	0.68±0.06	0.63±0.01	0.34±0.03
1-q_P	0.3±0.02	0.38±0.05	0.76±0.02	0.32±0.06	0.37±0.01	0.66±0.03
q_L	0.83±0.02	0.71±0.04	0.37±0.02	0.85±0.02	0.75±0.02	0.54±0.03
1-q_L	0.17±0.02	0.29±0.04	0.63±0.02	0.15±0.02	0.25±0.02	0.46±0.03
$\Phi_{PSIImax}$	0.42±0.01	0.43±0.02	0.49±0.01	0.46±0.01	0.43±0.02	0.54±0.01

Carotenoids function as accessory light harvesting pigments (Stamatakis et al., 2014) and are also involved in photoprotection to aid in quenching excess light (Schäfer et al., 2005; Sozer et al., 2010). Thus, we looked at the carotenoid content in the WT and Phe sink engineered strain at different light intensities. In both WT and M14.2, we found that the mean carotenoid content increased with light intensity. However, there was a statistically significant increase only between LL and HL conditions in both the WT and M14.2. Interestingly, we found that the total carotenoids increased significantly in M14.2 under all light conditions (Figure 4.8). Although the effect of increased carotenoid content needs to be studied further, it is possible that it helps with light harvesting at lower light intensities (LL and ML) and improves photoprotection at high light.

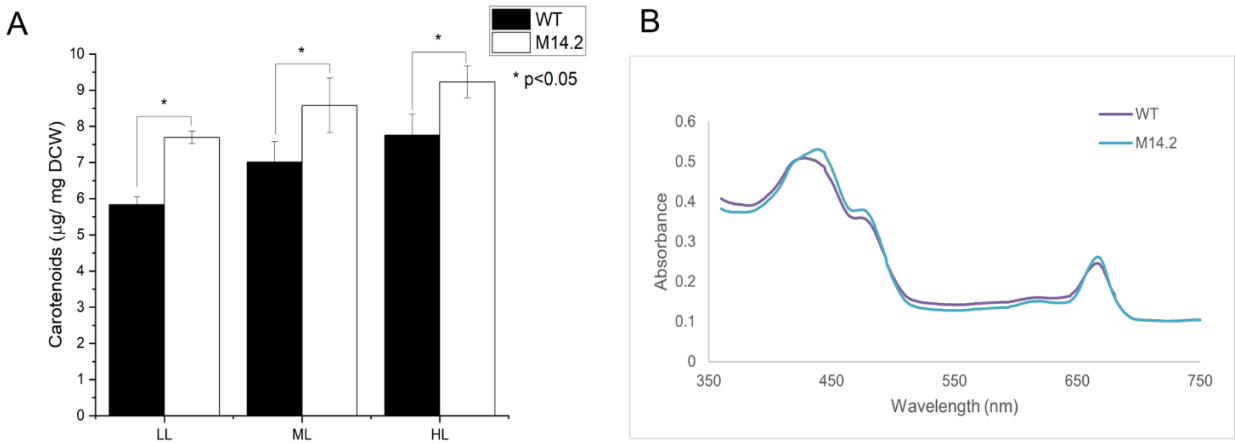

Figure 4.8 (A) Total carotenoid content of WT and M14.2 under different light conditions normalized to DCW. Data are the mean and standard deviation of three biological replicates grown at 38°C at ambient CO_2. (B) Absorbance spectra for WT and M14.2 normalized for OD_{730}. Cultures were grown at ML at 38°C and ambient CO_2.

4.4.3 Introduction of Phe sink alters cyclic electron flow

By generating additional ATP molecules, the cyclic electron flow balances the ATP/NADPH ratio[15]. In order to understand that effect of introduction of Phe sink on linear and cyclic electron flow, and thus ATP/NADPH production, we utilize P700 spectroscopy.

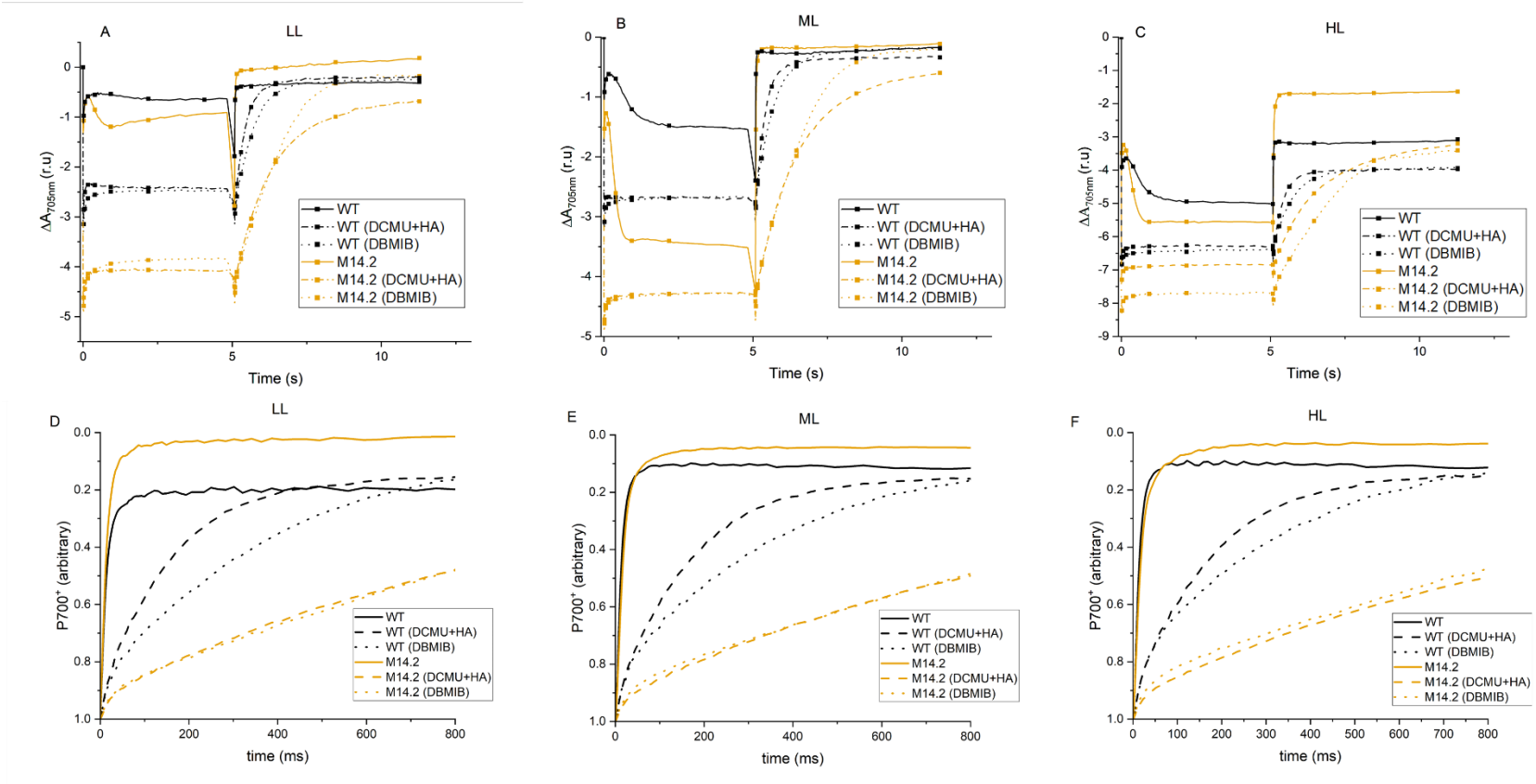

Figure 4.9 P700 absorbance kinetics of the WT (black) and M14.2 (yellow) with (dotted) and without (solid) inhibitors to block electron flow from PSII under (A) LL, (B) ML, and (C) HL conditions. P700 re-reduction kinetics for different light conditions (D) LL, (E) ML, and (F) HL are shown after normalization of the y-axis for easier comparison as described previously(Berla et al., 2015). All traces are the average of traces obtained from three biological replicates. Detailed description of the procedure is available in section 4.3

Since CEF returns electrons to the PQ pool, CEF activity can be estimated by blocking the electron flow from PSII using PSII specific inhibitors DCMU and HA. The dark rereduction rate of P700 was measured in the absence of inhibitors (total electron flow LEF+CEF) and in the presence of DCMU+HA (CEF around PSI) to calculate the %CEF in WT and M14.2 under LL, ML and HL conditions (Figure 4.10A). The %CEF in WT is higher than M14.2 at all light levels. The rereduction of P700 is significantly faster in DCMU and HA-treated WT compared to the corresponding M14.2 sample (Figure 5D-F). The %CEF is reduced to nearly 1% or to a negligible rate as observed under DBMIB due to the introduction of the Phe sink. Since DBMIB treatment should inhibit both linear and cyclic electron flow, the rereduction rate under it mostly originates from charge recombination in P700 or to a minor degree, incomplete inhibition of cyt b_6f. Since CEF generates only ATP, the decrease in %CEF by the introduction of the Phe sink will result in a decrease in the ATP/NADPH ratio in M14.2. This indicates that under the growth light intensities tested, Phe sink is likely to be more NADPH-intensive compared to the biomass sink. The introduction of the Phe sink thus results in a marked decline in %CEF, which helps to adjust the altered demand for energy and reductant towards this new sink. Our results do not indicate any change in %CEF as a function of light intensity. In WT, the only major sink is biomass and thus the demand for ATP and NADPH should be the same under different light levels. In M14.2, the flux towards the Phe sink is light dependent (figure 4.5 C). Since the ATP/NADPH requirements for the biomass and Phe sink differ, the change in flux to the Phe sink should change the net demand for ATP/NADPH. An increase in %CEF with light intensity might meet the increased demand for ATP. However, we do not find any change in %CEF with light intensity in M14.2 (Tukey's test for multiple comparison).

Figure 4.10B shows the relative electron transport through PSI (rETR1) to be significantly higher in the mutant at both ML and HL conditions than WT, with most of the increase in rETR1 arising from the increased LEF. The rETR1 and ΦPSI reflect the rate of both linear and cyclic flow while rETR2 and ΦPSII report only on the LEF. The enhancement in total electron flow as apparent from rETR1, is 86% at ML, and 83% at HL, comparable to the enhancement in carbon fixation (Figure 4.4).

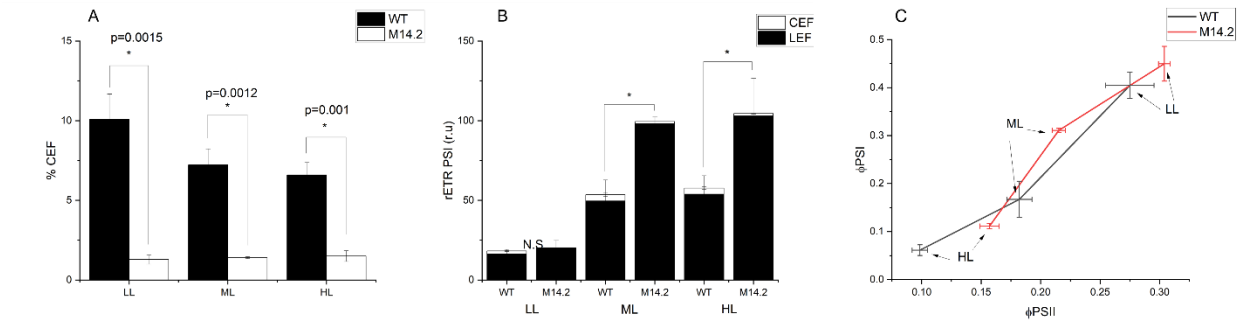

Figure 4.10 (A) P700 re-reduction kinetics were followed under different light conditions in the absence of inhibitors (LEF+CEF) and presence of DCMU+HA (CEF) to estimate the fraction of cyclic electron flow. (B) The relative total electron flow can be estimated from Y(I) and incident light intensities. (C) ΦPSI plotted vs ΦPSII for different light intensities as indicated in the graph. Data represents mean and standard deviation from three biological replicates.

4.4.4 Effect of introduction of Phe sink on PSI parameters

The introduction of Phe sink led to a substantial reduction in %CEF (Figure 4.10). Other than that it is unclear how does the Phe sink affect the PSI photochemical efficiency. We therefore determined the quantum yield as well as donor and acceptor side limitations of PSI from P700 redox kinetic data (Figure 4.9). As expected, ΦPSI of both the WT and M14.2 decreased with increase in light intensity due to an increase in the donor side inhibition Y(ND) of PSI (photosynthetic control) for avoiding photoinhibition of PSI (Kono & Terashima, 2016). However, the extent of the ΦPSI decrease at ML and HL was significantly lower in M14.2 compared to WT. The higher photochemical efficiency of PSI at ML and HL in M14.2 leads to a higher electron flow through PSI (Figure 4.10 B). Since the introduction of the Phe sink can generate a greater sink demand, we hypothesized that M14.2 would have lower PSI acceptor side limitation compared to WT, especially under high light conditions. At low light condition, we find no change between WT and M14.2 in the acceptor side limitations (Figure 4.11C). To our surprise, the introduction of the Phe sink led instead to a small increase in acceptor side limitations at ML and HL conditions. However, the largest loss in PSI efficiency was due to donor side limitation in both WT and M14.2. Interestingly, the donor side limitation was considerably lower in M14.2 compared to WT at ML and HL, thus accounting for its higher ΦPSI in those light conditions.

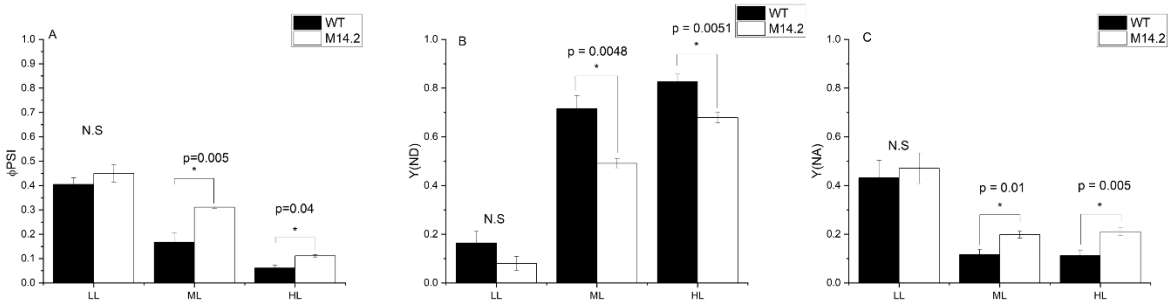

Figure 4.11 . Effect of Phe sink under different light conditions on (A) quantum yield of PSI; ΦPSI or Y(I), (B) non-photochemical energy dissipation due to donor side limitation; Y(ND) and (C) non-photochemical energy dissipation due to acceptor side limitation; Y(NA). Data represent mean and standard error of three biological replicates.

4.5 Discussion

Cyanobacteria have been increasingly investigated as sustainable chassis to produce biochemicals due to their ability to use CO_2 as the sole carbon source (Knoot et al., 2018). Several studies have engineered cyanobacteria for the production biofuels and biochemicals, however there are still hurdles before industrial application is feasible (Jaiswal et al., 2022). One way to improve feasibility is to improve the rate of carbon fixation which can then be diverted to the production of chemicals. Recently, the observation in a few studies that the introduction of a heterologous sink results in improved carbon fixation has proven to be an important finding and unintuitive strategy to further understand and develop to improve carbon fixation in cyanobacteria (Santos-Merino, Singh, et al., 2021).

In this work, we utilize randomly engineered Phe overproducing mutants of fast-growing strain *S. elongatus* PCC 11801 previously developed in our lab (Chapter 3) that showed increased carbon fixation compared to the WT strain. To study the effect of different light intensities on the enhancement in carbon fixation by quantifying the total carbon in biomass and Phe, the effect on the PSII and PSI parameters, and the cyclic and linear electron flow which is responsible to maintain the balance between the demand and production of ATP and NADPH.

Previously, it was suggested that a heterologous sink is necessary to relieve sink limitation (Santos-Merino, Singh, et al., 2021). We show that even an overflow homologous sink, such as Phe in this case can result in enhanced carbon fixation. In this work, we highlight the role of light intensity on enhancement in carbon fixation. The Phe sink competes with biomass under LL

whereas under ML and HL the enhancement is directed entirely to the engineered sink. This is similar to the observation made in lactate overproducing strain which under high light had a 22% improvement in net carbon fixation which was directed entirely to the lactate sink (Grund et al., 2022). This contrasts with 2,3 butanediol (2,3 BD) and sucrose sinks, where there was a reduction in the biomass although the total carbon fixation increased by addition of the sink (Abramson et al., 2016; Oliver & Atsumi, 2015). Phe derived 2-phenylethanol production also improved total carbon fixation where in the first 4 days there was a competition between biomass and product sinks whereas after 4 days, enhancement in carbon fixation was directed solely towards the product sink (Ni et al., 2018). These observations indicate that the sink product can influence behavior of the sink. Products such as 2-phenyl ethanol (Ni et al., 2018) and 2,3 BD (Oliver & Atsumi, 2015) can be toxic whereas the sucrose sink (Abramson et al., 2016) can osmotic pressure stress resulting in competition between biomass and product even under excess light. In contrast, a native (homologous) product such as Phe does not compete with biomass under excess light. In our work, the change in light intensity significantly affected the carbon partitioning to the Phe sink. This is similar to enhancement in carbon productivity attained in 2,3 butanediol production in *S. elongatus* 7942 when light intensity was increased from 50 µmol-photons/m^2/s to 250 µmol-photons/m^2/s (Oliver & Atsumi, 2015).

It is hypothesized that the excess light energy that is otherwise dissipated to non-photochemical quenching can be utilized by the introduction of an additional sink (Abramson et al., 2016). Our data provides additional support to this idea where we find improved quantum yield of PSII under ML and HL conditions whereas there is an insignificant improvement when light is limiting (figure 4.5). The photochemical quenching (q_P) is improved substantially under high light conditions. These results are similar to the observations made in sucrose (Abramson et al., 2016) and glycerol (Savakis et al., 2015) producing strains. This improvement in quantum yield leads to improvement the LEF that contributes to increased availability of ATP and NADPH to supply the additional demand created by the Phe sink.

There is an inherent imbalance between the production and demand of ATP/NADPH. The LEF generates ATP/NADPH in 1.38 whereas cyclic and other alternate electron flows such as Mehler reaction generate only ATP (Allen, 2003; Berla et al., 2015). The CBB cycle requires 3 ATP and 2 NADPH to fix one carbon. However, the ATP and NADPH requirement for biomass and other sinks can differ, often resulting in a mismatch between the production and consumption of ATP

and NADPH. The balanced synthesis of ATP and reductant is therefore a key impetus for the regulation of linear and cyclic electron transport. This facet of light reaction further represents an important avenue for improvement of photosynthetic efficiency and carbon fixation (Erdrich et al., 2014). Our data suggests that %CEF is decreased in response to the introduction of the Phe sink and under all light conditions. This suggests that the partitioning to the Phe sink is requires a lower ATP/NADPH ratio for production compared to biomass, which is the only sink in the WT. The biomass demand for ATP/NADPH is a minimum of 1.51 (Erdrich et al., 2014), while previous flux balance models predicted a demand as high as 1.73 (Shastri & Morgan, 2005). The estimate the demand for Phe to be 1.52. However, this demand can be slightly higher with ATP dependent amino acid uptake transporters (Luz Montesinos et al., 1997). Our results indicate that in the conditions tested, the demand of ATP/NADPH for biomass is higher than Phe resulting in lower %CEF in the Phe overproducing strains. This is consistent with expectations since Phe (degree of reduction = 4.44) is a more reduced product compared to biomass (degree of reduction ~ 4.26).

The decrease of CEF in mutant may have led to relaxation of an important safety mechanism of photosynthesis known as photosynthetic control (Berla et al., 2015; W. Huang et al., 2015). In photosynthetic control, the increased acidification of thylakoid lumen at high light intensities slows down the oxidation of PQH_2 at the Q_o-site of cyt b_6f complex, which in turn decreases the inter-photosystem electron transport. CEF is a key contributor towards proton gradient formation and photosynthetic control that protect PSI from photoinhibition. The establishment of photosynthetic control is evident in the increased donor side inhibition of PSI at ML and HL in both WT and M14.2 (Figure 4.11 B). However, the substantial decrease of CEF in M14.2 leads to lower photosynthetic control and donor side inhibition of PSI (Figure 4.11 B). This speeds up the LEF in M14.2 at ML and HL (Figure 4.10 B).

Although our data indicates an increase in the quantum yield of PSI with the introduction of the Phe sink, a large amount of energy is quenched by donor side limitation of PSI. Future work can be directed to addressing this inefficiency to further improve the carbon fixation (Mellor et al., 2019). Further work is required on understanding the molecular mechanisms responsible for sensing metabolic demands which are dynamic and change with the environment and how that regulates changes in the photosynthetic apparatus.

A key question that remains to be answered is why has evolution not fully optimized the photosynthetic capacity as the improvement of light utilization efficiency under heterologous and native overflow sink reveals additional underutilized photosynthetic potential. One possibility is that there is a tradeoff between maximizing biomass production and acclimating to different stressors that are encountered in the natural environment. Our low light data suggest that there is a competition between biomass and Phe production (figure 4.4) which could reduce the biomass accumulation and strain robustness under outdoor conditions.

Overall, our work adds to the emerging reports of enhancement in carbon fixation attained by engineering of a sink. Our study is also novel in that our sink is a native overflow sink whereas previous work has been solely on heterologous sinks. Sink engineering is a promising avenue to obtain enhancements in photosynthesis and biochemical production. With further work in understanding molecular mechanisms behind regulation of source/sink sensing and dynamic regulation under different conditions, accompanied with further metabolic engineering particularly on recently discovered fast-growing strains, cyanobacteria can be one step closer to being economically feasible chassis for biochemical production.

4.6 Conflict of Interest

I report that strains M14 and M14.2 which are part of this work are included in an US provisional patent application No. 63219691 filed by Purdue Research Foundation, Office of Technology Commercialization with inventors listed as Arnav Deshpande and John A. Morgan.

4.7 Acknowledgements

I would like to thank the National Biodiversity Authority of India for approval of strain procurement and Dr. Pramod Wangikar from Indian Institute of Technology, Bombay for providing the wild type *Synechococcus elongatus* PCC 11801. I would also like to thank Dr. Iskander Ibrahim for his help with setting up PAM and P700 spectroscopy measurements as well as critical review of the data.

4.8 References

Abramson, B. W., Kachel, B., Kramer, D. M., & Ducat, D. C. (2016). Increased photochemical efficiency in cyanobacteria via an engineered sucrose sink. *Plant and Cell Physiology*, *57*(12), 2451–2460. https://doi.org/10.1093/pcp/pcw169

Allen, J. F. (2003). Cyclic, pseudocyclic and noncyclic photophosphorylation: new links in the chain. *Trends in Plant Science*, *8*(1), 15–19. https://doi.org/https://doi.org/10.1016/S1360-1385(02)00006-7

Baker, N. R. (2008). Chlorophyll fluorescence: A probe of photosynthesis in vivo. *Annual Review of Plant Biology* (Vol. 59, pp. 89–113). https://doi.org/10.1146/annurev.arplant.59.032607.092759

Berla, B. M., Saha, R., Maranas, C. D., & Pakrasi, H. B. (2015). Cyanobacterial Alkanes Modulate Photosynthetic Cyclic Electron Flow to Assist Growth under Cold Stress. *Scientific Reports*, *5*. https://doi.org/10.1038/srep14894

Campbell, D., Hurry, V., Clarke, A. K., Gustafsson, P., & Quist, G. O. ¨. (1998). Chlorophyll Fluorescence Analysis of Cyanobacterial Photosynthesis and Acclimation. *Microbiology and Molecular Biology Reviews* (Vol. 62, Issue 3). https://journals.asm.org/journal/mmbr

Deshpande, A., Vue, J., & Morgan, J. (2020). *Combining Random Mutagenesis and Metabolic Engineering for Enhanced Tryptophan Production in Synechocystis sp. Strain PCC 6803*. https://doi.org/10.1128/AEM

Erdrich, P., Knoop, H., Steuer, R., & Klamt, S. (2014). Cyanobacterial biofuels: new insights and strain design strategies revealed by computational modeling. *Microbial Cell Factories*, *13*(1). doi: 10.1186/s12934-014-0128-x

Genty, B., Briantais, J. M., & Baker, N. R. (1989). The relationship between the quantum yield of photosynthetic electron transport and quenching of chlorophyll fluorescence. *Biochimica et Biophysica Acta - General Subjects*, *990*(1), 87–92. https://doi.org/10.1016/S0304-4165(89)80016-9

Grund, M., Jakob, T., Wilhelm, C., Bühler, B., & Schmid, A. (2019). Electron balancing under different sink conditions reveals positive effects on photon efficiency and metabolic activity of Synechocystis sp. PCC 6803. *Biotechnology for Biofuels*, *12*(1). https://doi.org/10.1186/s13068-019-1378-y

Grund, M., Torsten, J., Jörg, T., Andreas, S., Christian, W., Bruno, B., & Haruyuki, A. (2022). Heterologous Lactate Synthesis in Synechocystis sp. Strain PCC 6803 Causes a Growth Condition-Dependent Carbon Sink Effect. *Applied and Environmental Microbiology*, *0*(0), e00063-22. https://doi.org/10.1128/aem.00063-22

Holland, S. C., Artier, J., Miller, N. T., Cano, M., Yu, J., Ghirardi, M. L., & Burnap, R. L. (2016). Impacts of genetically engineered alterations in carbon sink pathways on photosynthetic performance. *Algal Research*, *20*, 87–99. https://doi.org/10.1016/j.algal.2016.09.021

Huang, Q., Jiang, F., Wang, L., & Yang, C. (2017). Design of Photobioreactors for Mass Cultivation of Photosynthetic Organisms. *Engineering*, *3*(3), 318–329. https://doi.org/10.1016/J.ENG.2017.03.020

Huang, W., Yang, Y. J., Hu, H., & Zhang, S. B. (2015). Different roles of cyclic electron flow around photosystem I under sub-saturating and saturating light intensities in tobacco leaves. *Frontiers in Plant Science*, https://doi.org/10.3389/fpls.2015.00923

Jaiswal, D., Sahasrabuddhe, D., & Wangikar, P. P. (2022). Cyanobacteria as cell factories: the roles of host and pathway engineering and translational research. *Current Opinion in Biotechnology* (Vol. 73, pp. 314–322). Elsevier Ltd. https://doi.org/10.1016/j.copbio.2021.09.010

Jaiswal, D., Sengupta, A., Sohoni, S., Sengupta, S., Phadnavis, A. G., Pakrasi, H. B., & Wangikar, P. P. (2018). Genome Features and Biochemical Characteristics of a Robust, Fast Growing and Naturally Transformable Cyanobacterium Synechococcus elongatus PCC 11801 Isolated from India. *Scientific Reports*, *8*(1). https://doi.org/10.1038/s41598-018-34872-z

Kirst, H., Formighieri, C., & Melis, A. (2014). Maximizing photosynthetic efficiency and culture productivity in cyanobacteria upon minimizing the phycobilisome light-harvesting antenna size. *Biochimica et Biophysica Acta - Bioenergetics*, *1837*(10), 1653–1664. https://doi.org/10.1016/j.bbabio.2014.07.009

Klughammer, C., & Schreiber, U. (1994). An improved method, using saturating light pulses, for the determination of photosystem I quantum yield via $P700^{+}$. *Planta*, *192*(2), 261–268. http://www.jstor.org/stable/23382564

Knoot, C. J., Ungerer, J., Wangikar, P. P., & Pakrasi, H. B. (2018). Cyanobacteria: Promising biocatalysts for sustainable chemical production. *Journal of Biological Chemistry* (Vol. 293, Issue 14, pp. 5044–5052). American Society for Biochemistry and Molecular Biology https://doi.org/10.1074/jbc.R117.815886

Kono, M., & Terashima, I. (2016). Elucidation of photoprotective mechanisms of PSI against fluctuating light photoinhibition. *Plant and Cell Physiology*, *57*(7), 1405–1414. https://doi.org/10.1093/pcp/pcw103

Kramer, D. M., & Evans, J. R. (2011). The importance of energy balance in improving photosynthetic productivity. *Plant Physiology*, *155*(1), 70–78. https://doi.org/10.1104/pp.110.166652

Liang, F., Lindberg, P., & Lindblad, P. (2018). Engineering photoautotrophic carbon fixation for enhanced growth and productivity. In *Sustainable Energy and Fuels* (Vol. 2, Issue 12, pp. 2583–2600). Royal Society of Chemistry. https://doi.org/10.1039/c8se00281a

Montesinos, M., Herrero, A., & Flores, E. (1997). Amino acid transport in taxonomically diverse cyanobacteria and identification of two genes encoding elements of a neutral amino acid permease putatively involved in recapture of leaked hydrophobic amino acids. *Journal Of Bacteriology*, *179*(3), 853-862. doi: 10.1128/jb.179.3.853-862.1997

Mellor, S. B., Vinde, M. H., Nielsen, A. Z., Hanke, G. T., Abdiaziz, K., Roessler, M. M., Burow, M., Motawia, M. S., Møller, B. L., & Jensen, P. E. (2019). Defining optimal electron transfer partners for light-driven cytochrome P450 reactions. *Metabolic Engineering*, *55*, 33–43. https://doi.org/10.1016/j.ymben.2019.05.003

Ni, J., Liu, H. Y., Tao, F., Wu, Y. T., & Xu, P. (2018). Remodeling of the Photosynthetic Chain Promotes Direct CO2 Conversion into Valuable Aromatic Compounds. *Angewandte Chemie - International Edition*, *57*(49), 15990–15994. https://doi.org/10.1002/anie.201808402

Nogales, J., Gudmundsson, S., Knight, E. M., Palsson, B. O., & Thiele, I. (2012). Detailing the optimality of photosynthesis in cyanobacteria through systems biology analysis. *Proceedings of the National Academy of Sciences of the United States of America*, *109*(7), 2678–2683. https://doi.org/10.1073/pnas.1117907109

Oliver, J. W. K., & Atsumi, S. (2015). A carbon sink pathway increases carbon productivity in cyanobacteria. *Metabolic Engineering*, *29*, 106–112. https://doi.org/10.1016/j.ymben.2015.03.006

Porra, R., Thompson, W., & Kriedemann, P. (1989). Determination of accurate extinction coefficients and simultaneous equations for assaying chlorophylls a and b extracted with four different solvents: verification of the concentration of chlorophyll standards by atomic absorption spectroscopy. *Biochimica Et Biophysica Acta (BBA) - Bioenergetics*, *975*(3), 384-394. doi: 10.1016/s0005-2728(89)80347-0

Ralph, P. J., & Gademann, R. (2005). Rapid light curves: A powerful tool to assess photosynthetic activity. *Aquatic Botany*, *82*(3), 222–237. https://doi.org/10.1016/j.aquabot.2005.02.006

Rippka, R., Stanier, R., Deruelles, J., Herdman, M., & Waterbury, J. (1979). Generic Assignments, Strain Histories and Properties of Pure Cultures of Cyanobacteria. *Microbiology*, *111*(1), 1-61. doi: 10.1099/00221287-111-1-1

Ritchie, R. J. (2006). Consistent sets of spectrophotometric chlorophyll equations for acetone, methanol and ethanol solvents. *Photosynthesis Research*, *89*(1), 27–41. https://doi.org/10.1007/s11120-006-9065-9

Santos-Merino, M., Singh, A. K., & Ducat, D. C. (2021). *6 Sink Engineering in Photosynthetic Microbes*.

Santos-Merino, M., Torrado, A., Davis, G., Röttig, A., Bibby, T., Kramer, D., & Ducat, D. (2021). Improved photosynthetic capacity and photosystem I oxidation via heterologous metabolism engineering in cyanobacteria. *Proceedings Of The National Academy Of Sciences*, *118*(11). doi: 10.1073/pnas.2021523118

Savakis, P., Tan, X., Du, W., Branco Dos Santos, F., Lu, X., & Hellingwerf, K. J. (2015). Photosynthetic production of glycerol by a recombinant cyanobacterium. *Journal of Biotechnology*, *195*, 46–51. https://doi.org/10.1016/j.jbiotec.2014.12.015

Schäfer, L., Vioque, A., & Sandmann, G. (2005). Functional in situ evaluation of photosynthesis-protecting carotenoids in mutants of the cyanobacterium Synechocystis PCC6803. *Journal of Photochemistry and Photobiology B: Biology*, *78*(3), 195–201. https://doi.org/https://doi.org/10.1016/j.jphotobiol.2004.11.007

Shastri, A., & Morgan, J. (2005). Flux Balance Analysis of Photoautotrophic Metabolism. *Biotechnology Progress*, *21*, 1617–1626. https://doi.org/10.1021/bp050246d

Sozer, O., Komenda, J., Ughy, B., Domonkos, I., Laczk-Dobos, H., Malec, P., Gombos, Z., & Kis, M. (2010). Involvement of carotenoids in the synthesis and assembly of protein subunits of photosynthetic reaction centers of synechocystis sp. PCC 6803. *Plant and Cell Physiology*, *51*(5), 823–835. https://doi.org/10.1093/pcp/pcq031

Stamatakis, K., Tsimilli-Michael, M., & Papageorgiou, G. C. (2014). On the question of the light-harvesting role of β-carotene in photosystem II and photosystem I core complexes. *Plant Physiology and Biochemistry*, *81*, 121–127. https://doi.org/10.1016/j.plaphy.2014.01.014

Ungerer, J., Tao, L., Davis, M., Ghirardi, M., Maness, P. C., & Yu, J. (2012). Sustained photosynthetic conversion of CO2 to ethylene in recombinant cyanobacterium Synechocystis 6803. *Energy and Environmental Science*, *5*(10), 8998–9006. https://doi.org/10.1039/c2ee22555g

Vega de Luna, F., Córdoba-Granados, J. J., Dang, K. van, Roberty, S., & Cardol, P. (2020). In vivo assessment of mitochondrial respiratory alternative oxidase activity and cyclic electron flow around photosystem I on small coral fragments. *Scientific Reports*, *10*(1). https://doi.org/10.1038/s41598-020-74557-0

Whitney, S. M., Houtz, R. L., & Alonso, H. (2011). Advancing our understanding and capacity to engineer nature's CO2-sequestering enzyme, Rubisco. *Plant Physiology*, *155*(1), 27–35. https://doi.org/10.1104/pp.110.164814

Zhang, A., Carroll, A. L., & Atsumi, S. (2017). Carbon recycling by cyanobacteria: Improving CO_2 fixation through chemical production. In *FEMS Microbiology Letters* (Vol. 364, Issue 16). Oxford University Press. https://doi.org/10.1093/femsle/fnx165

CONCLUSIONS AND FUTURE WORK

This dissertation aimed to showcase the potential of cyanobacteria as chassis for sustainable engineering of aromatic amino acids. It demonstrates the advantages of using modern synthetic biology tools for metabolic engineering and the challenges in their use in recently discovered cyanobacteria. It highlights the importance and power of random mutagenesis combined with appropriate selection, especially in newly discovered fast growing cyanobacteria such as *Synechococcus elongatus* PCC 11801. Although random mutagenesis is not a rational targeted process, this dissertation shows that genome sequencing and single nucleotide polymorphism identification can be used successfully to unravel the specific mutations due to the reduced cost of next generation sequencing techniques. It also showcases the benefits of tying together modern metabolic engineering with traditional random mutagenesis approaches which showed an improvement over either approach alone.

This dissertation also investigated the phenomenon of sink induced enhancement in carbon dioxide fixation. In the last several years, there have been observations that carbon fixation in cyanobacteria showed an enhancement when a heterologous pathway to a chemical sink was added. However, these observations were not the focus of those studies and were not investigated in detail. In this dissertation, we showed that this enhancement in carbon fixation can also be achieved by engineering overproduction and excretion of an endogenous product such as Phe. We also highlight of the effects of Phe overproduction on photosynthesis, in particular electron flow through photosystems I/II as described in chapter 4.

This dissertation also highlights some of the challenges that still remain to be addressed for cyanobacteria to be considered as industrial microbes. Although the phenylalanine overproducers developed as part of this dissertation have the potential to be superior to heterotrophs in land use as described in chapter 3, further translational research is must in order to scale up production. Future work should be focused on understanding resistance to various abiotic stressors that are encountered in outdoor settings such as diurnal cycles, temperature variation, resistance to population crashes. Furthermore, in-depth techno-economic analyses will be crucial for designing and selecting the optimal outdoor photobioreactor system. Outdoor pilot scale studies under different climates will prove important in order to make suitable assumptions for any techno-economic analyses. Furthermore, exploring the feasibility of using CO_2 containing flue gas streams

is important as this can not only reduce cost for CO_2 supply but also provide carbon credits to companies which will incentivize the development of cyanobacteria as hosts for biochemical production. Thus, future metabolic engineering efforts should be directed at improving productivity under outdoor conditions and not only under "ideal" laboratory conditions.

We describe improved carbon fixation in Phe overproducing strains in chapter 4, which resembles a "free lunch" scenario where our engineered strains make a product for no apparent cost. For example, the engineered strains produce several g/L of Phe without any loss of biomass accumulation. Although we identified the role of electron flow through the photosystems that enables this, there is much that remains unknown. For example, how the engineering of a secreted product alters the demand and production of ATP/NADPH by altering electron flow through the photosystems is still being understood. Along with the production and demand for ATP/NADPH, it is also crucial to study the NADPH/NADP+, ATP/ADP/AMP fractions in sink engineered strains. This is particularly important since photosynthesis and electron flow is linked to the redox state of NADPH. Effect of light on redox state of NADPH in sink engineered strains has not been investigated and can reveal further insight into the increase in net carbon fixation in sink engineered strains. Since sink engineered strains exhibit an increase in electron flow, the redox state of NADPH could be crucial in deciding if the fate of electrons from PSI to either produce NADPH or as thermal dissipation. Understanding the imbalance between sink and source as well as the redox status of NADPH can guide metabolic engineering efforts to achieve further enhancements in biochemical productivity.

Future work is also needed to address several questions that arise from this phenomenon such as how cyanobacteria sense an increase in demand of carbon (sink demand), if, and how the introduction of a carbon sink affects the transcriptome or proteome. Transcriptomic data has the potential to unravel novel transcriptional regulation, if any that coordinates the balance between the source and sink. Since, the protein levels may not correlate with the transcript abundance, proteomics could further enable us to understand which proteins are likely to play a role in this phenomenon. A systems biology analysis can yield insight and answer some of these questions. Furthermore, it is intriguing why evolution has not resulted in harnessing the improved carbon fixation for biomass in the wild. It might be due to a trade-off between strain robustness which in the natural environment is crucial to adapt to changing environmental conditions. Fundamental and systems levels research is needed to understand these observations and might provide insight

that will be crucial in further enabling research to address the current limitations of cyanobacteria such as slower growth, especially in comparison to heterotrophic organisms and improve adaptability under different environmental conditions.

Harnessing the previously untapped potential of cyanobacteria by source and sink engineering to improve carbon fixation, development of sophisticated synthetic biology tools for fast growing strains, metabolic engineering strategies for improving productivity and product titers as well as resistance to abiotic stressors and adaptability to outdoor conditions are the crucial next steps to realize cyanobacteria as commercially competitive, sustainable alternatives to current petroleum derived or heterotrophic production of chemicals.